Chemical Investigation of Alkaloids from Two Haplosclerida sponges collected in Papua New Guinea

MSc Chemistry

By

Denis Besliu

School of Biological and Chemical Sciences

2023

OLLSCOIL NA GAILLIMHE
UNIVERSITY OF GALWAY

Research MSc Thesis

Denis Besliu

School of Biological and Chemical Sciences

Chemical Investigation of Alkaloids from Two Haplosclerida sponges collected in Papua New Guinea

Denis Besliu – 17313581

Supervisor: Prof. Olivier P. Thomas

01/08/2023

Declaration

I declare that this material, which I now submit for assessment, is entirely my own work and has not been taken from the work of others, save and to the extent that such work has been cited and acknowledged within the text of my work. I understand that plagiarism, collusion, and copying are grave and serious offences in the university and accept the penalties that would be imposed should I engage in plagiarism, collusion or copying. I have read and understood the Assignment Regulations. I have identified and included the source of all facts, ideas, opinions, and viewpoints of others in the assignment references. Direct quotations from books, journal articles, internet sources, module text, or any other source whatsoever are acknowledged, and the source cited are identified in the assignment references. This assignment, or any part of it, has not been previously submitted by me or any other person for assessment on this or any other course of study.

Acknowledgements

I would like to express my gratitude to the marine bio-discovery group for their support, knowledge input at key stages and training with equipment usage.

Special thanks to:

Olivier P. Thomas

Shauna O'Brian

For their help at key stages through the project.

Summary/Abstract

The phylum Porifera contributes immensely to the repertoire of marine natural products amassed to date. Regions of the Pacific Ocean where chemical diversity was not previously assessed were analysed and samples of various organisms including sponges were collected during the *Tara* Pacific expedition in 2016. Two sponges of the family Haplosclerida were selected for chemical investigation due to their chemical profile where mass spectrometry analysis showed the presence of alkaloids. Marine alkaloids are known to possess high bioactivity against various diseases. The objectives of this Masters are to isolate alkaloids from these sponges, elucidate their structures using NMR and test their bioactivity in terms of cytotoxicity and antioxidant activity. This investigation lead to the discovery of 4 known compounds, 1 new compound and left us with highly interesting NMR results for 2 further compounds.

Table of contents

1. Introduction

1.1. The *Tara* pacific expedition (2016-2018)

Coral reef research in the Pacific Ocean is vital to the understanding of marine ecosystems. Inspired by previous expeditions like the Great Barrier Reef expedition of 1928, it is understood that coral reefs are great regions of biodiversity in the marine environment and their preservation crucial to maintaining the health of marine ecosystems.[1] Aquatic resources from organisms living in coral reefs have the potential to contribute immensely to the blue bioeconomy especially in areas such as food.

1.1.1. Objectives of the expedition

The principal objectives of this expedition are the census of biodiversity and marine life composing the endangered coral reef ecosystems in the Pacific Ocean.[1] This includes, eukaryotes, prokaryotes and viruses which are connected to corals, fish and the surrounding waters as a way to determine variation across different reefs in the ocean (Figure 1).[1]

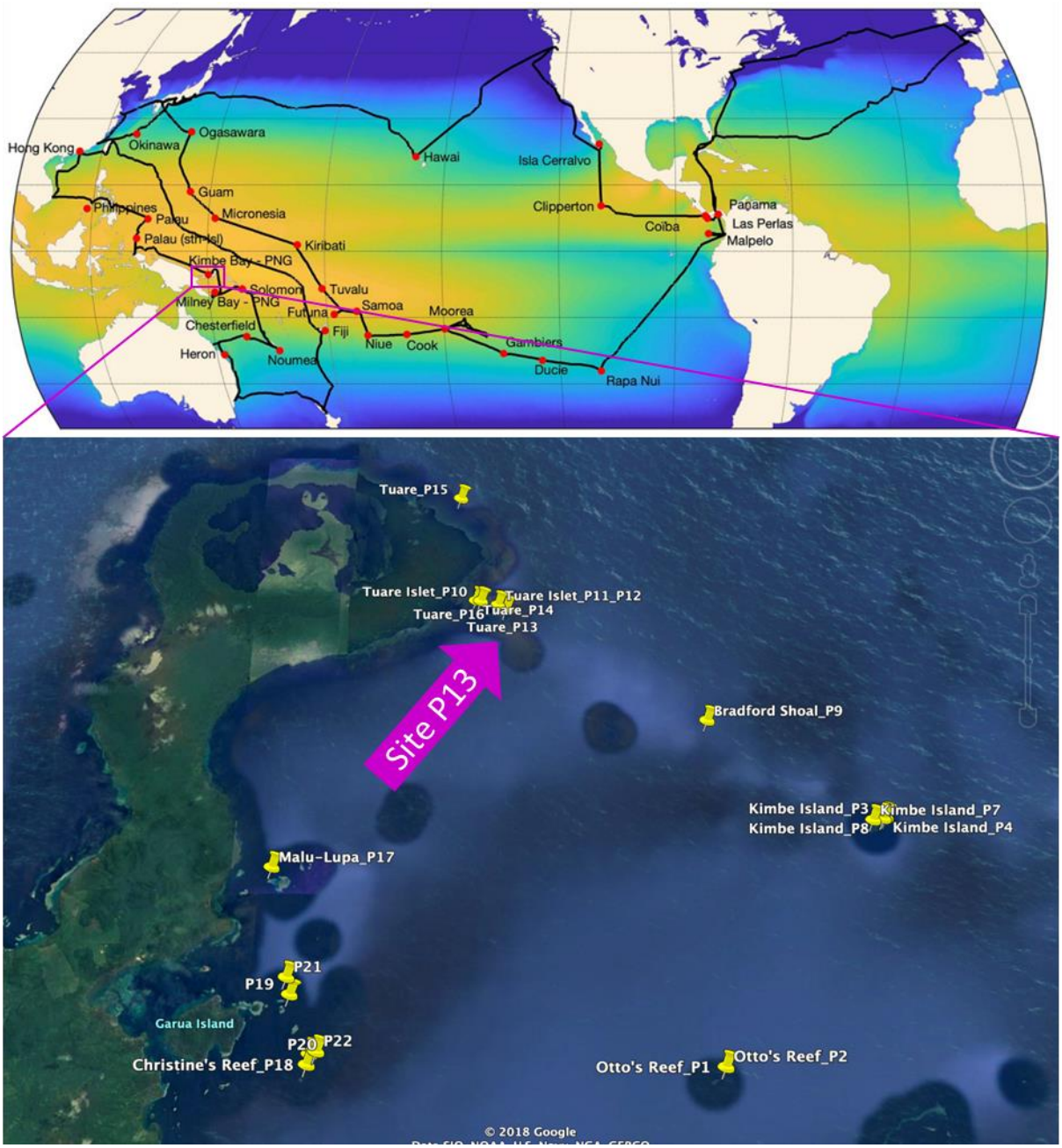

Figure 1 Route of the Tara Pacific expedition and key research areas.[1] Collection in Kimbe Bay Papua New Guinea, site P13.

1.1.2. An interest in Sponges

The collection and chemical investigation of sponges from coral reefs of the Pacific Ocean was a key objective, with the aim of assessing chemical diversity in these remote regions. During the expedition a biobank of sponges was generated from these unexplored regions and they were collected for the assessment of their chemical diversity.[2] Papua New Guinea (PNG) was one of the sites where sponge samples were collected. Located within the coral triangle, the coasts of PNG are known for their

extremely high level of marine biodiversity, this being a key reason for collecting biological samples in the region. The aim of collecting these samples is to discover new compounds from sponges and assess their chemical biodiversity.

1.2. Sponges

With oceans making 70% of the earth's surface, they are repository of organisms including 226,000 known eukaryotic species.[3] It is estimated that between one to two thirds of marine species are yet to be discovered, corresponding to a proposed 741,000 species.[3] Over the 2000 decade there have been more species described than any previous decade and the rate has not stopped growing towards the end of this decade.[3] With current trends in the description of marine species, it is possible that most species will be discovered by the end of this century, primarily due to the steady increase in active researchers on the matter.[3]

Sponges make up the phylum Porifera and are the oldest metazoan group present on earth, originating 800 million years ago.[4] These aquatic organisms are primarily found in the marine environment with very few species inhabiting fresh waters. Sponges are adapted to living in various marine habitats from Antarctic waters, to temperate and tropical oceans.[4, 5] They are filter-feeders, sessile and benthic, usually attached to a substrate like rocks or other hard surfaces.[4] These organisms produce secondary metabolites as chemical defences against predators and marine microorganisms. The phylum Porifera produces approximately one third of all metabolites in the Marinlit database.[6] Sponges may also have dead zones around them where no other organisms grow due to ecotoxic metabolites, preventing the growth of other organisms like corals in their proximity.[5] Sponges must counteract the action of pathogenic microorganisms, resulting in the production of antimicrobial marine natural products (MNP). It is still unclear whether sponges directly or their endosymbionts are responsible for the biosynthesis of these secondary metabolites.

1.3. Marine Natural Products and Drug Discovery

Firstly it is important to acknowledge the importance of natural products (NP) as a whole, before focusing on MNPs. A record of approved drugs is kept by Newman and Cragg from 1981 to 2019.[7] 23.5% of approved drugs have some connection to natural product chemistry, be it unaltered NPs or a NP derivative.[7] On top of these 11.5% of

drugs that are synthetic are still inspired by NPs (Figure 2).[7] This shows the importance of NPs for drug discovery to combat diseases and also their importance in providing scientists with inspiration for future drugs.

code	brief definition/year
B	biological macromolecule, 1997
N	unaltered natural product, 1997
NB	botanical drug (defined mixture), 2012
ND	natural product derivative, 1997
S	synthetic drug, 1997
S*	synthetic drug (NP pharmacophore), 1997
V	vaccine, 2003
/NM	mimic of natural product, 2003

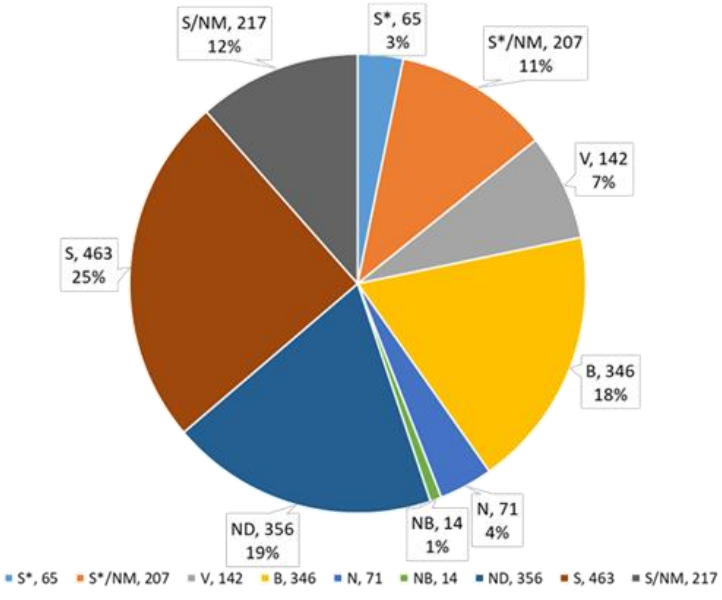

Figure 2 Approved Drugs Jan 1981 to Sept 2019 with their origin, including number of drugs for each category.[7]

The marine environment started to be studied for therapeutics and MNPs in the mid-1960s to 1970s and started picking up pace in the 1980s (Figure 3). This is relatively recent compared to the terrestrial environment. However, more advances are being made and more therapeutics come out regularly that are of marine origin, totalling 17 today. A molecular scaffold is the base or core structure of a molecule and generally has some connection to a molecule's overall bioactivity.[8] Approximately 71% of molecular scaffolds are used solely by marine life and in regards to terrestrial NPs, their marine counterparts are seen to be structurally more complex.[9, 10] This is likely due to millions of years of molecular adaptations where marine life had to continuously develop compounds to counteract predation and pathogenic microorganisms which can develop resistance to these compounds. This can be comparable to humanity's struggles against bacteria where antibiotics were and still are developed but, now antibiotic-resistant bacteria are becoming more prevalent and worrying, resulting in a need to modify existing antibiotics and find new sources of antimicrobial compounds. It is important to recognize the growth of MNP chemistry and the progress made in the number of isolated compounds over the past decades (Figure 3). Each decade corresponds to a further increase in the number of MNPs being

discovered. From 2010 where there were a total of approximately 9000 MNPs discovered, now with the use of Marinlit as a database, there are 39054 MNPs discovered in total.[6, 11] The discovery of new MNPs had a rate of growth of 500 in the 1990s and has increase over the 2000s reaching over 1000 new discoveries yearly.[12]

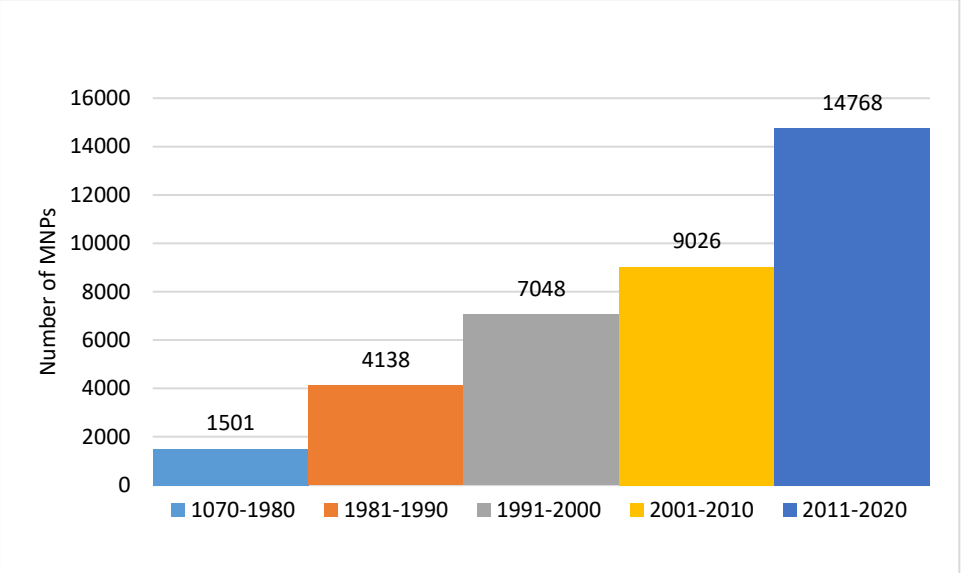

Figure 3 Number of MNPs isolated per decade from 1970 to 2010 according to Marinlit.[11]

When testing marine versus terrestrial bioactivity rates, it has been shown by the National Cancer Institute that only 0.1% of terrestrial compounds show cytotoxicity compared to 1% for MNPs.[13] Ziconotide is an example of a MNP success story, an analgesic drug that is extracted from the cone snail *Conus magnus* approved on the 12th of December 2005 by the Food and Drug Administration (FDA).[9, 14] The potency of ziconotide was determined to be 1000 times more powerful than morphine.[15]

From 2004 until 2013, 7 MNPs have been approved for clinical used by the FDA and European Medicines Evaluations Agency (EMEA).[16] This number increased to 13 by December 2020. Crucially there is the prevalence of sponge derived therapeutics, 3 of which are anticancer agents and 1 being an antiviral agent.[17] Therefore, it is essential to consider the study of MNPs for further therapeutic research especially those produced by sponges. Finally, in 2021 the FDA approved a total of 15 MNP clinical drugs and that number reaching 17 in the present day (Table 1).[18, 19]

Table 1 MNP therapeutics approved by the FDA.[18]

Compound Name	Year of FDA-Approval	Marine Organism	Disease Area
Cytarabine (Ara-C)	(1969)	Sponge	Cancer: Leukemia
Vidarabine (Ara-A)	(1976)	Sponge	Antiviral: Herpes Simplex Virus
Ziconotide	(2004)	Cone snail	Pain: Severe Chronic Pain
Omega-3-acid ethyl esters *status is debatable at the moment	(2004)	Fish	Hypertriglyceridemia
Eicosapenta enoic acid ethyl ester	(2012)	Fish	Hypertriglyceridemia
Omega-3-carboxylic acid	(2014)	Fish	Hypertriglyceridemia
Eribulin Mesylate (E7389)	(2010)	Sponge	Cancer: Metastatic Breast Cancer
Brentuximab vedotin (SGN-35)	(2011)	Mollusk/cyanobacterium	Cancer: Anaplastic large T-cell systemic maglinant lymphoma, Hodgkin's disease
Trabectedin (ET-743)	(2015)	Tunicate	Cancer: Soft Tissue Sarcoma and Ovarian Cancer
Panobinostat	(2015)	Sponge	Cancer: Multiple Myeloma
Plitidepsin	(2018) (Australia)	Tunicate	Cancer: Multiple Myeloma, Leukemia, Lymphoma
Polatuzumab vedotin (DCDS-4501A)	(2019)	Mollusk/cyanobacterium	Cancer: Non-Hodgkin lymphoma, Chronic lymphocytic leukemia, Lymphoma, B-Cell lymphoma, Folicular
Enfortumab Vedotin-ejfv	(2019)	Mollusk/cyanobacterium	Metastatic urothelial cancer
Lurbinectedin	(2020)	Tunicate	Cancer: Metastatic Small Cell Lung Cancer
Belantamab Mafodotin-blmf	(2020)	Mollusk/cyanobacterium	Cancer: Relapsed/refractory multiple myeloma
Disitamab Vedotin	2021 (China)	Mollusk/cyanobacterium	Cancer: Urothelial Carcinoma, Advanced Cancer, Gastric Cancer, HER2 Overexpressing Gastric Carcinoma, Advanced Breast Cancer, Solid Tumors
Tisotumab vedotin-tftv	(2021)	Mollusk/cyanobacterium	Metastatic cervical cancer

A lot of MNP drugs are monoclonal antibody conjugated. Along with these, 33 extra marine compounds are in clinical trials with 4 of these being in phase III trials.[19]

Table 2 MNP therapeutics in phase 3 clinical trials.[18]

Compound Name	Marine Organism	Disease Area
Plinabulin (NPI-2358)	Fungus	Cancer: Non-Small Cell Lung Cancer, Brain Tumor
Tetrodotoxin	Pufferfish	Pain: Chronic Pain
Marizomib (Salinosporamide A; NPI-0052)	Bacterium	Cancer: Non-Small Cell Lung Cancer, Pancreatic Cancer, Melanoma, Lymphoma, Multiple Myeloma
Plitidepsin	Tunicate	Coronavirus

1.4. Sponge MNPs

Up until 2008 around 75% of all MNPs were isolated from the phyla Porifera (Figure 4).[20] This constituted a number of just over 3500 MNPs. According to Marinlit, on the 14th of August 2022, 11849 out of 39054 corresponding to 30.3 % of MNPs are derived from phylum porifera. [6, 11] This constitutes a decrease in percentage due to the increasing interest in MNP chemistry and the study of other marine organisms, however sponges remain a promising source of new MNPs.

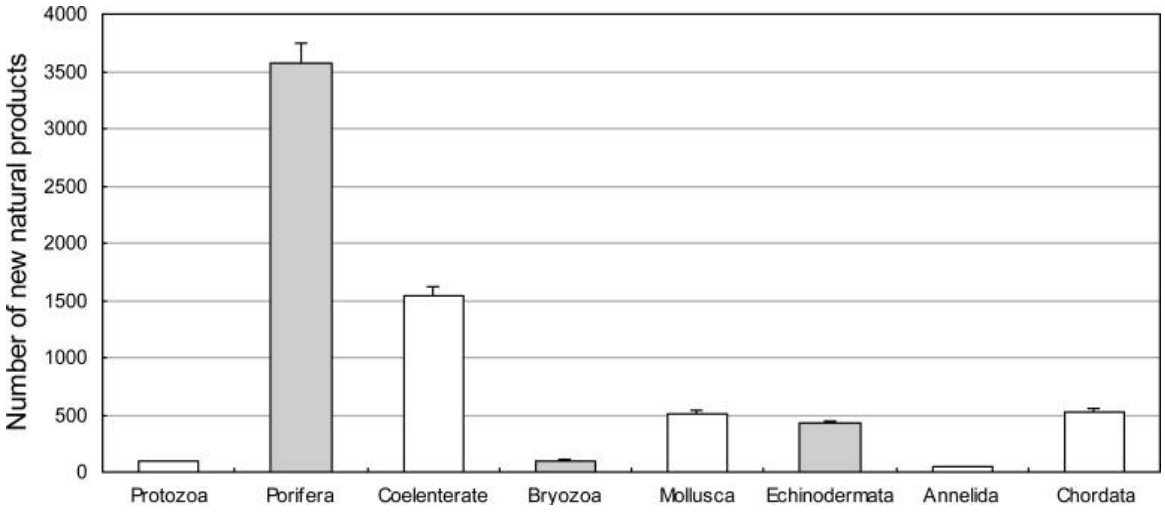

Figure 4 New compounds isolated from marine invertebrates between 1985 to 2008.[20]

Sponges show a large chemical diversity of MNPs, Roberto Mioso et al. have produced a review of cytotoxic MNPs from sponges between the years 2010 and 2012 comprising 62 sponges from the class Demospongiae.[21] They concluded that four

classes of compounds were most likely to result in bioactivity: terpenoids (41.9%), alkaloids (26.2%), macrolides (8.9%) and peptides (6.3%) (Figure 5).[21, 22]

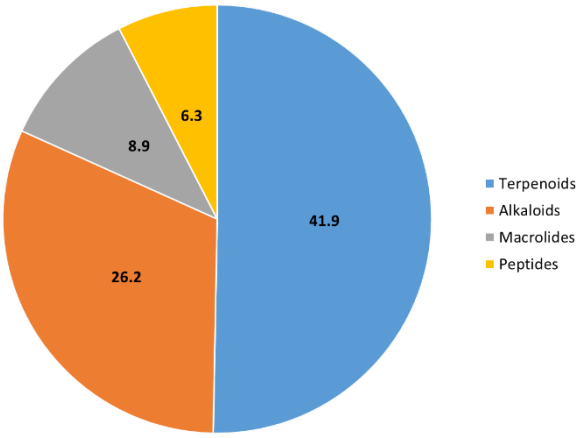

Figure 5 Chemical class of bioactive compounds isolated from sponges between 2010 and 2012.[21]

Sponges are known to produce bioactive compounds that are not only cytotoxic but have other functions such as: anti-inflammatories, immunosuppressants, neurosuppressants, antivirals, anti-fungals, anti-malarials and antibiotics among others.[23]

1.5. Main families of alkaloids from sponges

Secondary metabolites containing a basic nitrogen cycle are known as alkaloids and these can be both aromatic and non-aromatic.[24] It is crucial for these compounds to have basic pKa to be considered alkaloid NPs. These compounds are mostly known to be used for defence purposes against predators and microorganisms the sponges may encounter and represent close to one quarter of all sponge MNPs.[25, 26]

1.5.1. Alkaloids derived from aromatic amino acids

1.5.1.1. Tyrosine derived alkaloids

Using L-tyrosine as the building block for this class of alkaloids usually results in bromotyrosine MNPs from sponges. Examples like aplyzanzine B from *Jaspis* sp. and anomoian B from *Bubaris* sp. (Figure 6), both collected from Indonesia showing cytotoxic effects against colorectal adenocarcinoma, lung cancer and breast cancer cell lines.[27] Another example of a cytotoxic bromotyrosine MNP is purpuramine J from Fijian marine sponge *Druinella* sp. which shows the potential of this family of MNPs to combat various diseases.[28]

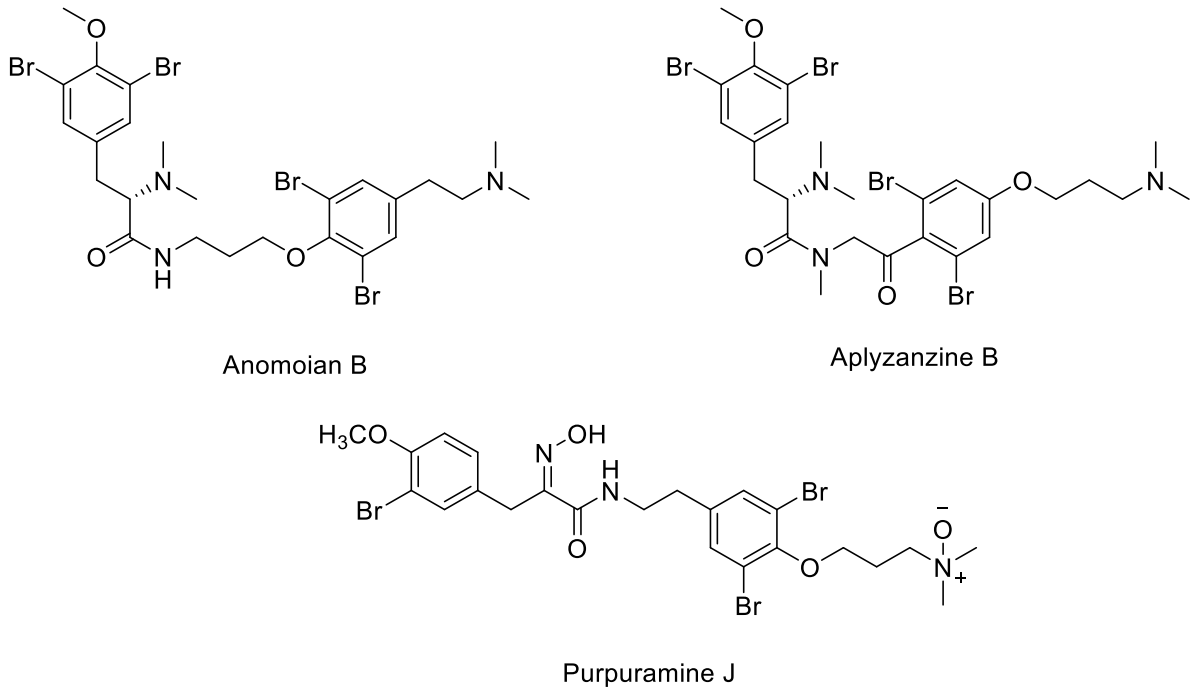

Figure 6 Structure of bioactive bromotyrosine MNPs.[27, 28]

1.5.1.2. Tryptophan derived alkaloids

1.5.1.2.1. Indole Alkaloids

The basic indole unit, the defining characteristic this family of alkaloids comes from L-tryptophan, an aromatic amino acid that in animals is usually derived through diet or via symbiotic bacteria.[24, 29] In the case of plants the shikimate pathway produces this amino acid.[24]

N-3′-Ethylaplysinopsin is an indole alkaloid isolated from Jamaican sponge *Smenospongia aurea* (Figure 7).[30, 31] It has been found that this MNP has high affinity for receptors 5-HT_{2A} and 5-HT_{2C} that mediate the effects of many compounds that act on diseases like depression, schizophrenia, dysthymia and neuro-endocrine functions.[31]

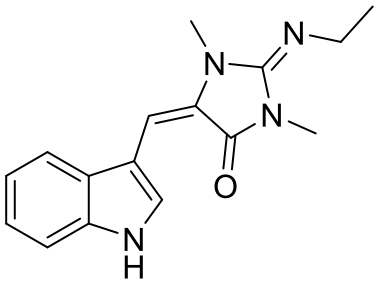

Figure 7 Structure of *N*-3′-Ethylaplysinopsin from *Smenospongia aurea*.[31]

Indole alkaloids also include bisindole and trisindole alkaloids which can be highly bioactive. Dragmacidin G and H are bisindole alkaloids from sponge *Lipastrotheya* sp. that have shown significant cytotoxic activity against HeLa cells (Figure 8).[32]

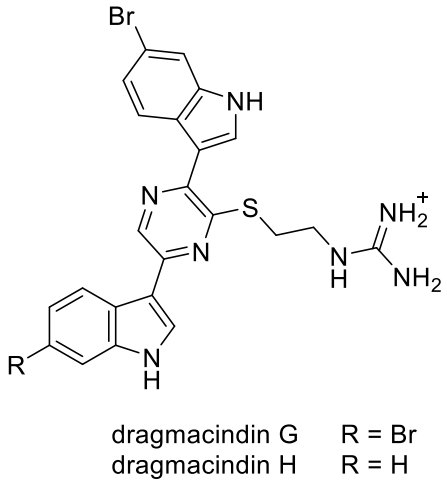

Figure 8 Structures of dragmacidin G and H from a from *Lipastrotheya* sp. Sponge.[32]

1.5.1.2.2. Quinoline alkaloids

This tryptophan derived alkaloid is based on the conversion of tryptophan to kynurenine and subsequently to kynurenic acid, the base structure for these alkaloids (Figure 9).[33] Due to losing the indole group, it is less obvious this type of alkaloids are tryptophan derived.

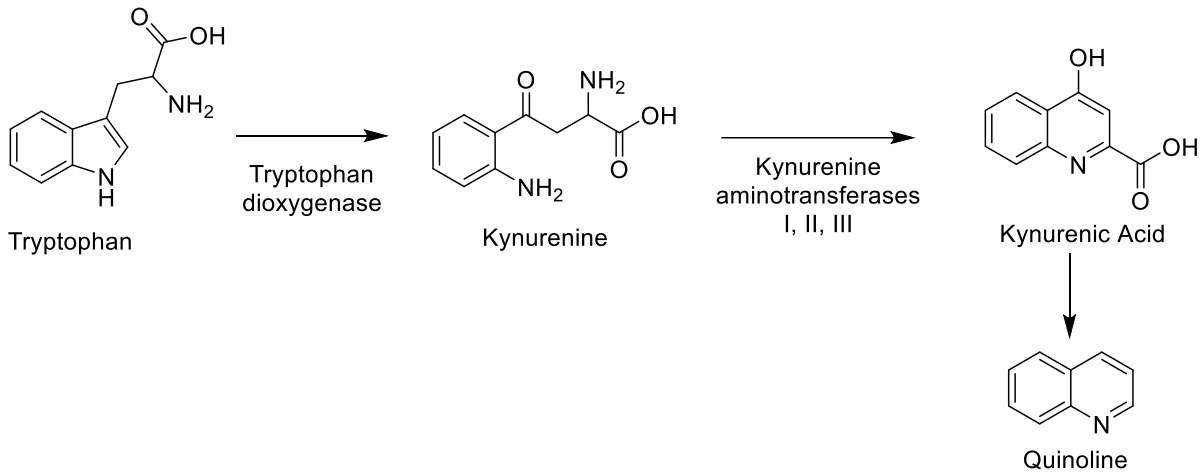

Figure 9 Quinoline pathway of tryptophan.[33]

4,5,8-trihydroxyquinoline-2-carboxylic acid is a MNP from the Antarctic sponge *Dendrilla membranosa* that has antimicrobial activity against *Staphylococcus aureus* (Figure 10).[34]

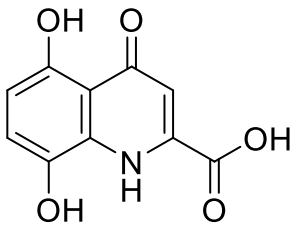

Figure 10 Structure of 4,5,8-trihydroxyquinoline-2-carboxylic acid from *Dendrilla membranosa*.[34]

1.5.1.3. Nicotinic acid derived alkaloids

1.5.1.3.1. Pyridine alkaloids

Nicotinic acid (vitamin B3/niacin) is the precursor to this family of alkaloids.[24] Animals obtain nicotinic acid via the degradation of L-tryptophan via the kynurenine pathway (Figure 11).[24, 35]

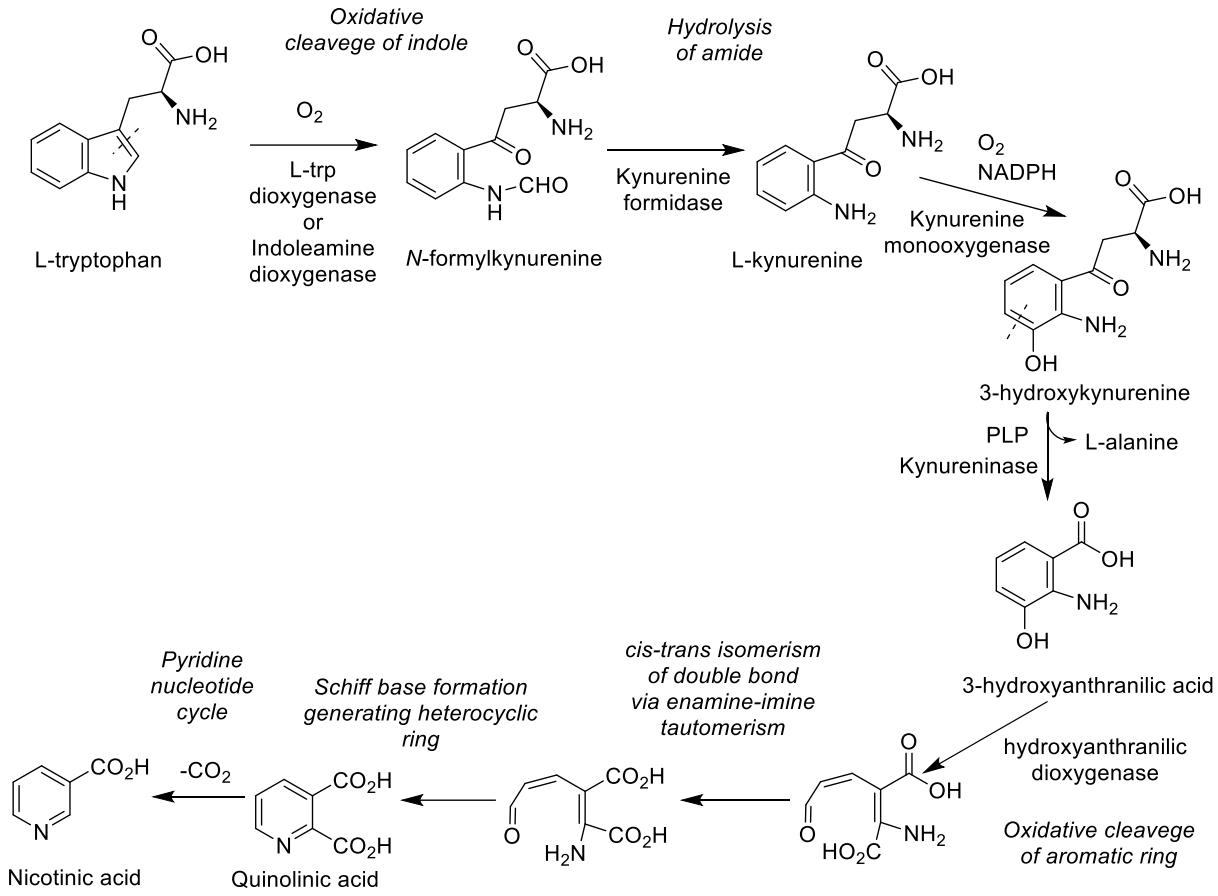

Figure 11 Biosynthesis of nicotinic acid via the kynurenine and 3-hydroxyanthranilic acid pathways.[24]

Like all MNPs such alkaloids have the potential for cytotoxicity, examples include the bis-pyridine alkaloids pyrinodemins B-D (Figure 12), from the Okinawa sponge *Amphimedon* sp.[36] Okinawa is an area known for its biodiversity and nitrogen containing MNPs with bioactivities against various diseases.[36] These compounds demonstrate high cytotoxic activity against murine leukemia cell line L1210.[36]

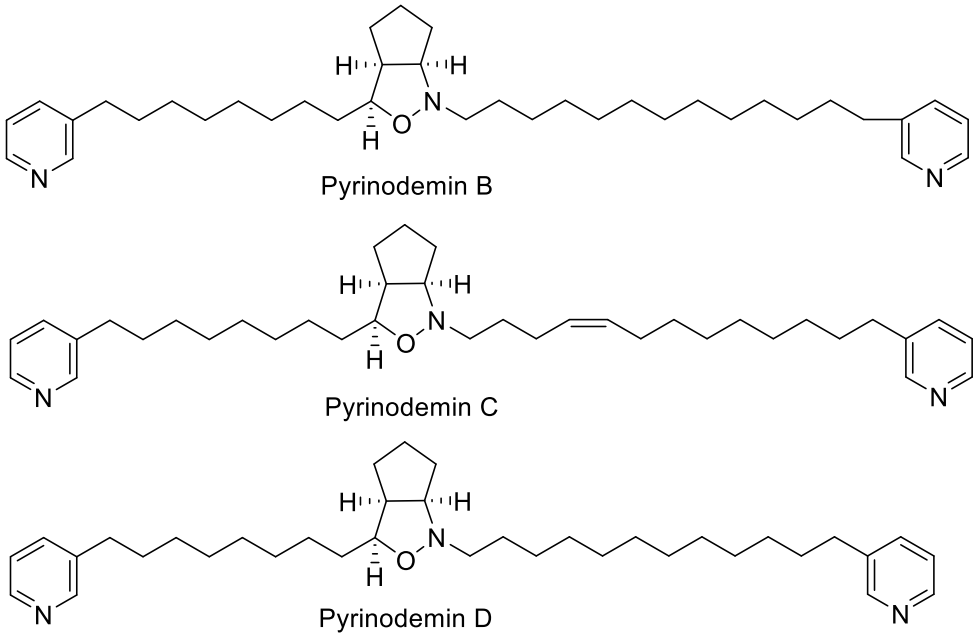

Figure 12 Structures of pyrinodemins B-D from *Amphimedon sp*.[36]

1.5.1.3.2. 3-alkyl piperidine alkaloids

These alkaloids are highly prelevant in sponges of the order Haplosclerida, mainly from the genus *Haliclona*.[37] Neopetrosiamine A is one such compound from the sponge *Neopetrosia proxima* of the order Haplosclerida collected from Mona Island in Puerto Rico (Figure 13).[38, 39] It has shown cytotoxic activity against melanoma, leukemia and breast cancer cell lines. However, it has also displayed activity against *Mycobacterium tuberculosis* and *Plasmodium falciparum*.[38]

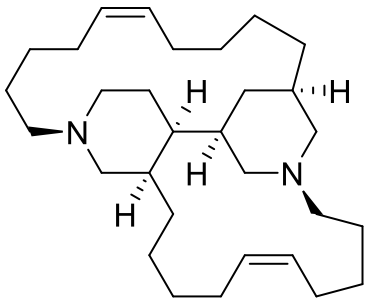

Figure 13 Structure of neopetrosiamine A from *Neopetrosi proxima.*[38]

1.5.2. Alkaloids derived from non-aromatic amino acids

1.5.2.1. Piperidine alkaloids

Lysine is a precursor of the ring piperidine, a C5N building block to this family of alkaloids.[24] The biosynthesis of piperidine involves the loss of a carboxyl group followed by the loss of the α-amino nitrogen, resulting in the formation of the imine piperideine and finally a reduction to form piperidine (Figure 14).[24, 40]

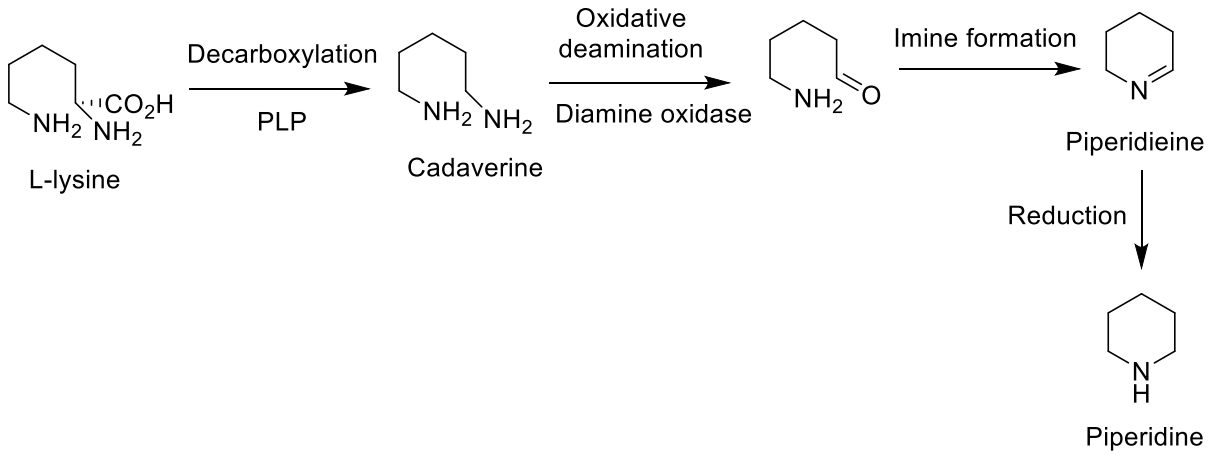

Figure 14 Biosynthetic pathway of piperidine from L-lysine.[40]

One MNP containing this feature is calyxamine B extracted from Puerto Rican sea sponge *Calyx podatypa* (Figure 15).[41] In more recent times, calyxamine B has been studied for acetylcholinesterase inhibition. It has been found that this MNP is a potent acetylcholinesterase inhibitor, with better IC_{50} than Ferulic acid.[42]

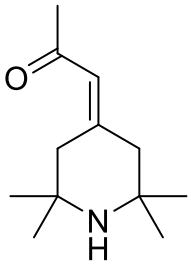

Figure 15 Structure of calyxamine B from Puerto Rican sponge *Calyx podatypa*.[41]

1.5.2.2. Pyrrole aminoimidazole alkaloids

These alkaloids are derived from the precursor oroidin and are known as downstream events (alkaloids whose precursor is oroidin). Such Alkaloids are known and accepted in the scientific community.[43] However, the upstream events or the biosynthetic

pathway to obtain oroidin are undefined. Using radiolabelling, it was found that proline and lysine are precursors to oroidin and a proposed biosynthetic pathway is given by Gregory Genta-Jouve et al. (Figure 16).[43]

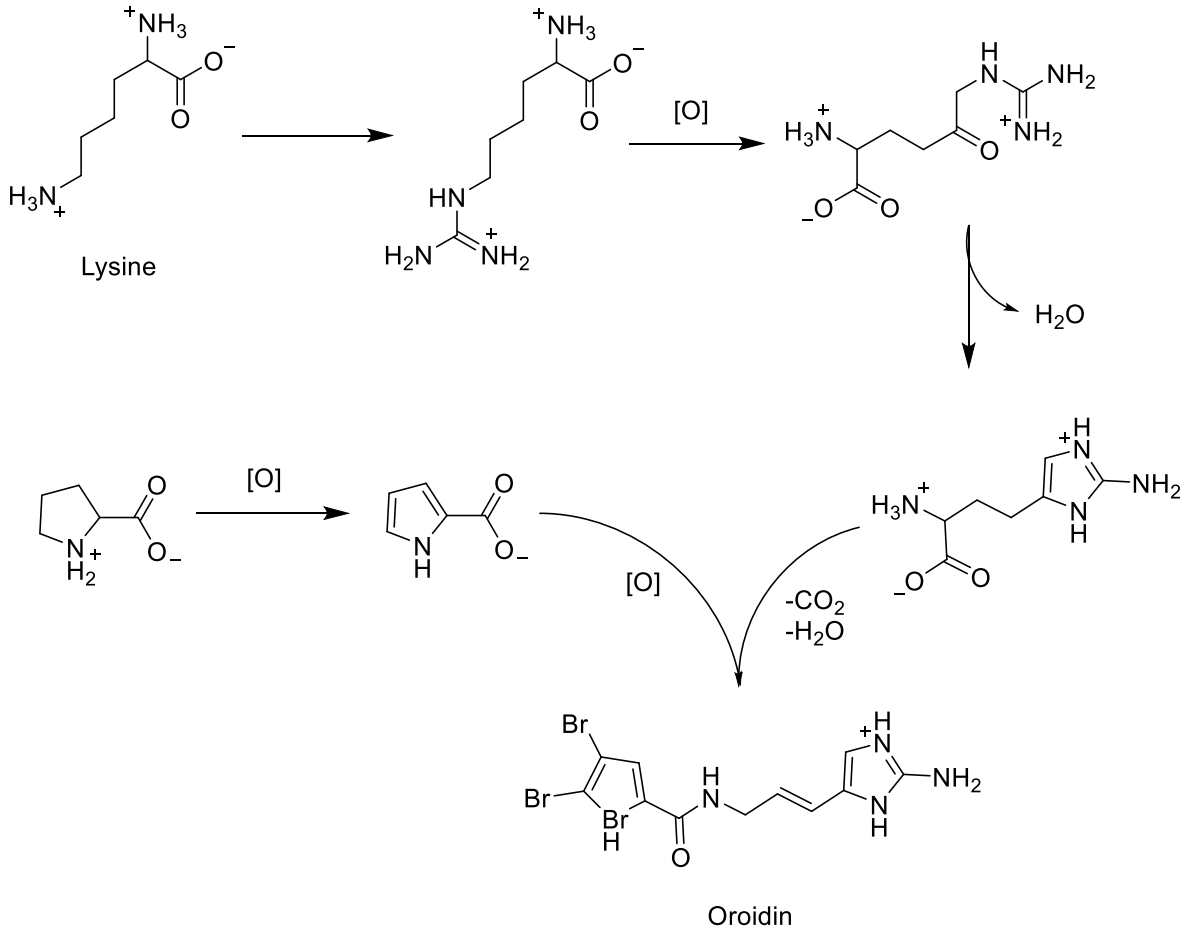

Figure 16 Proposed biosynthetic pathway of Oroidin.[43]

One such marine alkaloid is dispacamide A from Caribbean marine sponge *Agelas* dispar (Figure 17). This compound resulted in antihistamine activity against guinea pig ileum.[44, 45]

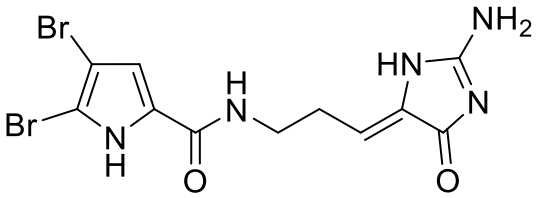

Figure 17 Structure of dispacamide A from Caribbean sponge *Agelas* dispar

1.5.2.3. Ornithine/Arginine derived cyclic guanidine alkaloids

The family Crambeidae of sponges is known to produce cyclic guanidine alkaloids.[46] The original hypothesis for the biosynthesis of these compounds by Snider et al. suggests a full polyketide origin for these compounds along with a late condensation reaction to add the guanidine group to the carbon backbone.[46, 47] However, a new hypothesis suggests a biosynthetic pathway of mixed origins where the amino acid L-arginine is the precursor for such alkaloids. The C4-guanidine unit forms a guanidinopyrrolinium which is used as a building block for this family of alkaloids.[46] This occurs via oxidative deamination, decarboxylation and cyclization of agmatine or 2-oxoarginine which are derived from arginine (Figure 18).[46, 48]

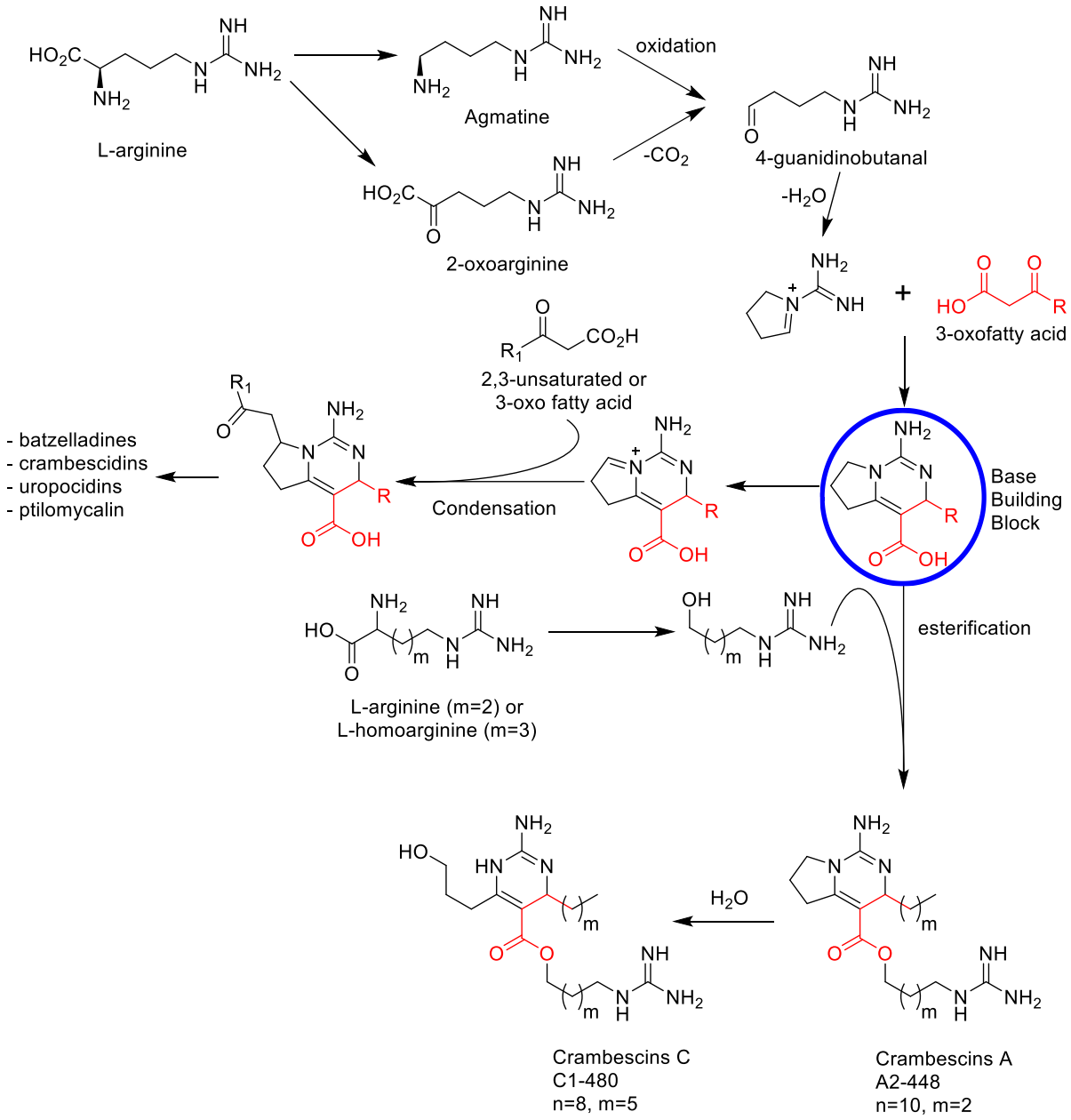

Figure 18 Amino acid based biosynthetic pathway hypothesis of cyclic guanidine alkaloids from marine sponges.[46]

Base Building block for suck alkaloids highlighted in blue.

Batzelladine A was isolated from Caribbean sponge *Batzella* sp. and proved to be a potent inhibitor of HIV (Figure 19).[49] Crambescin A2 and Crambescidin 800 were isolated from Mediterranean sponge *Crambe crambe* (Figure 19).[50, 51] Crambescidin 800 has been shown to exhibit cytotoxic activity against murine leukemia L1210 cell lines and also proves to be an inhibitor against *Herpes simplex* virus (HSV-1).[51] Crambescin A2-448 has not yet undergone bioassay screening however, crambescins A2 as a whole are known to exhibit antitumor and antimicrobial characteristics.[52]

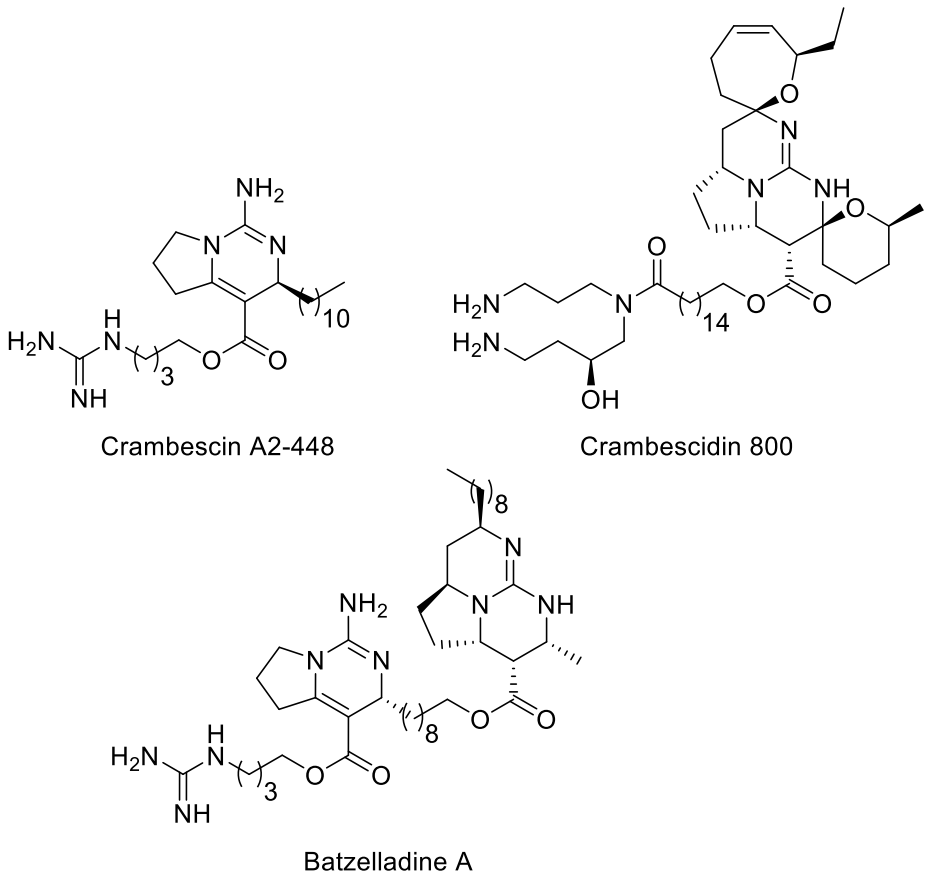

Figure 19 Structures of bioactive cyclic guanidine alkaloids.[46]

1.5.2.4. Polyamine alkaloids

Poly- as a prefix in chemical nomenclature is used to show multiple characteristics present in a molecules, in the case of polyamine alkaloids this denotes the presence of at least two amino groups that are part of a hydrocarbon chain.[53] These amino groups are separated by three or four methylenes and very rarely by two or five.[53] The adjacency of two or more nitrogen atoms in their chemical structure, result in polyamines having chemical reactivities different from monoamine compounds.[53] Ianthelliformisamine A is a polyamine from marine sponge *Suberea ianthelliformis* has shown antibiotic activity against *Pseudomonas aerguginosa* (Figure 20).[54, 55] Macrocyclic polyamines can also be seen such as motuporamines A-C isolated from marine sponge *Xestospongia exigua*, that present moderate cytotoxic activity.[55, 56]

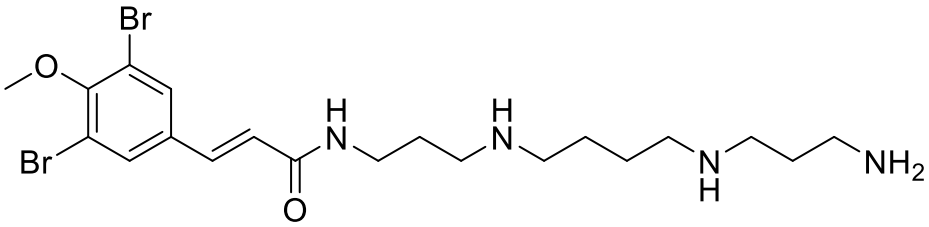

Ianthelliformisamine A

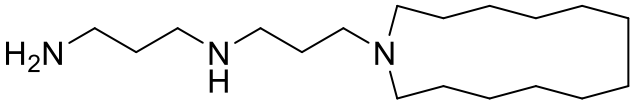

Motuproamine A

Figure 20 Structures of polyamines Ianthelliformisamine A and motuporamine A.[54, 56]

2. Marine Alkaloids from the Haplosclerida sponge sample MB NUIG 361

2.1. Preliminary screening and fractionation

The sponge sample was collected in the coral triangle in PNG and presented visual characteristics like vibrant orange colouring and the presence of a dead zone around it which seemed to stop the growth of coral. After a solid phase extraction (SPE), fractions 2 (H_2O:MeOH) and 3 (MeOH) underwent chemical analysis via mass spectrometry (MS). Furthermore, cytotoxicity screening was done by colleague Francesco Bertoni in Switzerland. Cytotoxicity screening showed activity against lymphoma cell lines OCILY10 and TMD8 resulting in their death. A control of CB33 human primary was also assayed and resulted in a reduction in proliferation however, it did not result in their death. *Vacuum* liquid chromatography (VLC) was applied to the extract to obtain 5 fractions of decreasing polarities (Table 3).

Table 3 VLC fractions, naming, composition and mass

Name	Fraction Composition	Fraction mass (g)
F1	H_2O	0.315
F2	H_2O:MeOH (1:1)	0.346
F3	MeOH	0.301
F4	MeOH:DCM (1:1)	0.366
F5	DCM	0.080

The profile of F3 by HPLC-DAD coupled to an evaporative light scattering detector (ELSD) using a standard gradient showed the presence of rather polar compounds absorbing only slightly in UV (Table 4, Figure 21). This fraction was then subjected to semi-preparative HPLC using a reverse phase C18 column which resulted in 5 compounds, 4 known and 1 new, all of which are marine alkaloids certainly from the polyamine family (Table 5, Figure 22).

Table 4 HPLC-DAD-ELSD analytical conditions for F3 using H_2O and acetonitrile (ACN)

Time (min)	Flow mL/min	A H_2O	B ACN
0	1	90	10
2	1	90	10
14	1	0	100
21	1	0	100
23	1	90	10
25	1	90	10

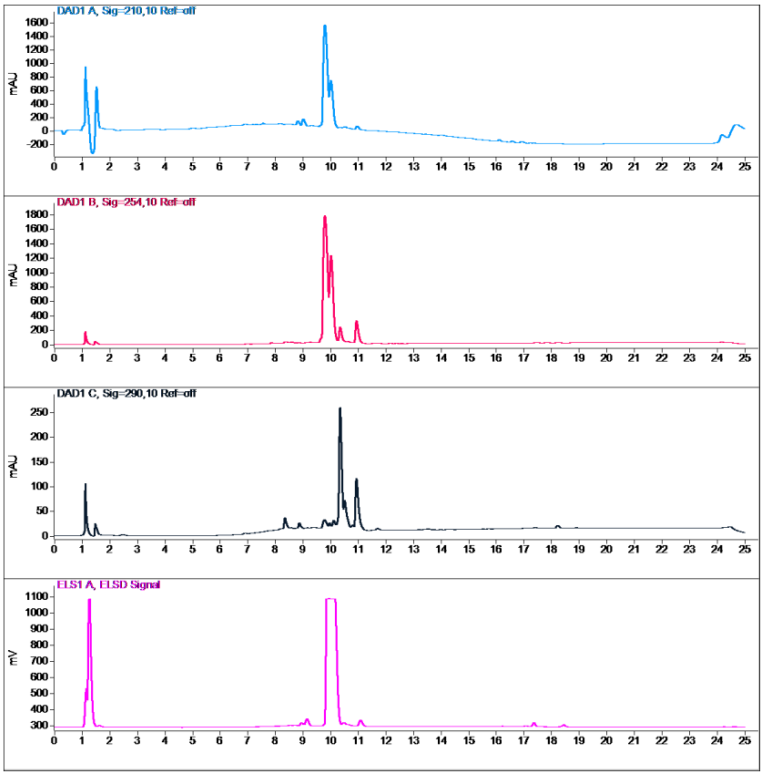

Figure 21 DAD (210 nm, 254 nm, 290 nm), ELSD and chromatograms for F3

Table 5 HPLC purification conditions for F3 using H_2O and ACN, both with 0.1% trifluoroacetic acid (TFA)

Time (min)	Flow mL/min	A H_2O+0.1% TFA	B ACN+0.1% TFA
0	3	70	30
5	3	70	30
30	3	50	50
40	3	50	50
41	3	70	30
42	3	70	30

Purified compounds include 6-epi-monanchorin (compound **1**) and monanchorin (compound **2**) which were compared to literature.[57] The major compounds purified are the known compounds papuamine (**3**) and haliclonadiamine (**4**).[58-60] Papuhydrazine (**5**) is a new minor compound structurally similar to **3** but with a new unique feature the hydrazine bond. Two further compounds were also pursued, however they presented low quality 1D and 2D NMR signals using different deuterated solvents which resulted in an inability to elucidate their respective structures.

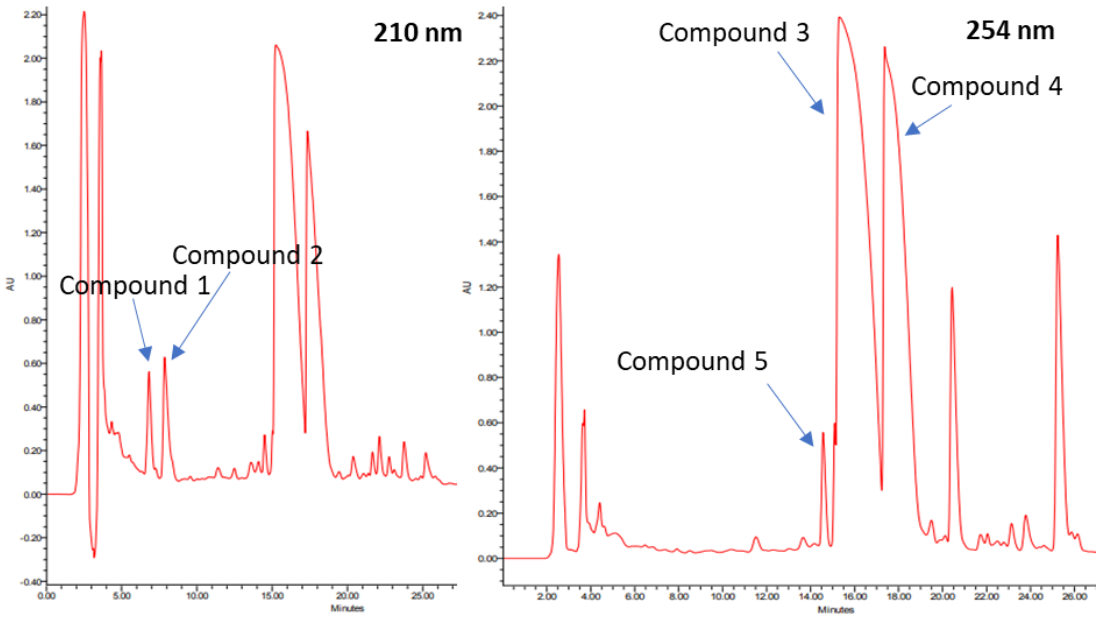

Figure 21 Chromatograms for F3 purification. 210 nm (left), 254 nm (right).

Table 6 Compounds ordered by mass obtained after purification.

Compound	Mass purified (mg)
Compound **1**	2.94
Compound **2**	1.71
Compound **3**	21.82
Compound **4**	10.70
Compound **5**	1.51

2.1.1. 6-epi-monanchorin

6-epi-monanchorin (**1)** is known and has been previously isolated by Abdjul et al. (Figure 23), and was isolated as a solid white crystal.[57] NMR data were recorded in CD_3OD (SI Figure 5), and thereafter in DMSO-d_6 due to the low quality of previous spectra and for comparison to literature (Figure 25, Table 7). MS data were also acquired which resulted in a *m/z* $[M+H]^+$ of 212.1757 corresponding to $C_{11}H_{22}N_3O^+$ (Figure 24).

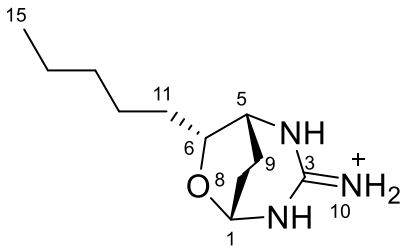

Figure 22 Structure of 6-epi-monanchorin (**1**)

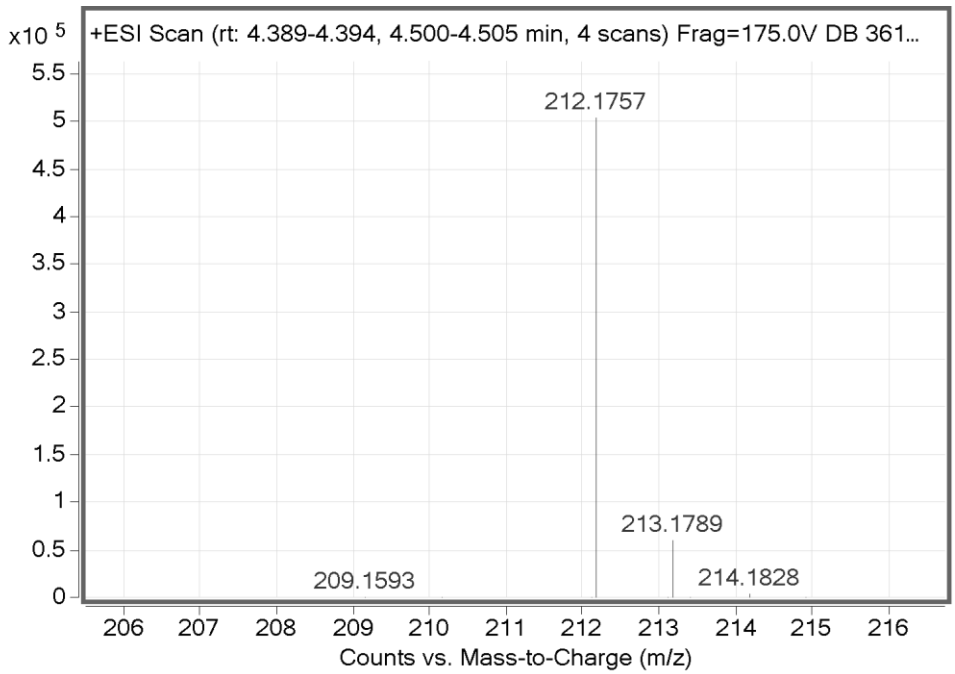

Figure 23 MS data for compound **1**

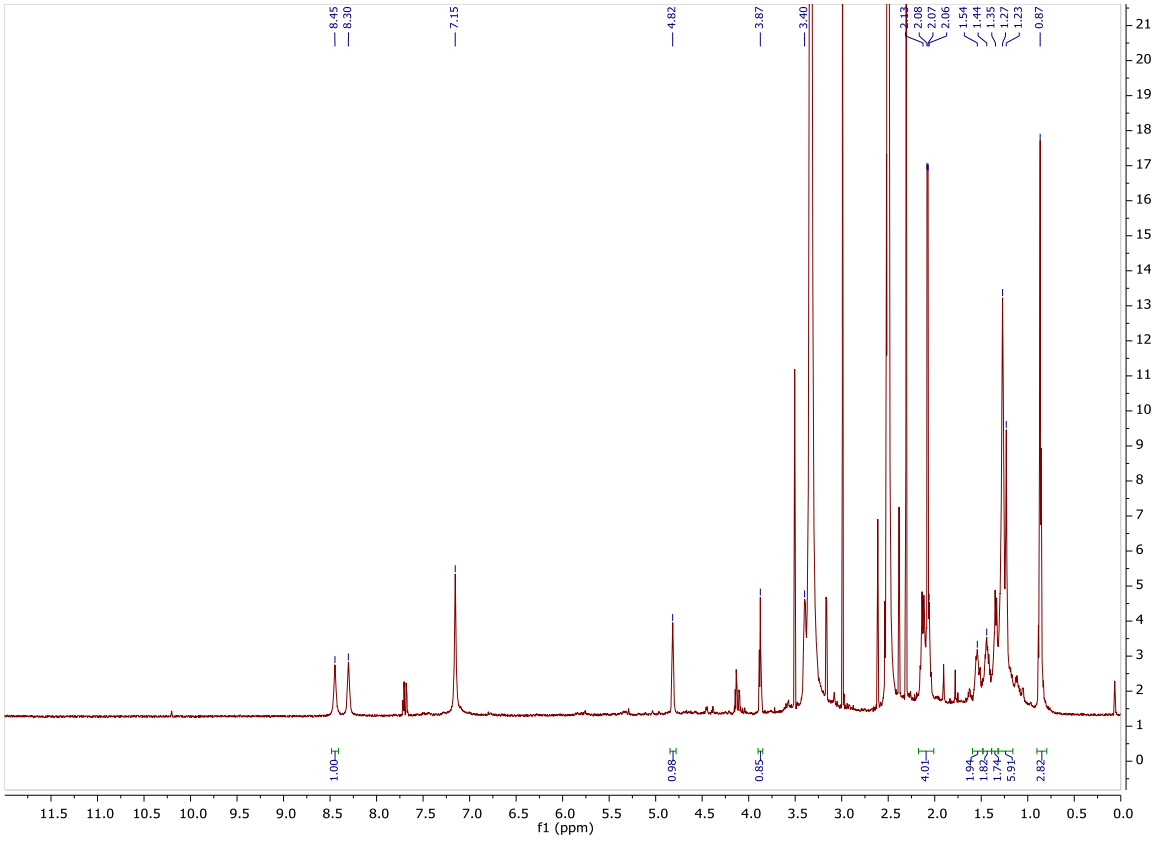

Figure 24 ^{1}H NMR (600 MHz, DMSO-d_6) of compound **1**

Table 7 ^{1}H NMR (600 MHz, DMSO-d_6) of compound **1** and **2** compared to literature ^{1}H NMR (400 MHz).

	δ_H mult. (*J* in Hz)			
No.	6-epi-monanchorin **(1)**	6-epi-monanchorin (Abdjul et al.)[57]	Monanchorin (**2**)	Monanchorin (Abdjul et al.)[57]
1	4.82 s	4.81 br s,	4.83 t (5.5)	4.82 br t (6)
2-NH	8.45 s	8.4 br s	8.57 s	8.68 br s
3	-	-	-	-
4-NH	8.30 s	8.25 br d (5.3)	8.43 s	8.56 br s
5	3.40 m	3.40 br s	3.30 m	3.28 m
6	3.87 s (6.5)	3.87 br t (6.5)	4.13 t (6)	4.13 br t (6.7)
7	-	-	-	-
8	2.06 m	2.04 m	1.83 m	1.86 m
	2.13 m	2.14 m	2.20 m	2.19 m
9	2.07 m	2.08 m	1.91 m	1.91 m
	2.08 m	2.10 m	2.03 m	2.02 m
10-NH_2	7.15 s	7.12 s	7.28 s	7.37 br t
11	1.44 m	1.43 m	1.46 m	1.45 m
	1.54 m	1.53 m	1.54 m	1.53 m
12	1.23 m	1.26 m	1.24 m	1.25 m
	1.35 m	1.36 m	1.37 m	1.35 m
13	1.23 m	1.26 m	1.24 m	1.24 m
14	1.23 m	1.26 m	1.24 m	1.24 m
15	0.87 m	0.86 t (6.8)	0.86 t (6.5)	0.85 t (6.6)

2.1.2. Monanchorin

Monanchorin (**2**) is known and has also been previously isolated by Abdjul et al. (Figure 26), and was isolated as a solid white crystal.[57] NMR data was collected in CD_3OD (SI Figures 6-10), and then in DMSO-d_6 due to the low quality of previous spectra and to compare to literature (Figure 28, Table 7). MS data was acquired which resulted in a *m/z* $[M+H]^+$ of 212.1757 corresponding to $C_{11}H_{22}N_3O^+$ (Figure 27).

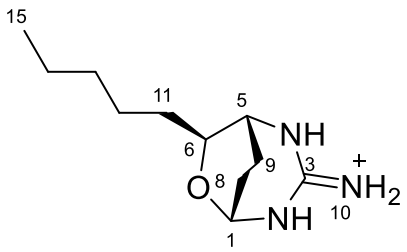

Figure 25 Structure of monanchorin (**2**)

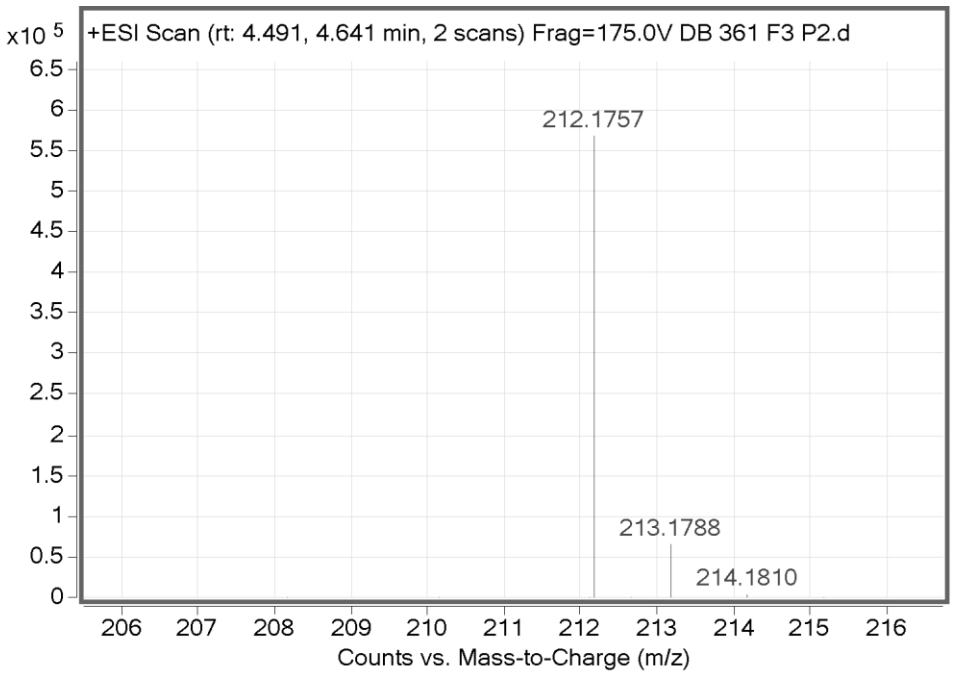

Figure 26 MS data for compound **2**

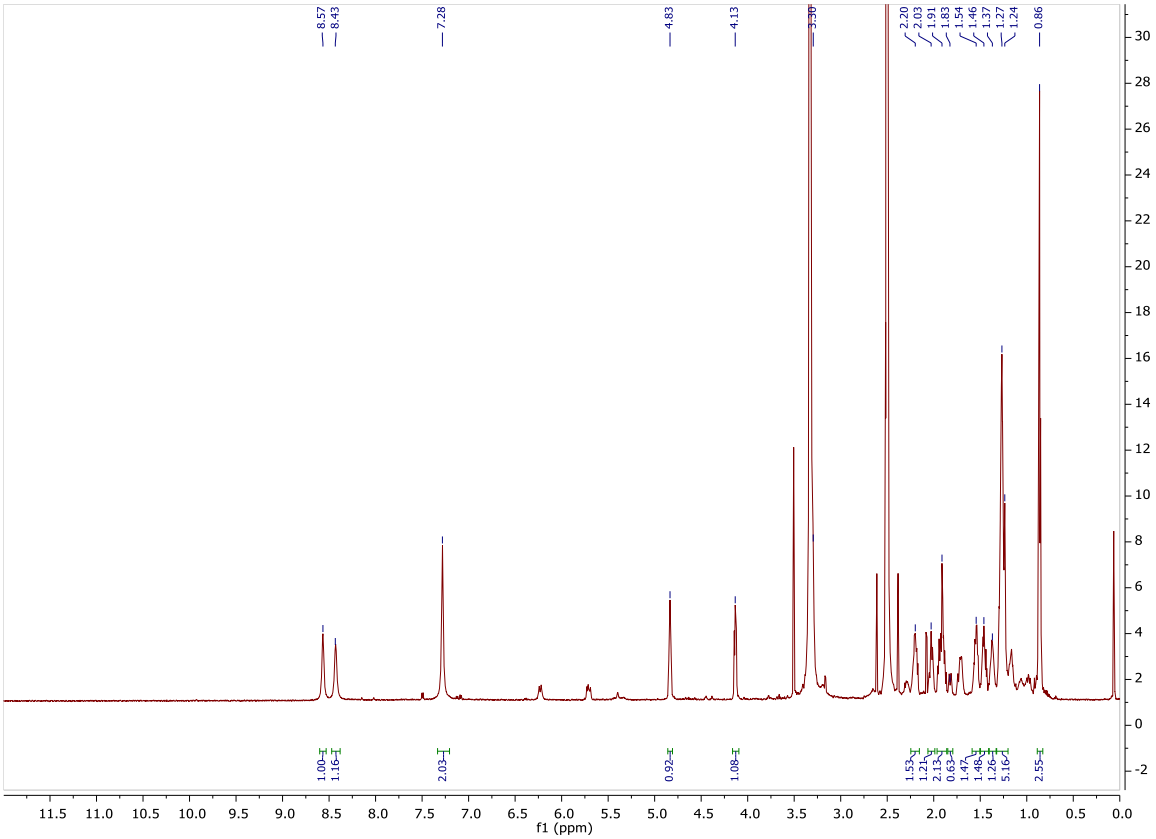

Figure 27 ^{1}H NMR (600 MHz, DMSO-d_6) for compound **2**

A full dataset was pursued in CD_3OD for compound **1** and **2** however, little compound was extracted and resulted in poor 2D NMR. For comparison to literature both **1** and **2** had their ^1H NMR done in DMSO-*d*6 too (Table7). A comparison with literature δ_H values in the ^1H NMR revealed high similarity between the two and with the MS as backup it was conclude that the compounds were previously isolated 6-epi-monanchorin (**1**) and monanchorin (**2**) (Table 7).[57]

2.2. Known papuamine and haliclonadiamine

2.2.1. Papuamine

Papuamine (**3**) is known and has been previously isolated by Bill Baker et al. from a sponge *Haliclona* sp. collected in PNG (Figure 30), and was isolated as a white solid crystal.[58] NMR data was recorded in CD_3OD (Figure 31, 32) and DMSO-d_6 (SI Figures 11-20). MS data was acquired which resulted in a *m/z* $[M+H]^+$ of 369.3266 corresponding to the molecular formula $C_{25}H_{41}N_2^+$ (Figure 29). Polarimetry results are comparable to literature, $[\alpha]_D^{20}$ −148 (c 6.60 mg.mL^{-1}, CH_3OH).[58] An electronic circular dichroism (ECD) spectrum and a UV spectrum were also recorded (SI Figures 21,22)

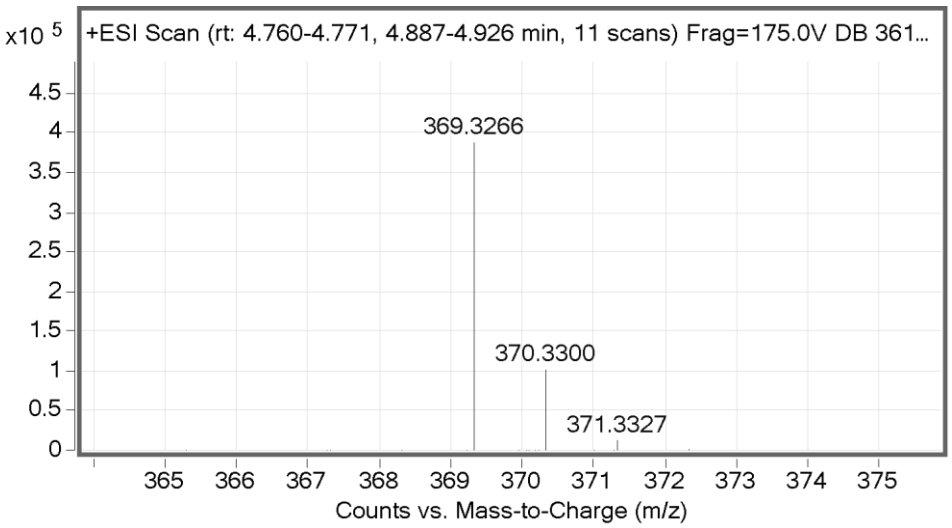

Figure 28 MS data for compound **3**

The ^{1}H NMR spectrum showed signals with integrations of value 2 (Figure 31). HSQC and HMBC data evidenced simultaneous ^1J and ^3J coupling occurring at δ_H 6.50 δ_C 136.1 meaning that C-16 and H-16 are correlated to their symmetric counterparts in H-17 and C-17 respectively (Figure 34). From this it was concluded that **3** is symmetric. Such symmetric MNPs are not very prevalent in nature. Here this gives the opportunity to study a symmetric compound and its non-symmetric analogues.

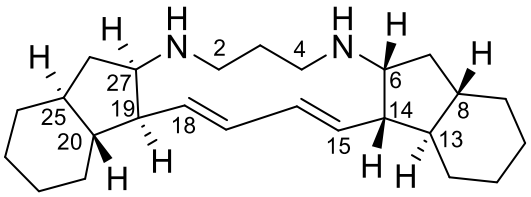

Figure 29 Structure of papuamine (**3**)

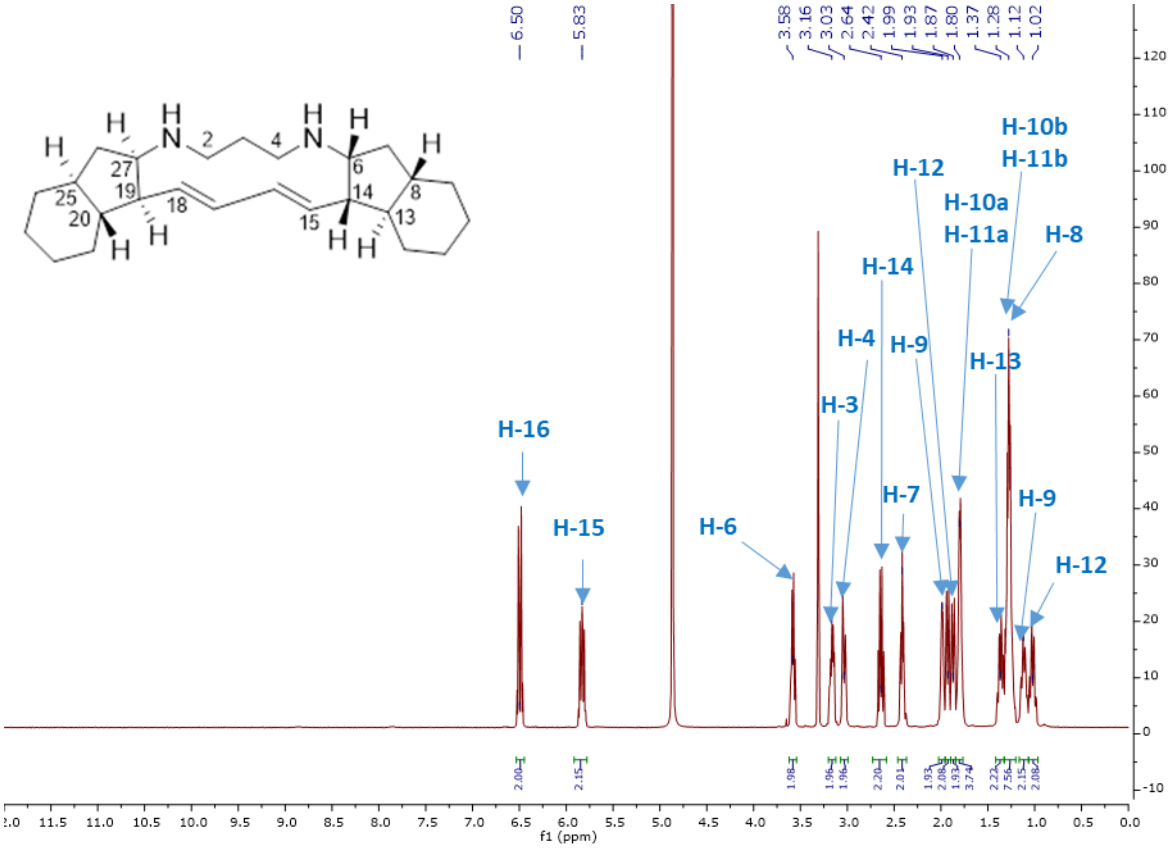

Figure 30 ^{1}H NMR (500 MHz, CD_3OD) of compound **3**

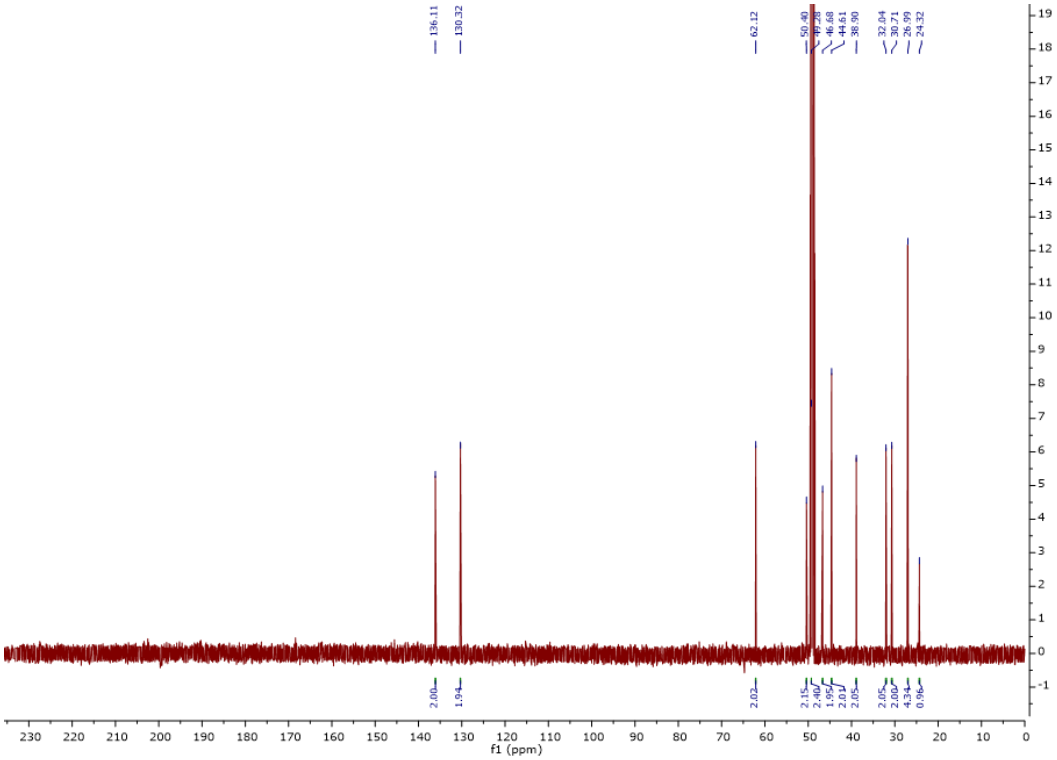

Figure 31 ^{13}C NMR (500 MHz, CD_3OD) of compound **3**

Another characteristic of **3** was the diene system δ_H 6.50, 5.83 in the s-*trans* conformation which was deduced by Hong-Bing Liu et al. *via* X-ray diffraction.[60] Using the COSY spectrum (Figure 33), two spin coupled systems were identified H-3/H-4 (SCS 1) and H-6/H-7 correlated to H-10/H-16 via COSY (SCS 2).

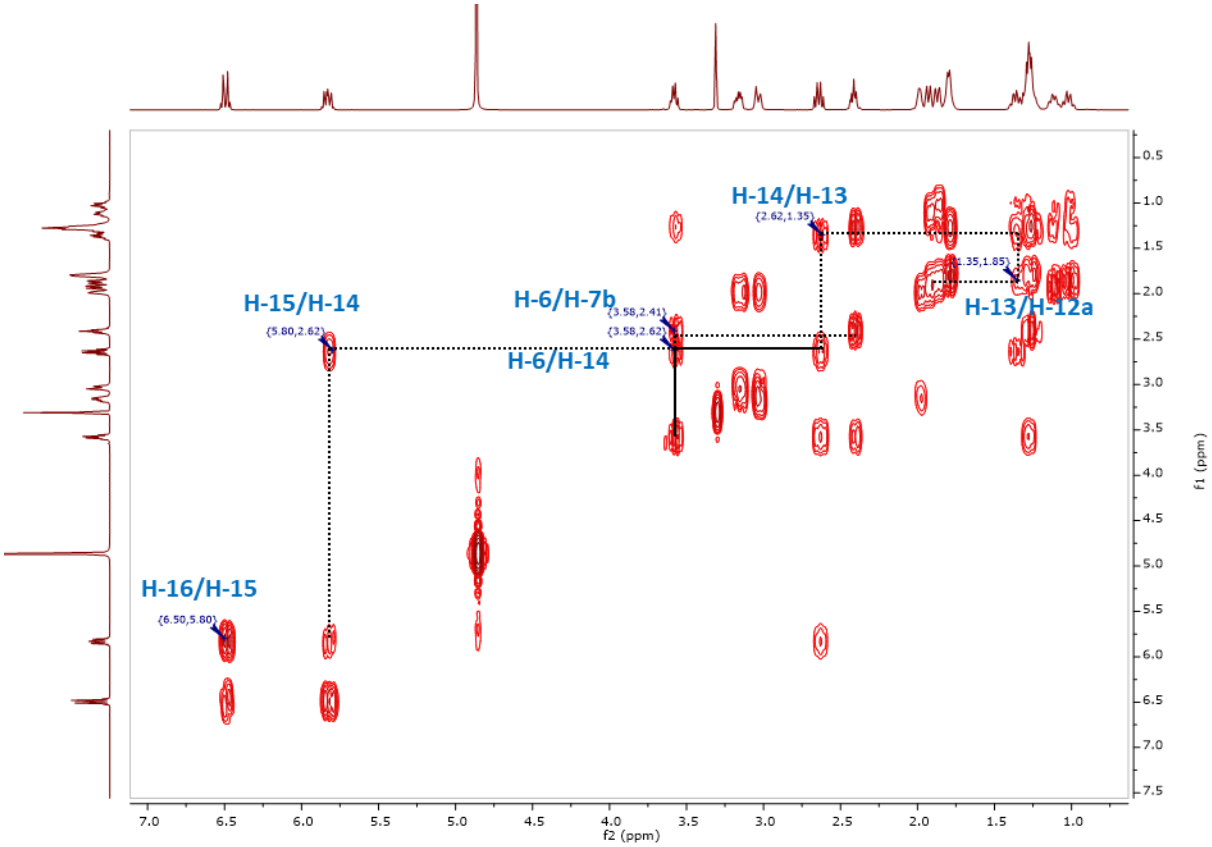

Figure 32 COSY spectrum (500 MHz, CD_3OD) of compound **3**. Showing SCS 2 key correlations.

Both SCS 1 and SCS 2 are connected which was seen *via* HMBC (Figure 34, 35) δ_H 3.16 (H-4) to δ_C 62.1 (C-6). Also using HMBC, a correlation was identified between δ_H 2.42 (H-7), 1.93 (H-9) and 1.87 (H-13) to δ_C 44.6 (C-6).

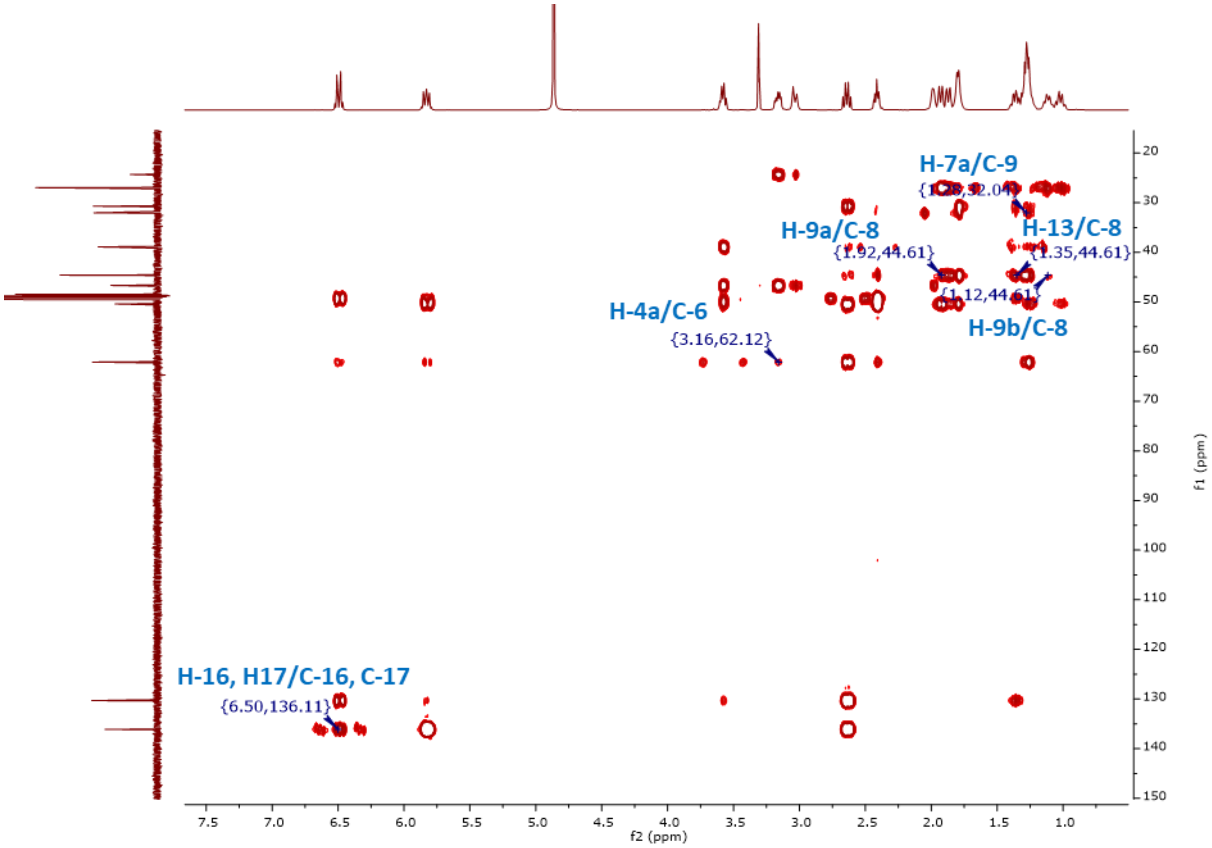

Figure 33 HMBC spectrum (500 MHz, CD_3OD) of compound **3**, highlighting key HMBC correlations

Finally, to complete the hydrindane ring δ_H 1.28 (H-9) was found to correlate with δ_C 27.0 (C-10) (Figure 35).

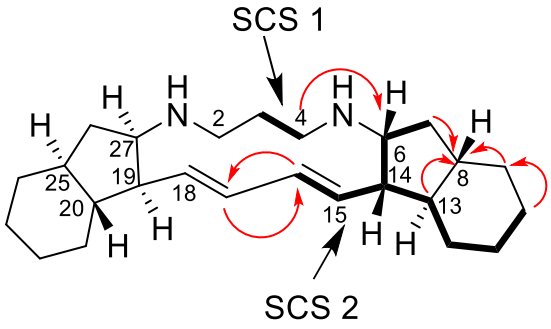

Figure 34 COSY and HMBC correlations in compound **3**

Table 8 ^{1}H (500 MHz) and ^{13}C (125 MHz) NMR data in CD_3OD for Compound **3**. Comparison to literature.[58]

No.	Papuamine (**3**)		Papuamine (Baker et al.)[58]
	δ_H, mult. (*J* in Hz)	δ_C mult.	δ_H mult. (*J* in Hz)
2a/4a	3.03 m	24.3 CH_2	2.98 br dt (3, 10.6)
2b/4b	3.16 m		3.19 br ddd (13.5)
3	1.99 s	46.7 CH_2	2.00 m
6/27	3.58 q (7.5, 8, 8.5)	62.1 CH	3.55 br ddd (8.2, 8.8)
7a/26a	1.28 m	38.9 CH	1.1-1.3 m
7b/26b	2.42 m		2.41 ddd (4.8, 8.8, 12)
8/25	1.28 m	44.6 CH	1.1-1.3 m
9a/24a	1.93 d (11)	32.0 CH_2	1.6-1.9 m
9b/24b	1.13 m		1.1-1.3 m
10a/23a	1.80 s	27.0 CH_2	1.6-1.9 m
10b/23b	1.28 m		1.1-1.3m
11a/22a	1.80 s	27.0 CH_2	1.6-1.9 m
11b/22b	1.28 m		1.1-1.3 m
12a/21a	1.87 d (13)	30.7 CH_2	1.6-1.9 m
12b/21b	1.02 q (3, 12)		1.00 ddd (3, 10.2, 12.6)
13/20	1.37 q (11)	50.4 CH	1.40 dddd (10.6)
14/19	2.64 q (9, 11)	49.3 CH	2.63 br ddd (9.3 10.6)
15/18	5.83 dt (11)	130.3 CH	5.89 dd (8.3, 15.8)
16/17	6.50 dt (15)	136.1 CH	6.50 dd (10.5, 15.8)

2.2.2. Haliclonadiamine

Compound **4** is also known and has been previously isolated by Eoin Fahy et al. from a sponge *Haliclona* sp. collected in Palau (Figure 37). It was isolated as a solid white crystalline substance like compound **3**. NMR data were collected in CD_3OD (SI Figures 31-33), $CDCl_3$ (SI Figures 34, 35) for comparison with literature and DMSO-d_6 (SI Figures 23-30). MS data was acquired which resulted in a *m/z* $[M+H]^+$ of 369.3265 corresponding to $C_{25}H_{41}N_2^+$ (Figure 36). Polarimetry results are comparable to literature $[\alpha]_D^{20}$ −17 (c 2.92 mg.mL^{-1}, CH_3OH).[59] The ECD and UV spectra were also obtained for this compound (SI Figures 36, 37). It was found by Eoin Fahy et al., the compound is similar to compound **3** however, initially in 1988 they established the difference to be one change at one chiral centre which results in a non-symmetric structure.[59] However, Hong-Bing Liu et al., through x-ray crystallography revised the structure of **4** and demonstrated that the change is not at one chiral centre only.[60] They

concluded that all but one chiral centre out of the 8 remained similar to papuamine that being the hydrogen at position (H-6).[60]

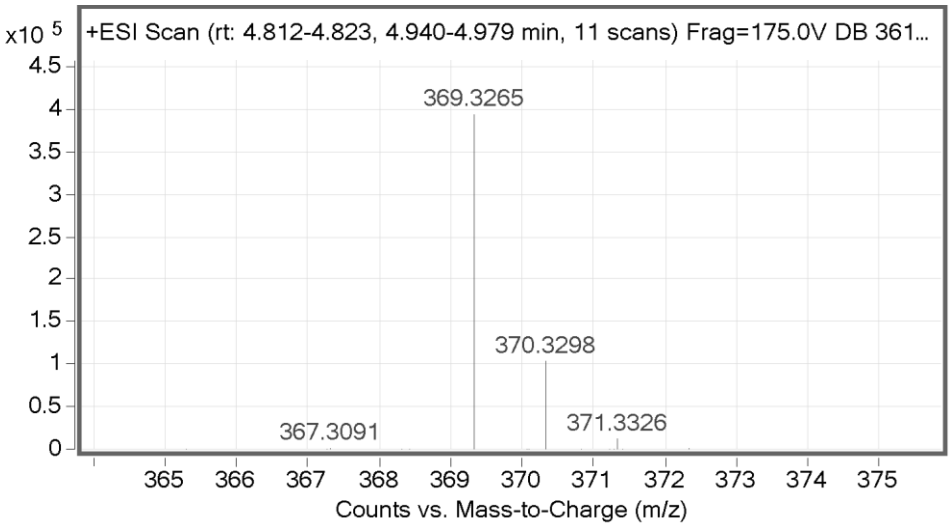

Figure 35 MS data for compound **4**

The loss of symmetry could be seen in the ^{13}C NMR spectrum with the increase in signals from 12 in compound **3** to 26 signals in compound **4** (Figure 39, Table 9). However, it is important to notice that the ^{1}H NMR signals in CD_3OD of the diene system δ_H 6.47 (H) 5.66 (H) are still overlapping (Figure 38). In DMSO-d_6 these olefinic signals were shown to be separate, and each unique proton signal could be seen (Figure 38).

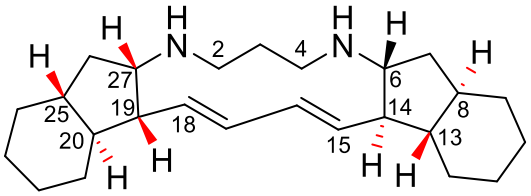

Figure 36 Structure of haliclonadiamine (**4**). In red are differences observed between compound **3** and **4**.

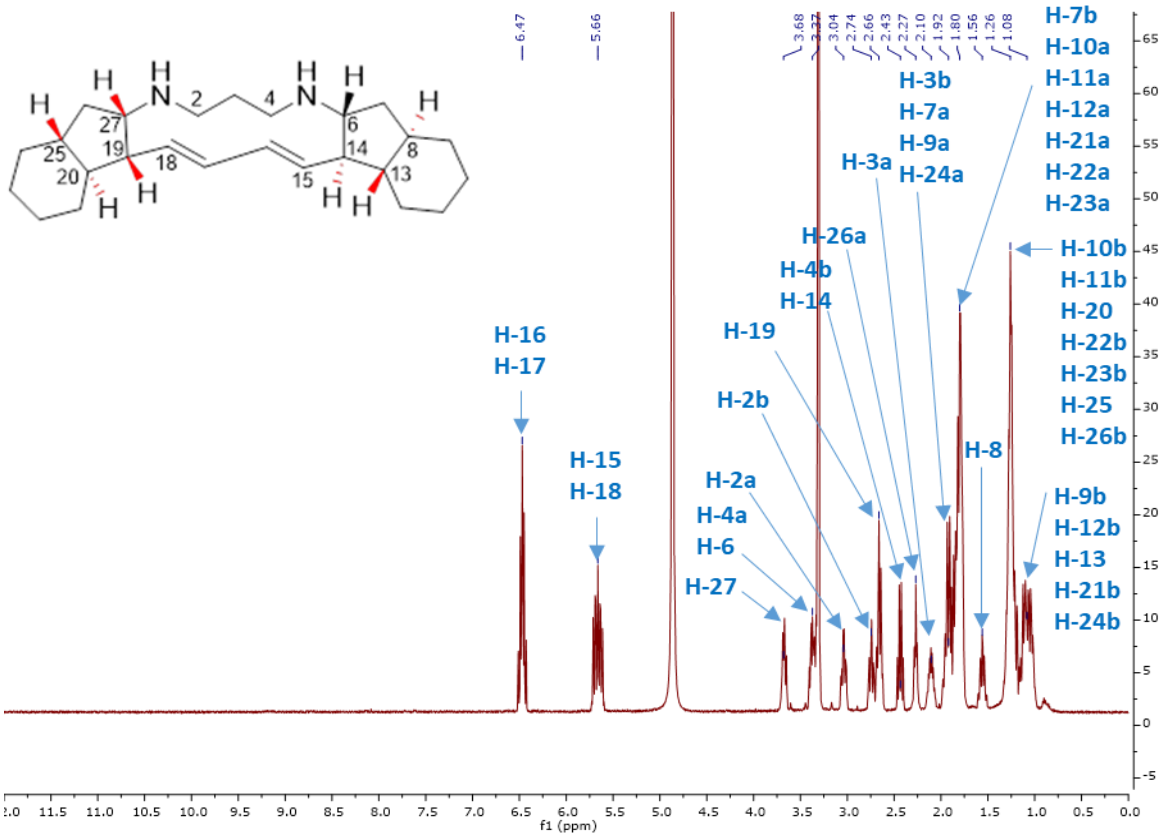

Figure 37 ^{1}H NMR (500 MHz, CD_3OD) of compound **4**

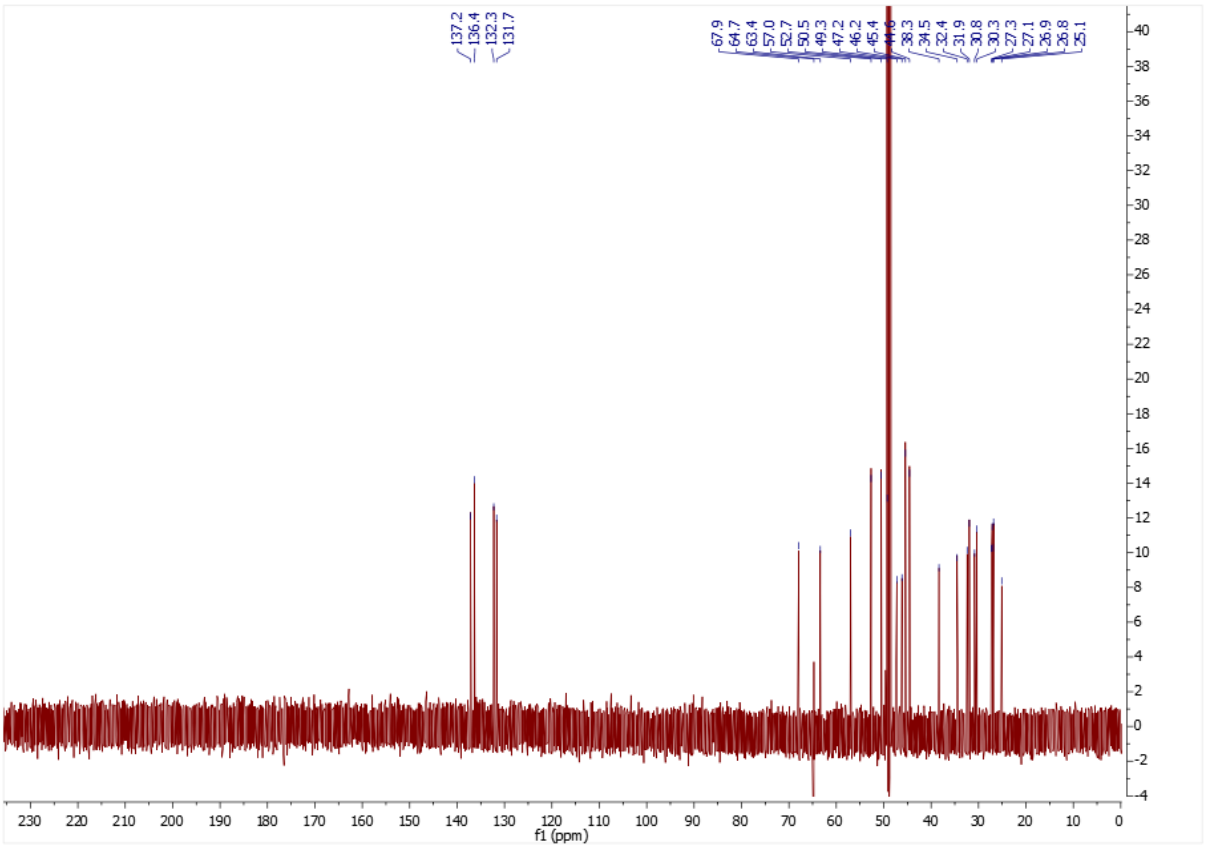

Figure 38 ^{13}C NMR (500 MHz, CD_3OD) of compound **4**

Table 9 ^{1}H (500 MHz) and ^{13}C (125 MHz) NMR data in CD_3OD for compound **3** and **4** for comparison.

No.	Haliclonadiamine (**4**)		No.	Papuamine (**3**)	
	δ_H mult. (*J* in Hz)	δ_C mult.		δ_H mult. (*J* in Hz)	δ_C mult.
1	-	-	-	-	-
2a	3.04 m	46.2 CH_2	-	-	-
2b	2.74 m		-	-	
3a	2.10 m	25.1 CH_2	3	1.99 s	46.7 CH_2
3b	1.92 m			-	-
4a	3.32 m	47.2 CH_2	2a/4a	3.03	24.3 CH_2
4b	2.66 m		2b/4b	3.16 m	
5	-	-	5	-	-
6	3.37 m	67.9 CH_2	6/27	3.58 q (7.5, 8, 8.5)	62.1 CH
7a	1.92 m	34.5 CH	7a/26a	1.28 m	38.9 CH
7b	1.80 m		7b/26b	2.42 m	
8	1.56 quin (10.5, 11)	45.4	8/25	1.28 m	44.6 CH
9a	1.87 m	32.4 CH_2	9/24	1.93 d (11)	32.0 CH_2
9b	1.08 m		9/24	1.13 m	
10a	1.80 m	26.8 CH_2	10a/23b	1.80 s	27.0 CH_2
10b	1.26 m		10b/23b	1.28 m	
11	1.80 m	27.3 CH_2	11a/22a	1.80 s	27.0 CH_2
11b	1.26 m		11b/22b	1.28 m	
12a	1.80 m	30.3 CH_2	12a/21a	1.87 d (13)	30.7 CH_2
12b	1.05 m		12b/21b	1.02 q (3, 12)	
13	1.20 m	50.5 CH	13/20	1.37 q (11)	50.4 CH
14	2.43 q (10, 11)	57.0 CH	14/19	2.64 q (9, 11)	49.3 CH
15	5.66 m (15)	132.3 CH	15/18	5.83 dt (11)	130.3 CH
16	6.47 m (16.5)	136.4 CH	16/17	6.50 dt (15)	136.1 CH
17	6.47 m (16.5)	137.2 CH			
18	5.66 m (15)	131.7 CH			
19	2.66 m	49.3 CH			
20	1.26 m	52.7 CH			
21a	1.80 m	30.8 CH_2			
21b	1.08 m				
22a	1.80 m	27.1 CH_2			
22b	1.26 m				
23a	1.80 m	26.9 CH_2			
23b	1.25 m				
24a	1.92 m	31.9 CH2			
24b	1.08 m				
25	1.26 m	44.6 CH			
26a	2.27 m	38.3 CH_2			
26b	1.26 m				
27	3.68 m	63.4 CH			

2.3. New papuhydrazine: publication in preparation

Contributions:

Denis Besliu: Purification and structure elucidation.

Rebeca Alvarino, Amparo Alfonso, Luis M. Botana: Bioassays.

Maggie Reddy: Sponge taxonomy.

Olivier P. Thomas: Review and supervision.

2.3.1. Abstract

Following chemical screening of a sponge inventory collected from Papua New Guinea during the *Tara* Pacific expedition, using mass spectrometry and cytotoxicity bioassay screening, four known compounds, 6-epi-monanchorin (**1**), monanchorin (**2**), papuamine (**3**), haliclonadiamine (**4**), were isolated along with a new compound, a papuamine derivative, papuhydrazine (**5**) which is characterised by a hydrazine bond. Their structures were identified using Mass Spectrometry, NMR data and cross referencing with literature. Papuamine and haliclonadiamine are known to exhibit strong cytotoxic activity and this activity was compared to papuhydrazine.

2.3.2. Introduction

Papua New Guinea is part of the coral triangle and classified as a megadiverse region due to its high level of biodiversity and especially marine biodiversity. Much emphasis has been put on marine life in this region, but especially sponges due to their secondary metabolites which have been reported as having various biological activities from antibiotic to cytotoxic among others.[5, 11] A sponge specimen identified as haplosclerida was collected among other sponges and other cnidarians. It presented interesting visual characteristics: a dead zone where the growth of corals was halted was present around this sponge indicating the potential presence of ecotoxic metabolites being produced and its highly vibrant colouring which in a lot of species is a sign of toxin presence.

In this study, the isolation and structure elucidation of four known compounds: 6-epi-monanchorin (**1**), monanchorin (**2**), papuamine (**3**), haliclonadiamine (**4**), together with a new papuamine derivative named papuhydrazine (**5**) from this unidentified

haplosclerida sponge are reported (Figure 40). Their structures were identified using 1D and 2D NMR data in combination with MS data. Compound **3** was discovered in 1988 from a marine sponge *Haliclona* sp. collected in PNG and its structure elucidated with a unique 13-membered ring connecting two hydrindanes resulting in a symmetric compound, this is reflected in its ^{13}C NMR spectrum when compared to compound **4** which has lost that symmetry.[58] Compound **4** was also discovered in 1988 from a marine sponge *Haliclona* sp. collected in Palau. and its structure elucidated, similar to papuamine but losing its symmetry due to a change in the configuration of one or more chiral centers.[59] Initially, it was determined to be due to a change at one chiral centre at position C-8 however, haliclonadiamine had its structure revised and corrected by Hong-Bing Liu et al. where the chiroptical properties of the compound were analysed and its structure determined via X-ray diffraction.[59, 60] This showed a change in all but one chiral centre C-6, correcting the previous structure from 1988.[60] In 1996 a total synthesis has been elaborated and resulted in a synthetic papuamine that is identical in the ^{1}H NMR spectrum as natural papuamine.[61] Compounds **3** and **4** are known to be cytotoxic compounds when tested against Huh-7 hepatoma cell lines.[57] Papuamine has also been found to be cytotoxic against non-small cell lung cancer cells *in vitro* by inducing mitochondrial dysfunction, this type of effect on mitochondria is also demonstrated on MCF-7 breast cancer cells.[62, 63] However, a control of a normal human cell line was not used and this is required to confirm specificity towards cancer cells and in the advancement towards *in vivo* trials.[64] Both guanidine alkaloids **1** and **2** were isolated previously by Abdjul et al., with their bioactivity assayed, and showing no cytotoxic or antimicrobial activity. [57]

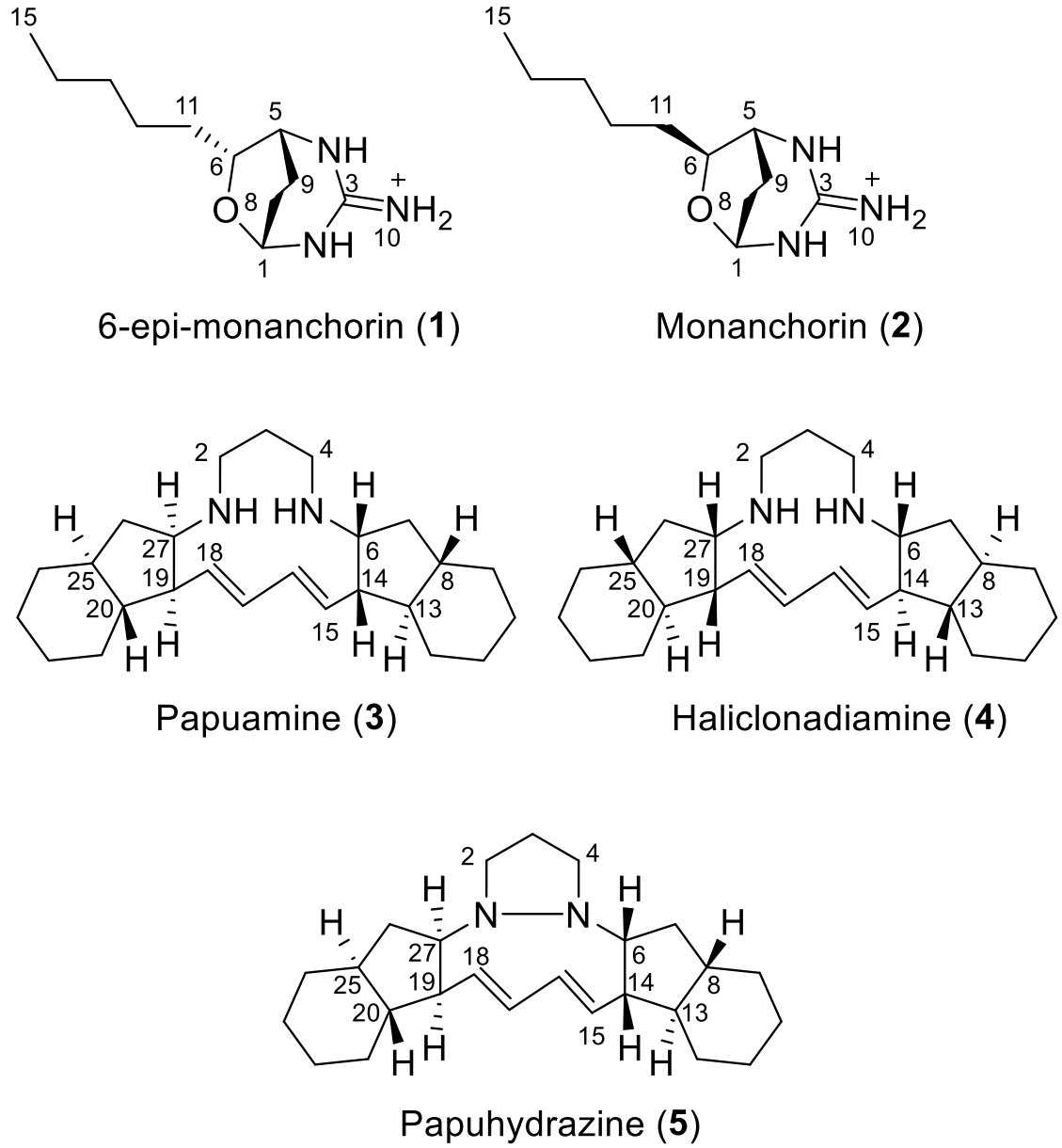

Figure 39 Structures of compounds **1**-**5** isolated from a haplosclerida sponge

2.3.3. Results and Discussion

Compound **5** was isolated as a white solid crystal. The molecular formula of **3** was identified as $C_{25}H_{38}N_2$ based on the molecular ion of *m/z* $[M+H]^+$ 367.3112 which meant the presence of an additional index of hydrogen deficiency (SI Figure 38). 1D and 2D NMR were performed in DMSO-d_6 (SI Figures 39-46). Polarimetry was also done on this compound: $[\alpha]_D^{20}$ −27 (c 0.26 mg.mL^{-1}, CH_3OH). ECD and UV spectra were recorded (SI Figures 47, 48). The lack of additional olefinic signals in the ^1H and ^{13}C NMR spectra for compound **5** meant that there was no additional unsaturation

compared to **3** and **4** leading to the presence of an additional cycle. With the same number of methines and methylenes, a hydrazine bond was proposed to be created between the two nitrogen atoms at positions N-1 and N-5. Symmetry for this compound was inferred from the ^{1}H and ^{13}C NMR spectra of **5** and comparison with those of **3**. To confirm the presence of the hydrazine bond, the NMR spectra of **3**, **4** and **5** was ran in DMSO-d_6. The ^{1}H NMR spectra of **3** and **4** showed two sets or four sets of exchangeable protons respectively (Figure 41), while no exchangeable proton was evidenced in the spectrum of **5** confirming the aforementioned hydrazine hypothesis.

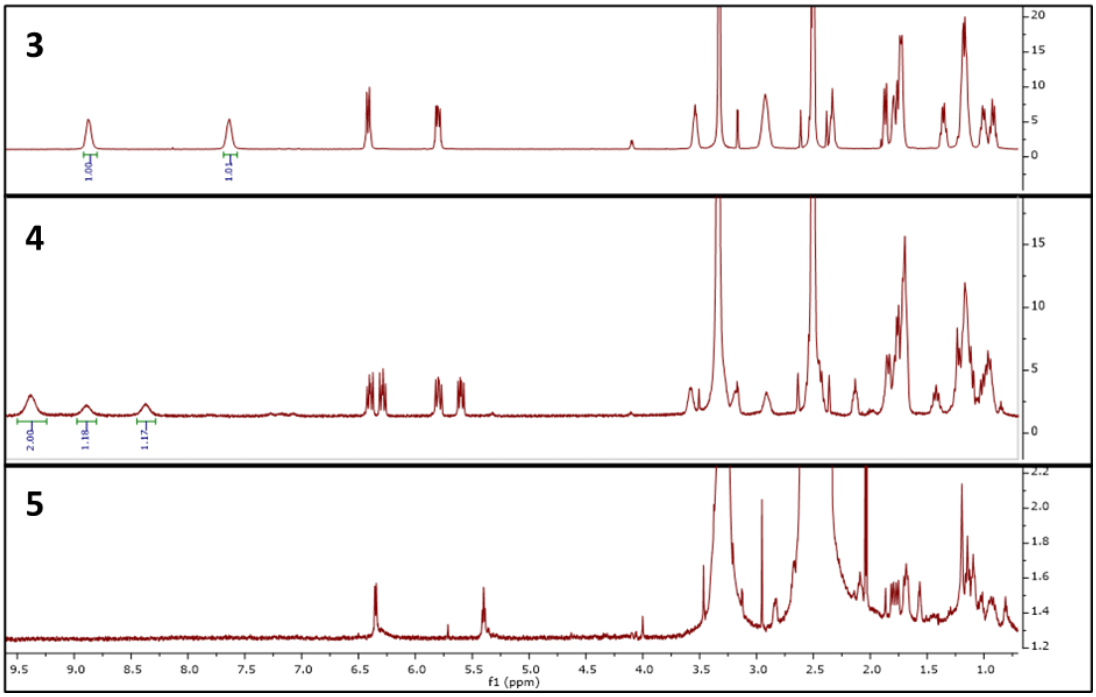

Figure 40 ^{1}H NMR comparison of compound **3, 5** (600 MHz, DMSO-d_6) and compound **4** (500 MHz, DMSO-d_6)

Using ^{1}H NMR, COSY, HSQC, HMBC all signals were assigned resulting in the elucidation of the structure for compound **5** which only slightly differs from the one of **3** (Figure 41, Table 10). Furthermore, 25 carbon atoms composed the molecule, most of the signals corresponding to two or four equivalent carbon atoms each due to the symmetry of **5,** with the exception of the signal at δ_C 21.51 (C-3). Two olefinic carbons are observed at δ_C 128.10, 131.94 (C-15, 16 and C-17, 18). For compound **5** the integration of H-3 has a value of 2, which also occurred in compound **3**. A diene system is present in both compounds, for **5** this is composed of 4 hydrogen atoms: H-15 and H-18 which are equivalent δ_H 5.40; H-16 and H-17 also being equivalent δ_H 6.35. Another difference between **3** and **5** could be seen in their olefinic coupling

constants, while **3** has δ_H 6.41 (14.8 Hz) 5.80 (10.7 Hz) compound **5** has δ_H 6.35 (8.5 Hz) 5.40 (7.9 Hz). These changes could be due to the strain between bonds that the extra hydrazine bond creates, shortening the ring system from being 13-membered to being 10-memebred, potentially resulting in the shift in coupling constant values. However, this requires further analysis to confirm because the coupling constant values can also indicate a transition from the E configuration to Z for the olefinic system.

Table 10 ^{1}H NMR for compound **3** (600 MHz, DMSO-d_6), **4** (500 MHz, DMSO-d_6), **5** (600 MHz, DMSO-d_6).

No.	**Papuamine (3)**		No.	**Haliclonadiamine (4)**		No.	**Papuhydrazine (5)**	
	δ_H mult. (*J* in Hz)	δ_C mult.		δ_H mult. (*J* in Hz)	δ_C mult.		δ_H mult. (*J* in Hz)	δ_C mult.
-	-	-	1	9.38 s	NH	-	-	-
-	-	-		8.37 s		-	-	-
-	-	-	2	3.18 m	45.3 CH_2	-	-	-
-	-	-		2.45 m		-	-	-
3	1.79 s	22.7 CH_2	3	1.79 m	33.3 CH_2	3	1.57 m	21.5 CH_2
4a	2.92 m	44.7 CH_2	4	2.91 m	44.4 CH_2	4	2.84 m	44.2 CH_2
4b	2.92 m			2.54 m			2.61 s	
5	8.88 s	NH	5	9.38 s	NH	5	-	-
	7.64 s			8.89 s			-	-
6	3.54 m	59.7 CH	6	3.58 m	61.0 CH	6	3.38 m	56.6 CH
7	1.15 m	37.4 CH	7	2.13 m	36.6 CH_2	7	2.09 m	29.7 CH_2
	2.33 m			1.23 m			1.03 m	
8	1.15 m	42.9 CH	8	1.42 quint. (10)	43.6 CH	8	1.09 m	42.1 CH
9	1.76 m	29.1 CH_2	9	1.79 m	30.9 CH_2	9	1.81 m	30.0 CH_2
	0.92 m			1.03 m			0.95 m	
10	1.73 m	25.6 CH_2	10	1.71 m	25.4 CH_2	10	1.68 m	24.9 CH_2
	1.17 m			1.17 m			1.14 m	
11	1.73 m	25.6 CH_2	11	1.71 m	25.8 CH_2	11	1.68 m	24.9 CH_2
	1.17 m			1.17 m			1.14 m	
12	1.87 m	30.8 CH_2	12	1.70 m	29.4 CH_2	12	1.75 m	29.0 CH_2
	1.01 m			0.94 m			0.92 m	
13	1.36 q (10)	47.2 CH	13	1.17 m	50.6 CH	13	1.09 m	49.5 CH
14	2.52 m	47.5 CH	14	2.54 m	47.4 CH	14	2.67 m	44.7 CH
15	5.80 dt (11)	128.3 CH	15	5.80 dd (5, 10)	131.1 CH	15	5.40 m (8)	131.9 CH
16	6.41 q (7.5, 14)	133.3 CH	16	6.40 dd (5, 10.5)	134.8 CH	16	6.35 t (8.5)	128.1 CH
			17	6.29 dd (5, 10.5)	134.4 CH			
			18	5.60 dd (5, 10)	131.0 CH			
			19	2.43 m	54.5 CH			
			20	1.12 m	48.6 CH			
			21	1.26 m	28.9 CH_2			
				0.94 m				
			22	1.71 m	25.7 CH_2			
				1.17 m				
			23	1.71 m	25.5 CH			
				1.17 m				
			24	1.84 m	30.6 CH			
				1.03 m				
			25	1.17 m	42.7 CH			
			26	-	-			
				-				
			27	3.29 m	65.14 CH			

Compounds **3** and **4** are known to be cytotoxic when tested against hepatoma cells, lung cancer cells and breast cancer cells. When the compounds were tested against neuroblastoma cell lines (SH-SY5Y) they showed cytotoxicity under 10 μM (Table 11, Figure 42, SI Figure 1). At a concentration between 1 mM and 10 mM the compounds showed some level of neuroprotective and antioxidant properties, resulting in reduced reactive oxygen species (ROS) levels and increased glutathione (GSH) levels when under oxidative stress conditions (SI figures 2, 3, 4). Control groups of normal cells were also tested unlike previous studies done on these compounds.

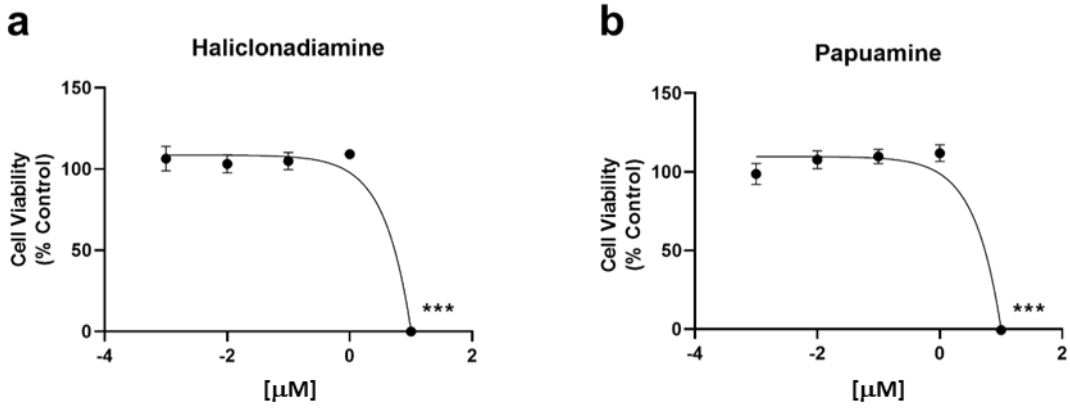

Figure 41 **Effect of haliclonadiamine and papuamine on cell viability in SHSY5Y cells**. Dose-response curves. Cells were treated with haliclonadiamine (a) and papuamine (b) at different concentrations (0.01, 0.1, 1, and 10 μM) for 6 hours. Cell viability was measured by MTT assay. The values are shown as the difference between control cells versus cells treated by ANOVA statistical analysis followed by post hoc Dunnet's t-test. ***$p < 0.001$. IC50 Haliclonadiamine: 3.69 μM [1.83-7.53] IC50 Papuamine: 3.83 μM [1.82-8.21]

Table 11 Compounds **3**-**5** cytotoxic activity in SH-SY5Y cell line

Compound	Cytotoxicity (IC_{50} μM, SH-SY5Y cell line)
3	3.83
4	3.69
5	non toxic

Although its biosynthetic pathway is unknown, Robert Adlington et al. have proposed a biosynthetic pathway for papuamine and haliclonadiamine.[65] In nature these compounds could start as C_{22} hydrocarbon chains or polyketides which would be cyclised via tandem ene cyclisation reactions.[65]

2.4. Discussion

The pursuit of marine alkaloids with bioactive properties and especially cytotoxic activity is highly important in the pursuit of a cure for cancer. Since many marine compounds approved for clinical use or in clinical trials are of sponge origin and are cancer targets, the interest to study sponges and their compounds is vital. Marine alkaloids are highly important in this quest and they present over one quarter of all bioactive MNPs isolated from sponges.

In this project compounds **3** and **4** are presented, these show significant cytotoxic activity against hepatoma cell lines. Furthermore, **3** is known to be cytotoxic against breast cancer cells and large cell lung cancer which have previously been described in literature. However, the provision of new biological assay results expand this knowledge pool where it is show that bioactivity against a neuroblastoma cell line (SH-SY5Y) also occurs. It has been demonstrated that at lower concentrations these compounds show neuroprotective activity. Furthermore, antioxidant activity is concluded via the analysis of intracellular ROS. With this already being proven, it is important to consider further testing, perhaps even in vivo studies on mice of these compounds to assess their effectiveness in combatting various cancers.

Compound **3** has previously been synthesised, with the synthetic version showing identical NMR characteristics to the natural version (Figure 43). Although the yield was fairly low, it shows that if this compound becomes of greater interest via more anticancer testing and even in vivo testing on animals in the future, the possibility of its synthesis has already been proven by Anthony Barrett et al. which eliminates the need to collect further samples and perform more isolation experiments.[61]

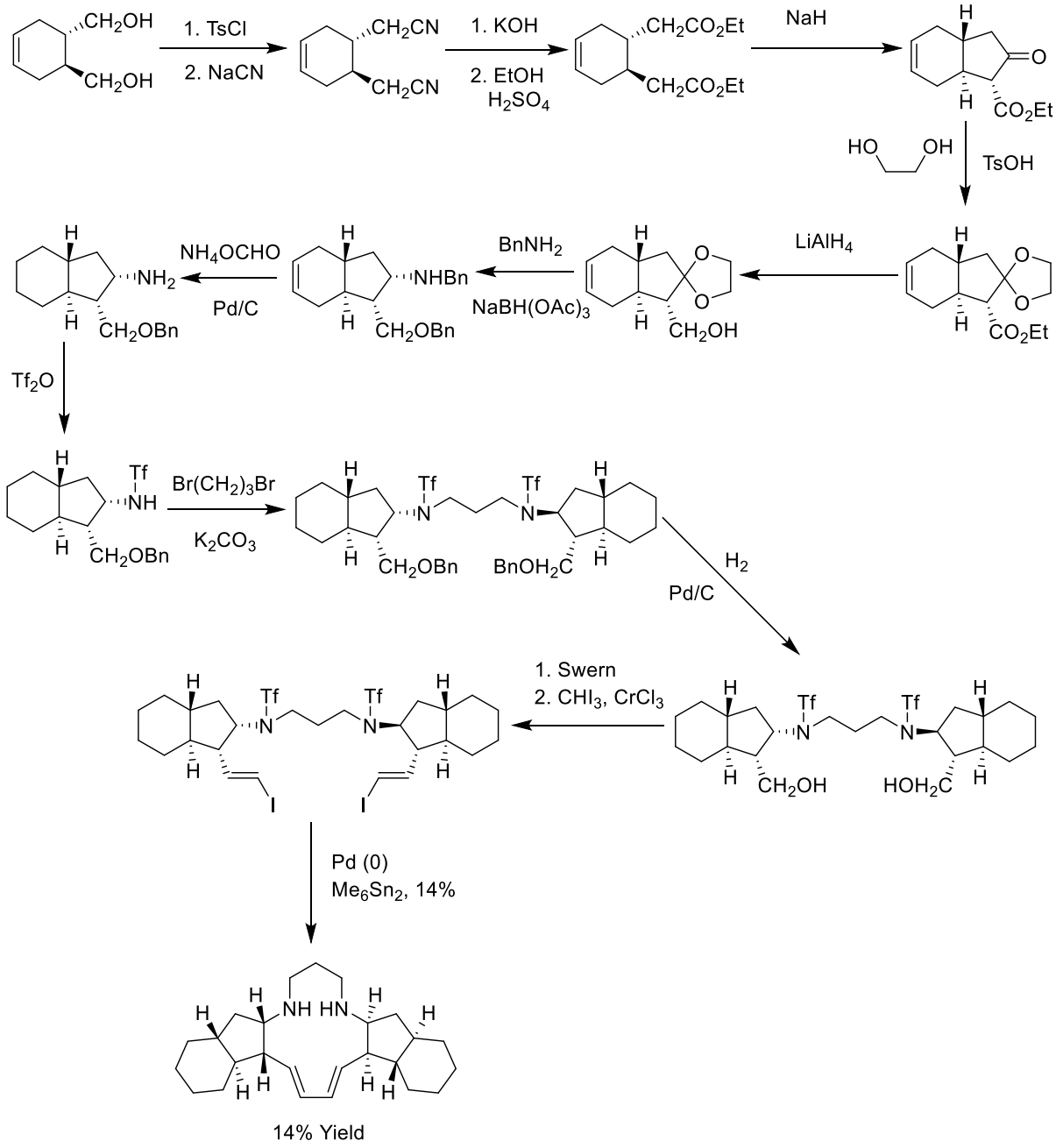

Figure 42 Synthesis of papuamine (simplified).[61]

Hydrazine MNPs are rare in nature.[66, 67] The formation of the hydrazine bond does not have a clear origin in most cases however *N*-nitrosation and *N*-hydroxylation are thought to be steps involved in the process.[67] In nature most of these compounds come from bacteria which use hydrazine-synthase in anaerobic activities to produce such compounds. Marine hydrazines are especially scarce therefore, there are not many similar compounds that papuhydrazine can be compared with.[67] Currently there are 4 hydrazine containing NPs, three from plants and one from a marine source.[67] From plants there are: N-amino-D-proline

from a flax seed *Linum usitatissimum* which shows antimicrobial activity, Munroniamide from plant *Munronia henryi* shows antifeedant activity against *Pieris brassicae*, an indole alkaloid braznitidumine from the bark of *Aspidosperma nitidum* (Figure 44).[67] The marine environment only presents ostrerine A from a marine mollusc *Ostrea rivularis* (Figure 44).[67]

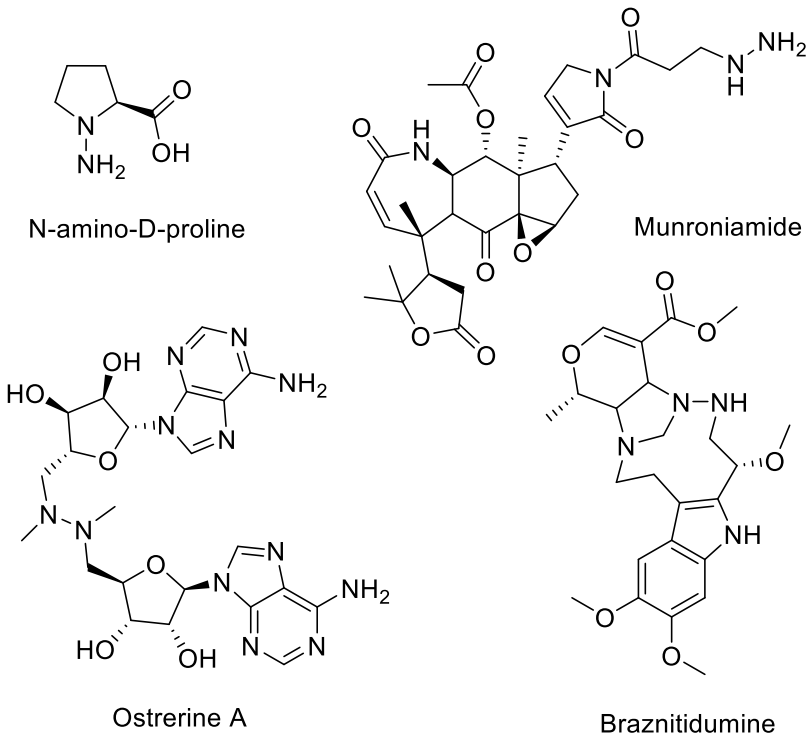

Figure 43 Structures of natural hydrazine containing NPs.[67]

With a critically small sample size to work from it is clear such compounds are of great interest and are not too well understood, from their biosynthetic pathways, to their various activities and even why these compounds are so rare in the marine environment.[68] With the activity of compounds **3** and **4** which are analogues to papuhydrazine it is important to recognize the effect of the additional bond on bioactivity. Furthermore, the lack of such compounds in the marine environment is of itself an interesting fact to consider as papuhydrazine would only be the second hydrazine MNP to be discovered. A key to understanding the lack of such compounds is their biosynthetic pathways which are currently unknown which could help bring to light the reason for the lack of such compounds.

3. Marine Alkaloids from the Haplosclerida sponge sample MB NUIG 368

3.1. Preliminary screening and fractionation

Sponge sample MB NUIG 368 was collected in PNG and presented a white colouring. SPE was done and fractions 2, 3 and 4 were chemically screened using MS which showed an abundance of potential compounds. This resulted in the decision to extract and isolated compounds from this specimen. VLC was done on the extract for separation into 5 fractions (Table 12).

Table 12 VLC fraction name, composition and mass

Name	Fraction Composition	Fraction mass (g)
F1	H_2O	0.883
F2	H_2O:MeOH (1:1)	0.210
F3	MeOH	0.536
F4	MeOH:DCM (1:1)	0.224
F5	DCM	0.035

3.2. Fraction 3

UPLC-DAD-ELSD using a standard gradient was used and showed the presence of polar compounds with retention times and UV profiles very similar to those of the alkaloids isolated from the previous sponge sample MB NUIG 361 (Table 13, Figure 45). This fraction was then subjected to semi-preparative HPLC using a reverse phase C18 column.

Table 13 UPCL-DAD-ELSD analytical conditions for F3 using H_2O and ACN

Time (min)	Flow mL/min	A H_2O	B ACN
0	1	90	10
2	1	90	10
8	1	0	100
12	1	0	100
14	1	90	10

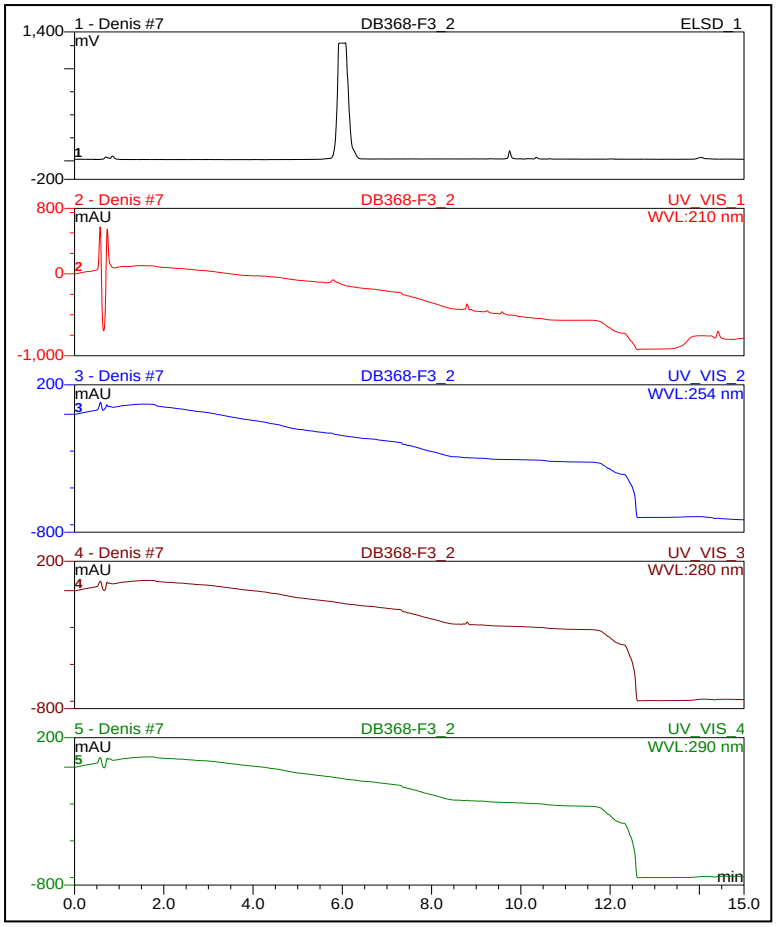

Figure 44 ELSD and DAD (210 nm, 254 nm, 280 nm, 290 nm) chromatograms for F3

At first the purification process was attempted with MeOH co-solvent. However, it turns out that that the targeted compounds are too non-polar to elute using this polar mobile phase, here 6 peaks were collected. Peaks 1-6 underwent a ^{1}H NMR, which showed the presence of compounds being present only in peak 6 which was collected when cleaning the column with 100% MeOH. The mobile phase was exchanged to acetonitrile (ACN) and re-purified the final peak resulting in 4 new peaks of which compound **3** and **4** were analysed further (Table 14, Figure 46).

Table 14 HPLC re-purification conditions for F3 using H_2O and ACN

Time (min)	Flow mL/min	A H_2O	B ACN
0	3	90	10
5	3	90	10
25	3	0	100
30	3	0	100
32	3	90	10

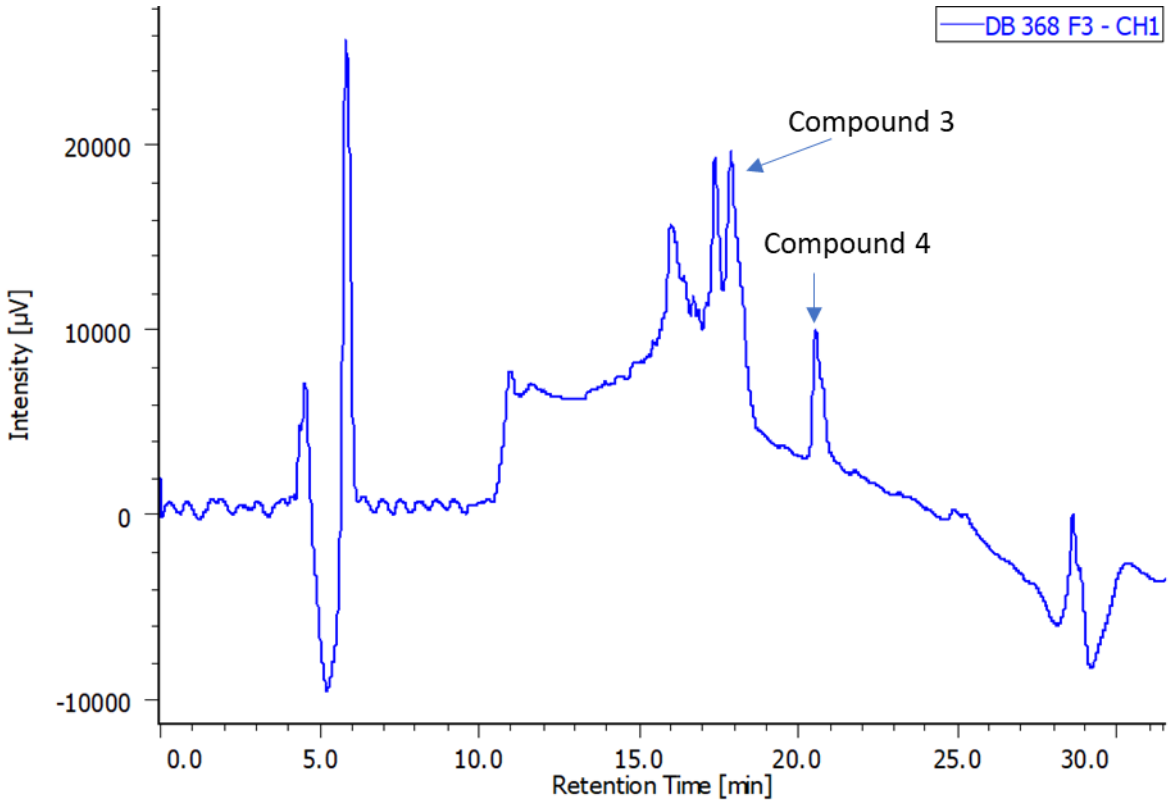

Figure 45 HPLC re-purification chromatogram for F3 at 210 nm

Compounds **3** and **4** were also further re-purified due to their ^{1}H NMR spectra and chemical shifts being very similar. However, the compounds turned out to be pure and this resulted in an interesting find where two compounds which are identical could elute at different times when undergoing purification, namely at 17 min for compound **3** and 20 min for compound **4**. This resulted in compound **3** (m = 25.8 mg) and **4** (m = 4.70 mg).

3.3. Compounds 3 and 4 structure elucidation

Fraction 3 was chosen for compound isolation as it contained the targeted compounds. Compound **3** and **4** have a *m/z* $[M+H]^+$ of 469.4518 and 469.4519 respectively, both corresponding to $C_{32}H_{57}N_2^+$ (Figure 47, 48, 49). When comparing the *m/z* ratio and chemical formula to the Marinlit database a similarity was observed to halichondramine and haliclonacyclamine A and B.[6] This means the compound would be a tetracyclic 1,3-alkyl piperidine alkaloid. NMR data was recorded in CD_3OD.

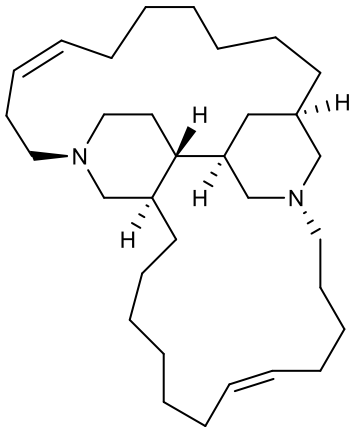

Halichondramine

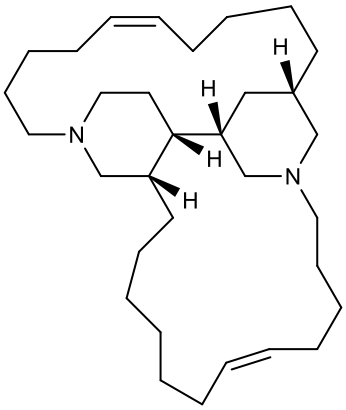

Haliclonacyclamine A

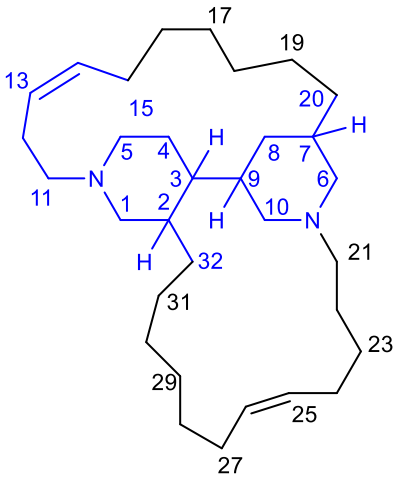

Compound **3** and **4**

Figure 46 Structures of halichondramine and haliclonacyclamine A for reference.[69, 70] Structure of compound **3** and **4**, in blue has been described using 1D and 2D NMR. In black undescribed parts of the alkyl chain.

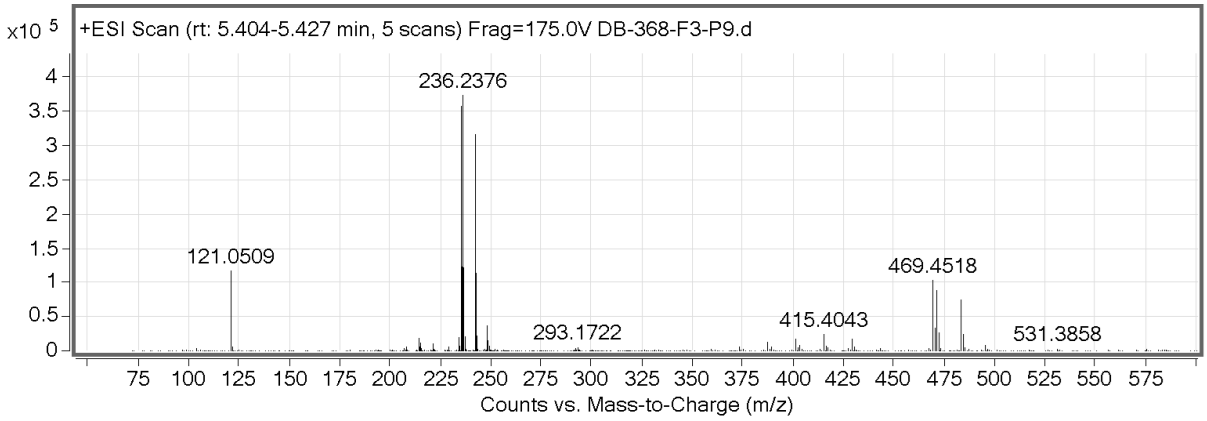

Figure 47 MS data for compound **3**

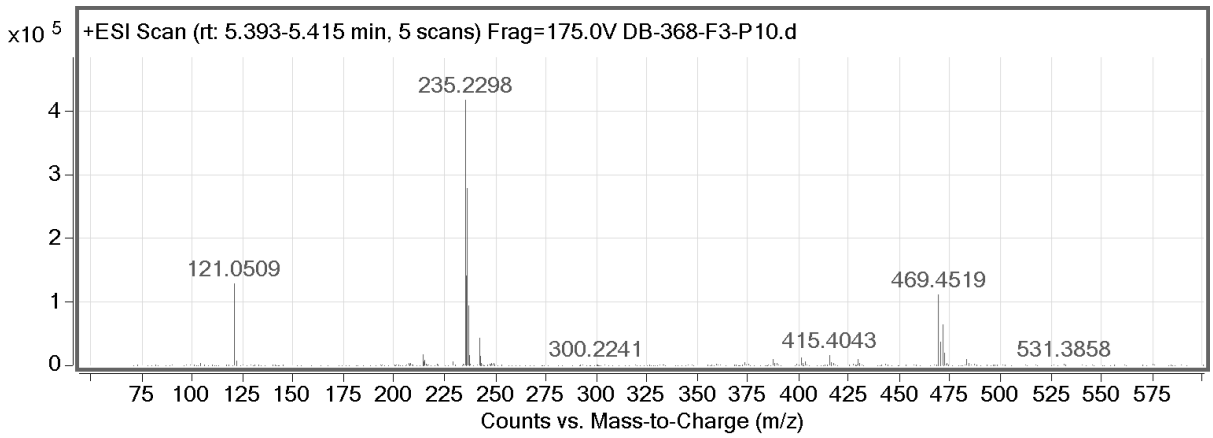

Figure 48 MS data for compound **4**

1D and 2D NMR for compounds **3** and **4** were performed in CD_3OD (SI Figures 49-58). For both compounds, the ^1H NMR spectrum showed identical chemical shifts and the ^{13}C showed matching results (Figure 50, Table 15, SI Figures 49, 50, 54, 55). This demonstrates both compounds are identical. The *J* coupling constant of 8.50 Hz at δ_H 5.32 indicate a Z olefinic configuration for C-13 and C-14.

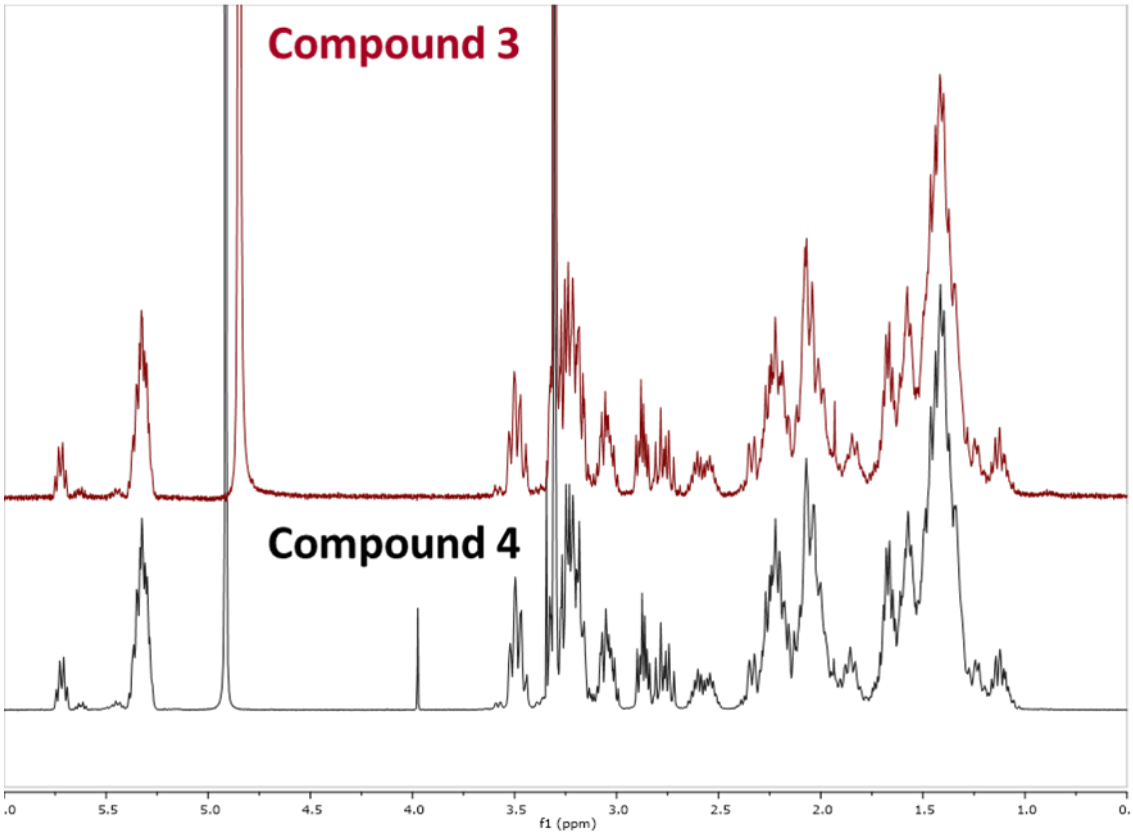

Figure 49 ^1H NMR (500 MHz, CD_3OD) of compound **3** and **4**

Using the COSY spectrum for compound **4** (Figure 51), two SCS' were identified. C-1/C-10 and including C-20 and C-32 (SCS1) making up the 3,4'-bipiperidine core (Figure 52). C-11/C-15 (SCS2), made up part of the first alkyl chain along with the unsaturation at C-13 and C-14 (Figure 52, 53). Due to overlapping of the COSY signals, it was impossible to fully describe both alkyl chains.

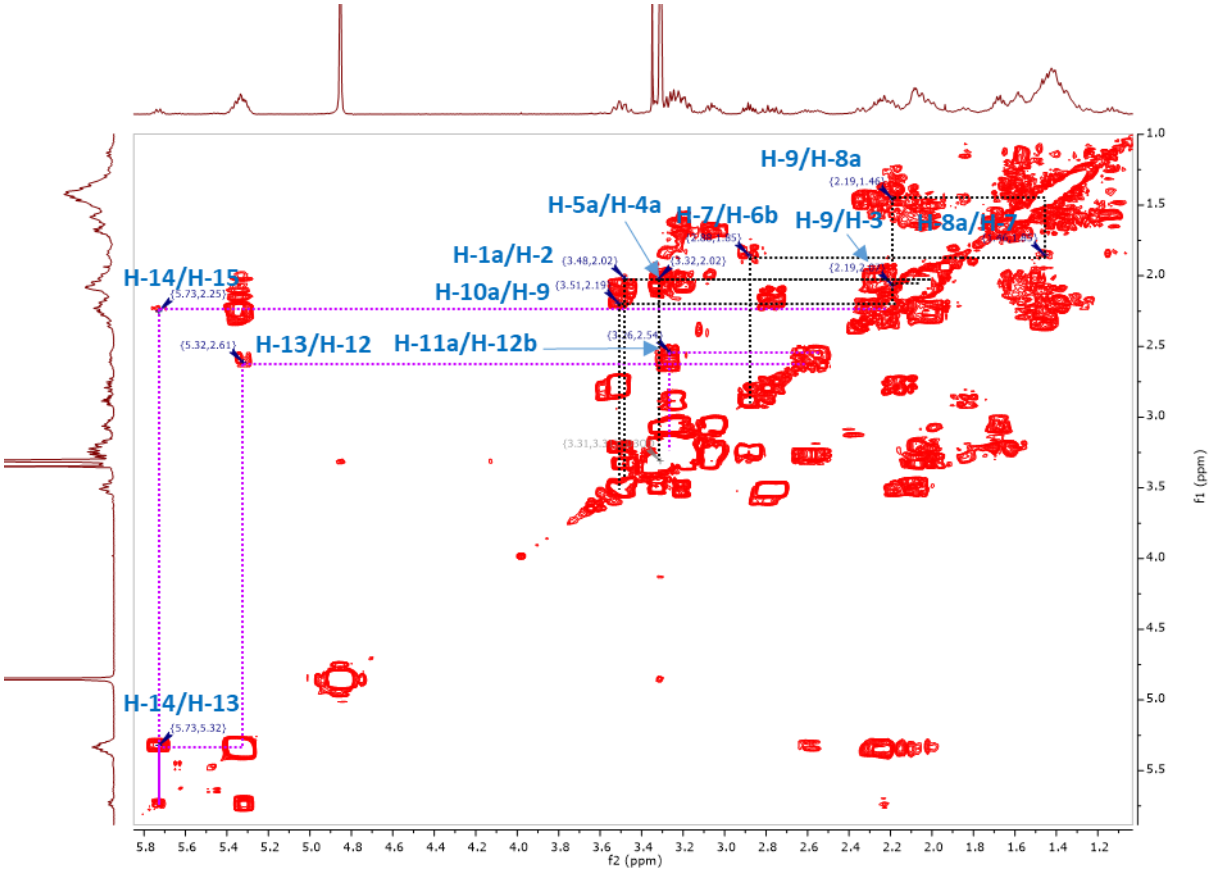

Figure 50 COSY spectrum (500 MHz, CD_3OD) of compound **3** and **4**. Identical to compound **3**. Highlighting key correlations.

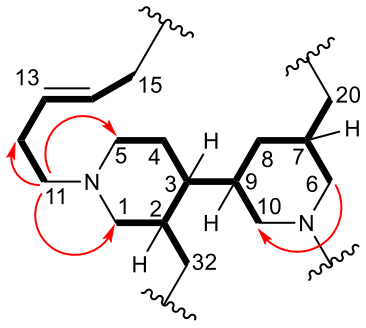

Figure 51 COSY and HMBC correlations in compound **3** and **4**

Variable temperature (VT) NMR was done on compound **4** (Figure 53). In the range of δ_H 3.06 to δ_H 1.58 there were either: peaks separating to form distinct signals or

peaks merging. For δ_H 2.62 and 2.55 at 25 °C it was seen that when lowering temperature the signals would separate from each other. This was also observed at signals at δ_H 2.23, δ_H 2.06 and δ_H 1.85 (C-7) which could be due to an interchange between S and R configurations of the chiral centre. At 25 °C for δ_H 2.88 there was a merging of two triplets where the signal becomes a single triplet at lower temperature. This same effect of temperature was also detected for δ_H 2.77. Also, there was a broadening of the signal at δ_H 3.50 and a merging of signals between δ_H 3.16 and 3.28 all of which are close to a nitrogen atom. This effect of temperature is also noticed for δ_H 2.77 where two triplets merge to form a single triplet. Finally, signals between 1.42 and 1.68 would merge and show less defined peaks. All of these results suggested a locking of the configuration around the ring system resulting in clear defined signals in ^{1}H NMR when reducing temperature.

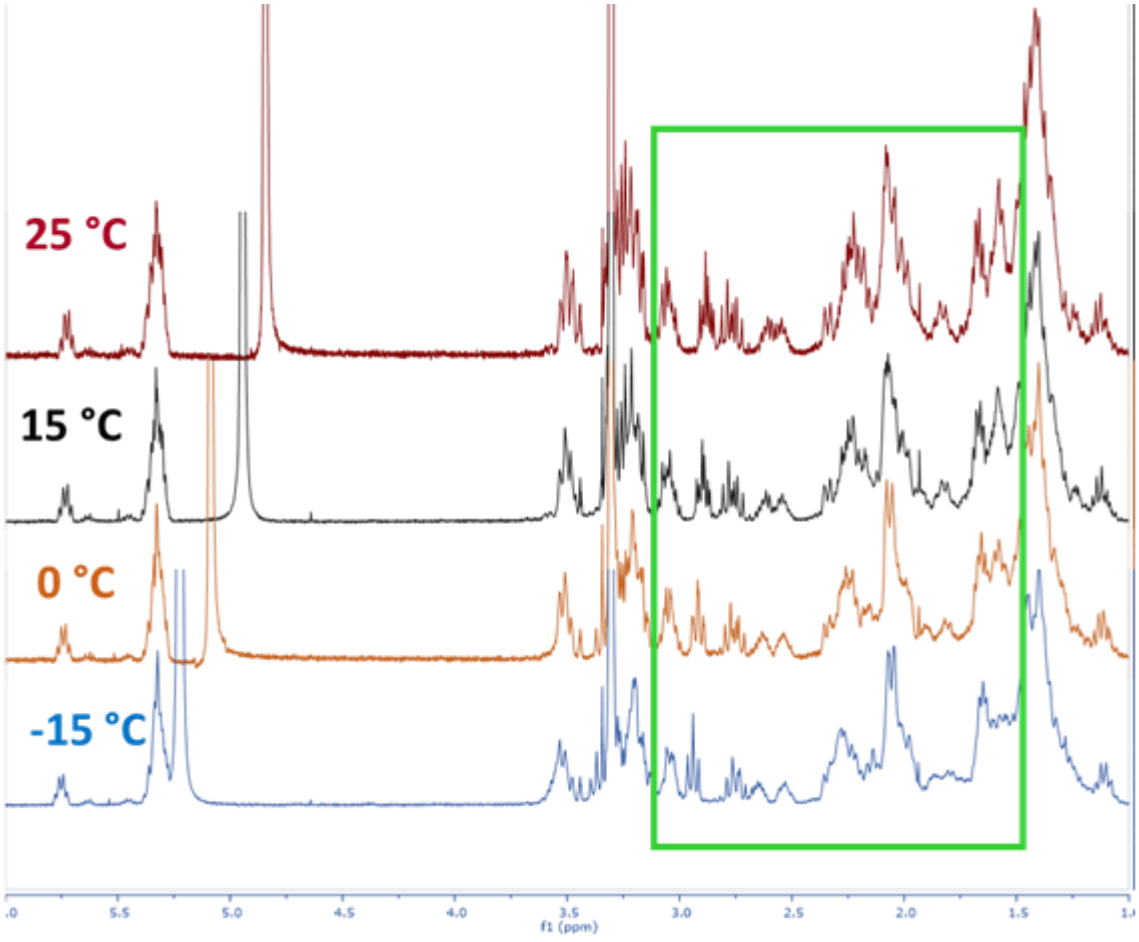

Figure 52 VT ^{1}H NMR (500 MHz, CD_3OD) of compound **4**

Table 15 ^{1}H (500 MHz, CD_3OD) and ^{13}C (125 MHz, CD_3OD) NMR of compound **3** and **4**

No.	**Compound 3** and **4**	
	δ_H mult. (*J* in Hz)	δ_C mult.
1a	3.48 m	48.1 CH_2
1b	3.31 m	
2	2.02 m	40.4 CH
3	2.06 m	32.7 CH
4a	2.02 m	27.1 CH_2
4b	2.06 m	
5a	3.32 m	53.2 CH_2
5b	3.18 m	
6a	3.40 m	58.1 CH_2
6b	2.88 m	
7	1.85 m	36.6 CH
8a	1.46 m	27.3 CH_2
8b	1.41 m	
9	2.19 m	42.4 CH
10a	3.51 m	57.2 CH_2
10b	2.79 m	
11a	3.26 m	56.4 CH_2
11b	3.18 m	
12a	2.62 m	20.7 CH_2
12b	2.55 m	
13	5.32 m	123.9 CH
14	5.73 (8.50)	134.7 CH
15a	2.23 m	27.3 CH_2
15b	2.07 m	
20a	1.15 m	33.8 CH_2
20b	1.12 m	
32a	1.5 m	27.3 CH_2
32b	1.46 m	

3.4. Discussion

MS data resulted in a molecular formula prediction of $C_{32}H_{56}N_2$. A comparison to Marinlit resulted in two possible structures being considered. Their defining feature being a 3,4'-bipiperidine system. Using 1D and 2D NMR the chemical shifts for this system were assigned, confirming its presence and also found that the *J* coupling constant at C-14 shows a cis olefinic system. The rest of the alkyl chain was hard to

assign due to the similarity and overlap of many signals in the COSY spectrum. Thus, from the aforementioned results it was concluded that the structure is similar to halichondramine however, its full structure was unable to be assigned (Tabe 15, Figure 52).

The hypothesis for the difference in the retention times of compound **3** and **4** however, with identical ^{1}H and ^{13}C NMR is that there are two different yet highly structurally similar compounds in the F3 fraction, potentially epimers around the chiral centres of the bipiperidine system that are stable during the HPLC purification process or they are rotamers. However, upon heating during the evaporation process which is done using N_2 evaporation, this can reach a temperature of 40°C where an energy barrier could be crossed and these compounds become identical. This can be seen in the VT NMR (Figure 53) which shows that at higher temperatures there is a separation of peaks which can mean a differentiation of two compounds. At lower temperatures however, some peaks merge resulting in triplets meaning that there is a locking of configuration on and close around the bipiperidine system resulting in clear NMR signals. This result means it is highly likely the two compounds are rotamers whose signals become clearer with lower temperature and a locking of configuration. Some NMR signals separate at low temperature demonstrating where the two rotamers differ.

When consulting literature it is obvious that under normal circumstances the separation of rotamers is impossible, and it can only be done under specific conditions involving great changes in temperature.[71, 72] In the case of sample MB NUIG 368 it is highly likely that when the compound is found in solution during the purification phase two compounds can be separated using HPLC. However, during the evaporation phase heating occurs resulting in the rotamers becoming indistinguishable via NMR. One possible way to study these compounds is their separation using HPLC at extremely cold temperatures. This could be followed by VT NMR to establish their individual structures.

4. Conclusion

Sponge sample MB NUIG 361 resulted in the isolation of 3 compounds, two known compounds (3 and 4) along with one new compound (5). NMR spectroscopy was used to elucidate the structure of all compounds and their signals compared to literature in the case of compounds 3 and 4. Compound 3 exhibits anticancer activity against breast cancer cells and large cell lung cancer. During this research it was found that the mixture of both known compounds is cytotoxic to lymphoma cell lines as well as individually having cytotoxic effects on neuroblastoma cell lines. At low concentrations compounds 3 and 4 have neuroprotective effects. With the use of NMR spectroscopy the structural elucidation of papuhydrazine (5) was achieved, uncovering a new hydrazine bond not present in the known compounds. Hydrazine NPs are scarce and with only one other MNP containing this feature coming from a marine mollusc, this is the first hydrazine containing MNP coming from a sponge. The future of this compound is dependent on further research 70 and assays to be completed which can then be used to compare this new compound with papuamine and haliclonadiamine. Sponge sample MB NUIG 368 resulted in the isolation of 2 compounds (3 and 4). These compounds underwent extensive purification and re-purification which resulted in clear NMR spectra which as used to elucidate the core structure of these molecules. However, both compounds are identical in the NMR spectrum but with completely different HPLC elution times. VT NMR was performed on compound 4 showing significant difference when going down in temperature. This led to the hypothesis that both compounds are rotamers that are interchangeable after nitrogen evaporation where they are heated and pass an energy barrier therefore, unable to be distinguished using NMR spectroscopy. However, they are separable during HPLC due to the lower temperature. With more time and different methods other equipment and techniques could have been used to further study these interesting compounds. To conclude, sponges have provided and still provide a diverse array of compounds that have not yet been discovered like papuhydrazine. They provide compounds that are unmatched in complexity with the potential to be highly useful in terms of medicinal application. Many sponge derived compounds have proved to be effective against various diseases when applied in cell lines, and with the increasing advancement of MNP drugs making

their way on the pharmaceutical market it is important to continue studying sponges and the compounds they produce.

5. Materials and Methods

5.1. General experimental procedures

Optical rotations were measured on Rudolph Research Analytical autopol v plus automatic polarimeter (Hackettstown, NJ, USA). CD spectra were measured on an Applied Photonics Chirascan V100. NMR spectra were measured on an Agilent Technologies 600/54 Premium Compact (500 and 125 MHz for ^{1}H and ^{13}C, respectively) and Varian 500 MHz AR NMR spectrometers (600 and 150 MHz for ^{1}H and ^{13}C, respectively) (Varian, Palo Alto, CA, USA); Chemical shifts (d) are reported in CD_3OD or DMSO-d_6 with reference to the solvent signals and coupling constants (*J*) in Hz. Waters SymmetryPrep C18 7μm 7.8x300mm Column for HPLC. Semi-preparative HPLC was performed on a Alliance Waters 2695 Separation Module (Milford, Massachusetts, USA) system equipped with a Waters 2487 Dual λ Absorbance Detector at 210 and 254 nm by eluting with CH3CN-H2O system at 3 $mL.min^{-1}$. All solvents used for CC and HPLC were of analytical grades (Shanghai Chemical Reagents Co., Ltd.) and chromatographic grade (Dikma Technologies Inc.), respectively. Mass spectrometry was done on an Agilent 1290 infinity UPLC coupled to a Agilent Technologies 6540 Accurate-Mass Q-TOF LC/MS. ELSD was measured on an Agilent Technologies 1260 infinity coupled to a 380-ELSD; the column used for this was XBridge C18 3.5 μL 4.6x100 mm. ELSD for sample 368 was measured using a Dionex UltiMate 3000 (Sunnyvale, CA, USA) coupled to an Agilent 385-ELSD via a Acquity UPLC BEH 1.7 μm 2.1x75 mm (Milford, Massachusetts, USA).

5.2. Experimental: MB NUIG 361

5.2.1. Biological material

The specimen was collected in Papua New Guinea, located in the coral triangle of the Pacific Ocean, and identified as belonging to the order Haplosclerida. Collection occurred during the *Tara* Pacific expedition of 2016.

5.2.2. Sample preparation

The samples were frozen at −80 °C followed by lyophilisation. After this, the sample was ground down to a powder and stored in a −80 °C freezer until ready for analysis.

5.2.3. Chemical screening and preliminary bioassay activity

SPE was done on a small amount of dried biomass (~1.00 g). A mixture of standard solvents were used to produce 5 fractions of decreasing polarity H_2O (F1), H_2O:MeOH 1:1 (F2), MeOH (F3), MeOH:DCM 1:1 (F4), DCM (F5). Chemical screening occurred via MS analysis of F2 and F3 which showed a high level of potential compounds. Biological assays to test for bioactivity were done against lymphoma cell lines, by collaborator Francesco Berri in Switzerland which resulted in the affirmation that fractions F2 and F3 were highly active against cancer cells and somewhat active against regular human cell lines, however, not as active as on cancer cells.

5.2.4. MB NUIG 361 (order haplosclerida)

The freeze-dried sponge (7.25g) was kept in a −80℃ freezer. Extraction was done using MeOH:DCM (1:1). The sample was placed in a conical flask where 200 mL of the 1:1 mixture was added. This was then ultra-sonicated for 15 minutes. The liquid is then transferred into a round bottomed flask. The aforementioned is done in triplicated. The extract is then evaporated using a rotary evaporator to leave a dry extract. The extract is then dissolved using some (MeOH: DCM) (1:1), transferred to a 20 mg vial and evaporated again. The extract is then weighed (3.03 g). A vacuum liquid chromatography (VLC) is performed using C18 (75.78 g) as the stationary phase. 5 Fractions were collected using 200 mL of mobile phase for each, H_2O (F1),

H_2O:MeOH 1:1 (F2), MeOH (F3), MeOH:DCM 1:1 (F4), DCM (F5). The analytical profiles were recorded using an Agilent HPLC-DAD-ELSD using a C18 analytical column (XBridge C18 3.5 μm 4.6x100 mm). Semi-preparative HPLC purification was done on a Waters system using a C18 column (Waters SymmetryPrep C18 7μm 7.8x300mm). The solvents used were H_2O+0.1% TFA (A) and ACN+0.1% TFA (B).

Fraction 3 isocratic for 0-5 min with A 70, B 30; linear gradient 5-30 min until A 50, B 50; isocratic 30-40 min A 50, B 50; linear gradient 40-41 min until A 70 B 30; isocratic 41-42 min A 70 B 30. A flow rate of 3 $mL.min^{-1}$ and dual UV detection at 210 nm and 254 nm. This fraction resulted in 5 compounds being isolated, compound **1**-**5** from MB NUIG 361.

Fraction 4 isocratic for 0-25 with A 55, B 35. A flow rate of 3 $mL.min^{-1}$ and dual UV detection at 210 nm and 254 nm. 2 compounds were isolated, these being papuamine and haliclonadiamine.

Fraction 2 semi-preparative HPLC done on a JASCO HPLC system using a T3 column (XSelect HSS T3 5μm 10x250 mm). Isocratic for 0-5 min with A 80, B 20; linear gradient 5-30 min until A 30, B 70; isocratic 30-40 min A 30, B 70; linear gradient 40-41 min until A 80 B 20; isocratic 41-42 min A 80 B 20. A flow rate of 3 $mL.min^{-1}$ and dual UV detection at 210 nm. This fraction resulted in 5 compounds, the known papuamine and haliclonadiamine, and 3 compounds which were not described due to poor 1D and 2D NMR resolution.

5.3. Experimental: MB NUIG 368

5.3.1. Biological material

As in MB NUIG 361.

5.3.2. Sample preparation

As in MB NUIG 361.

5.3.3. Chemical Screening

SPE was done on 1.04 g of dried biomass. A mixture of standard solvents were used to produce 5 fractions of decreasing polarity H_2O (F1), H_2O:MeOH 1:1 (F2), MeOH (F3), MeOH:DCM 1:1 (F4), DCM (F5). The analytical profiles were recorded using a Dionex UPLC-DAD-ELSD using a C18 analytical column (Acquity UPLC BEH 1.7 μm 2.1x75 mm) for F2, F3 and F4 with F3 being most promising.

5.3.4. MB NUIG 368 (order haplosclerida)

The freeze-dried sponge (6.38g) was kept in a −80℃ freezer. Extraction was done using MeOH:DCM (1:1). The sample was placed in a conical flask where 200 mL of the 1:1 mixture was added. This was then ultra-sonicated for 15 minutes. The liquid is then transferred into a round bottomed flask. The aforementioned is done in triplicate. The extract is then evaporated using a rotary evaporator to leave a dry extract. The extract is then dissolved using some MeOH: DCM (1:1), transferred to a 20 mg vial and evaporated again. The extract is then weighed (2.62 g). VLC is performed using C18 (33.6 g) as the stationary phase. 5 Fractions were collected using 200 mL of mobile phase for each, H_2O (F1), H_2O:MeOH 1:1 (F2), MeOH (F3), MeOH:DCM 1:1 (F4), DCM (F5). The analytical profiles were recorded using a Dionex UPLC-DAD-ELSD using a C18 analytical column (Acquity UPLC BEH 1.7 μm 2.1x75 mm). Semi-preparative HPLC purification was done on a JASCO system using a C18 (VP 250/10 NUCLEODUR 18 HTec, 5μm).

Fraction 3 was first purified using H_2O+0.1% TFA (A) and MeOH+0.1% TFA (B). However, no compounds were isolated except for the final peak which contained the overwhelming amount of compounds of interest. This was further re-purified with H_2O+0.1% TFA (A) and ACN+0.1% TFA (B) instead of MeOH. Isocratic for 0-5 min with A 90, B 10; linear gradient 5-25 min until A 0, B 100; isocratic 25-30 min A 0, B 10; linear gradient 30-32 min until A 90 B 10. A flow rate of 4 $mL.min^{-1}$ and dual UV detection at 210 nm. This fraction resulted in the isolation of two compounds, compounds **3** and **4** from MB NUIG 368.

6. References

1. S. Planes, D. Allemand, S. Agostini, B. Banaigs, E. Boissin, E. Boss, G. Bourdin, C. Bowler, E. Douville, J. M. Flores, D. Forcioli, P. Furla, P. E. Galand, J.-F. Ghiglione, E. Gilson, F. Lombard, C. Moulin, S. Pesant, J. Poulain, S. Reynaud, S. Romac, M. B. Sullivan, S. Sunagawa, O. P. Thomas, R. Troublé, C. de Vargas, R. Vega Thurber, C. R. Voolstra, P. Wincker, D. Zoccola and C. the Tara Pacific, *PLOS Biol.*, 2019, **17**, DOI: 10.1371/journal.pbio.3000483 .
2. M. Miguel-Gordo, S. Gegunde, K. Calabro, L. K. Jennings, A. Alfonso, G. Genta-Jouve, J. Vacelet, L. M. Botana and O. P. Thomas, *Mar. Drugs*, 2019, **17**, 319.
3. W. Appeltans, Shane T. Ahyong, G. Anderson, Martin V. Angel, T. Artois, N. Bailly, R. Bamber, A. Barber, I. Bartsch, A. Berta, M. Błażewicz-Paszkowycz, P. Bock, G. Boxshall, Christopher B. Boyko, Simone N. Brandão, Rod A. Bray, Niel L. Bruce, Stephen D. Cairns, T.-Y. Chan, L. Cheng, Allen G. Collins, T. Cribb, M. Curini-Galletti, F. Dahdouh-Guebas, Peter J. F. Davie, Michael N. Dawson, O. De Clerck, W. Decock, S. De Grave, Nicole J. de Voogd, Daryl P. Domning, Christian C. Emig, C. Erséus, W. Eschmeyer, K. Fauchald, Daphne G. Fautin, Stephen W. Feist, Charles H. J. M. Fransen, H. Furuya, O. Garcia-Alvarez, S. Gerken, D. Gibson, A. Gittenberger, S. Gofas, L. Gómez-Daglio, Dennis P. Gordon, Michael D. Guiry, F. Hernandez, Bert W. Hoeksema, Russell R. Hopcroft, D. Jaume, P. Kirk, N. Koedam, S. Koenemann, Jürgen B. Kolb, Reinhardt M. Kristensen, A. Kroh, G. Lambert, David B. Lazarus, R. Lemaitre, M. Longshaw, J. Lowry, E. Macpherson, Laurence P. Madin, C. Mah, G. Mapstone, Patsy A. McLaughlin, J. Mees, K. Meland, Charles G. Messing, Claudia E. Mills, Tina N. Molodtsova, R. Mooi, B. Neuhaus, Peter K. L. Ng, C. Nielsen, J. Norenburg, Dennis M. Opresko, M. Osawa, G. Paulay, W. Perrin, John F. Pilger, Gary C. B. Poore, P. Pugh, Geoffrey B. Read, James D. Reimer, M. Rius, Rosana M. Rocha, José I. Saiz-Salinas, V. Scarabino, B. Schierwater, A. Schmidt-Rhaesa, Kareen E. Schnabel, M. Schotte, P. Schuchert, E. Schwabe, H. Segers, C. Self-Sullivan, N. Shenkar, V. Siegel, W. Sterrer, S. Stöhr, B. Swalla, Mark L. Tasker, Erik V. Thuesen, T. Timm, M. A. Todaro, X. Turon, S. Tyler, P. Uetz, J. van der Land, B. Vanhoorne, Leen P. van Ofwegen, Rob W. M. van Soest, J. Vanaverbeke, G. Walker-Smith, T. C. Walter, A. Warren, Gary C. Williams, Simon P. Wilson and Mark J. Costello, *Curr. Biology*, 2012, **22**, 2189-2202.
4. R. W. M. Van Soest, N. Boury-Esnault, J. Vacelet, M. Dohrmann, D. Erpenbeck, N. J. De Voogd, N. Santodomingo, B. Vanhoorne, M. Kelly and J. N. A. Hooper, *PLOS One*, 2012, **7**, DOI: 10.1371/journal.pone.0035105.
5. P. Proksch, *Toxicon*, 1994, **32**, 639-655.
6. MarinLit, https://marinlit-rsc-org.nuigalway.idm.oclc.org/, (accessed 25/07/2022).
7. D. J. Newman and G. M. Cragg, *J. Nat. Prod.*, 2020, **83**, 770-803.
8. N. Mishra, V. K. Tiwari and R. R. Schmidt, in *Carbohydrates in Drug Discovery and Development*, ed. V. K. Tiwari, Elsevier, 2020, 1-69.
9. R. Montaser and H. Luesch, *Future Med. Chem.*, 2011, **3**, 1475-1489.
10. D. X. Kong, Y. Y. Jiang and H. Y. Zhang, *Drug Discov. Today*, 2010, **15**, 884-886.

11. M. F. Mehbub, J. Lei, C. Franco and W. Zhang, *Mar. Drugs*, 2014, **12**, 4539-4577.
12. G.-P. Hu, J. Yuan, L. Sun, Z.-G. She, J.-H. Wu, X.-J. Lan, X. Zhu, Y.-C. Lin and S.-P. Chen, *Mar. Drugs*, 2011, **9**, 514-525.
13. M. H. Munro, J. W. Blunt, E. J. Dumdei, S. J. Hickford, R. E. Lill, S. Li, C. N. Battershill and A. R. Duckworth, *J. Biotechnol.*, 1999, **70**, 15-25.
14. Drug Approval Package, https://www.accessdata.fda.gov/drugsatfda_docs/nda/2004/21-060_Prialt.cfm, (accessed 24/07/2022).
15. J. G. McGivern, *Neuropsychiatr. Dis. Treat.*, 2007, **3**, 69-85.
16. A. Martins, H. Vieira, H. Gaspar and S. Santos, *Mar. Drugs*, 2014, **12**, 1066-1101.
17. E. Cappello and P. Nieri, *Life*, 2021, **11**, 1390.
18. Approved Mar. Drugs, https://www.marinepharmacology.org/approved, 24/07/2022).
19. A. C. Wu, K. K. Jelielek, H. Q. Le, M. Butt, D. J. Newman, K. B. Glaser, M. L. Pierce and A. M. Mayer, *FASEB J.*, 2022, **36**, DOI: 10.1096/fasebj.2022.36.S1.L7586.
20. G. P. Hu, J. Yuan, L. Sun, Z. G. She, J. H. Wu, X. J. Lan, X. Zhu, Y. C. Lin and S. P. Chen, *Mar. Drugs*, 2011, **9**, 514-525.
21. R. Mioso, F. J. Marante, R. S. Bezerra, F. V. Borges, B. V. Santos and I. H. Laguna, *Molecules*, 2017, **22**, 208.
22. E. R. Abdelaleem, M. N. Samy, S. Y. Desoukey, M. Liu, R. J. Quinn and U. R. Abdelmohsen, *RSC Adv.*, 2020, **10**, 34959-34976.
23. K. Anjum, S. Q. Abbas, S. A. A. Shah, N. Akhter, S. Batool and S. S. u. Hassan, *Biomol. Ther.*, 2016, **24**, 347-362.
24. P. M. Dewick, in *Medicinal Natural Products: A Biosynthetic Approach*, Wiley, Chichester, 2009, 311-420.
25. M. Assmann, E. Lichte, J. R. Pawlik and M. Köck, *Mar. Ecol. Prog. Ser.*, 2000, **207**, 255-262.
26. M. S. Laport, O. C. S. Santos and G. Muricy, *Curr. Pharm. Biotechnol.*, 2009, **10**, 86-105.
27. G. Tarazona, G. Santamaría, P. G. Cruz, R. Fernández, M. Pérez, J. F. Martínez-Leal, J. Rodríguez, C. Jiménez and C. Cuevas, *ACS Omega*, 2017, **2**, 3494-3501.
28. J. N. Tabudravu and M. Jaspars, *J. Nat. Prod.*, 2002, **65**, 1798-1801.
29. K. Yao, J. Fang, Y. L. Yin, Z. M. Feng, Z. R. Tang and G. Wu, *FLB*, 2011, **3**, 286-297.
30. N. Netz and T. Opatz, *Mar. Drugs*, 2015, **13**, 4814-4914.
31. J.-F. Hu, J. A. Schetz, M. Kelly, J.-N. Peng, K. K. H. Ang, H. Flotow, C. Y. Leong, S. B. Ng, A. D. Buss, S. P. Wilkins and M. T. Hamann, *J. Nat. Prod.*, 2002, **65**, 476-480.
32. Y. Hitora, K. Takada, Y. Ise, S. Okada and S. Matsunaga, *J. Nat. Prod.*, 2016, **79**, 2973-2976.
33. M. D. Lovelace, B. Varney, G. Sundaram, M. J. Lennon, C. K. Lim, K. Jacobs, G. J. Guillemin and B. J. Brew, *Neuropharmacology*, 2017, **112**, 373-388.
34. T. F. Molinski and D. J. Faulkner, *Tetrahedron Lett.*, 1988, **29**, 2137-2138.
35. V. Gasperi, M. Sibilano, I. Savini and M. V. Catani, *Int. J. Mol. Sci.*, 2019, **20**, 974.

36. K. Hirano, T. Kubota, M. Tsuda, Y. Mikami and J. i. Kobayashi, *Chem. Pharm. Bull.*, 2000, **48**, 974-977.
37. G. Genta-Jouve and O. P. Thomas, *Adv. Mar. Biol.*, 2012, **62**, 183-230.
38. X. Wei, K. Nieves and A. D. Rodríguez, *Bioorganic Med. Chem. Lett.*, 2010, **20**, 5905-5908.
39. A. M. Elissawy, E. Soleiman Dehkordi, N. Mehdinezhad, M. L. Ashour and P. Mohammadi Pour, *Biomolecules*, 2021, **11**, 258.
40. B. Chopra, A. Dhingra, R. Kapoor and D. Prasad, *Open Chem. J.*, 2016, **3**, 75-96.
41. A. D. Rodríguez, O. M. Cóbar, O. L. Padilla and C. L. Barnes, *J. Nat. Prod.*, 1997, **60**, 1331-1333.
42. R.-L. Meza-León, A. Dávila-García, F. Sartillo-Piscil, L. Quintero, M. S. Rivadeneyra and S. Cruz-Gregorio, *Tetrahedron Lett.*, 2013, **54**, 6852-6854.
43. G. Genta-Jouve, N. Cachet, S. Holderith, F. Oberhänsli, J. L. Teyssié, R. Jeffree, A. Al Mourabit and O. P. Thomas, *Chembiochem.*, 2011, **12**, 2298-2301.
44. B. Forte, B. Malgesini, C. Piutti, F. Quartieri, A. Scolaro and G. Papeo, *Mar. Drugs*, 2009, **7**, 705-753.
45. F. Cafieri, E. Fattorusso, A. Mangoni and O. Taglialatela-Scafati, *Tetrahedron Lett.*, 1996, **37**, 3587-3590.
46. S. B. L. Silva, F. Oberhänsli, M.-A. Tribalat, G. Genta-Jouve, J.-L. Teyssié, M.-Y. Dechraoui-Bottein, J.-F. Gallard, L. Evanno, E. Poupon and O. P. Thomas, *Angew. Chem. Int. Ed.*, 2019, **58**, 520-525.
47. D. S. Coffey, A. I. McDonald, L. E. Overman, M. H. Rabinowitz and P. A. Renhowe, *J. Am. Chem. Soc.*, 2000, **122**, 4893-4903.
48. G. Genta-Jouve, J. Croué, L. Weinberg, V. Cocandeau, S. Holderith, N. Bontemps, M. Suzuki and O. P. Thomas, *Phytochem. Lett.*, 2014, **10**, 318-323.
49. A. D. Patil, N. V. Kumar, W. C. Kokke, M. F. Bean, A. J. Freyer, C. D. Brosse, S. Mai, A. Truneh and B. Carte, *J. Org. Chem.*, 1995, **60**, 1182-1188.
50. S. Bondu, G. Genta-Jouve, M. Leirós, C. Vale, J.-M. Guigonis, L. M. Botana and O. P. Thomas, *RSC Adv.*, 2012, **2**, 2828-2835.
51. E. A. Jares-Erijman, R. Sakai and K. L. Rinehart, *J. Org. Chem.*, 1991, **56**, 5712-5715.
52. R. G. S. Berlinck, A. F. Bertonha, M. Takaki and J. P. G. Rodriguez, *Nat. Prod. Rep.*, 2017, **34**, 1264-1301.
53. S. Bienz, P. Bisegger, A. Guggisberg and M. Hesse, *Nat. Prod. Rep.*, 2005, **22**, 647-658.
54. M. Xu, R. A. Davis, Y. Feng, M. L. Sykes, T. Shelper, V. M. Avery, D. Camp and R. J. Quinn, *J. Nat. Prod.*, 2012, **75**, 1001-1005.
55. S. Négrel and J. M. Brunel, *Curr. Med. Chem.*, 2021, **28**, 3406-3448.
56. D. E. Williams, P. Lassota and R. J. Andersen, *J. Org. Chem.*, 1998, **63**, 4838-4841.
57. D. B. Abdjul, H. Yamazaki, S. Kanno, O. Takahashi, R. Kirikoshi, K. Ukai and M. Namikoshi, *J. Nat. Prod.*, 2016, **79**, 1149-1154.
58. B. J. Baker, P. J. Scheuer and J. N. Shoolery, *J. Am. Chem. Soc.*, 1988, **110**, 965-966.
59. E. Fahy, T. F. Molinski, M. K. Harper, B. W. Sullivan, D. J. Faulkner, L. Parkanyi and J. Clardy, *Tetrahedron Lett.*, 1988, **29**, 3427-3428.
60. H.-B. Liu, G. H. Imler, K. K. Baldridge, R. D. O'Connor, J. S. Siegel, J. R. Deschamps and C. A. Bewley, *J. Am. Chem. Soc.*, 2020, **142**, 2755-2759.

61. A. G. M. Barrett, M. L. Boys and T. L. Boehm, *J. Org. Chem.*, 1996, **61**, 685-699.
62. H. Y. Min, Y. Jung, K. H. Park and H. Y. Lee, *Anticancer Res.*, 2020, **40**, 323-333.
63. S. Kanno, S. Yomogida, A. Tomizawa, H. Yamazaki, K. Ukai, R. E. Mangindaan, M. Namikoshi and M. Ishikawa, *Int. J. Oncol.*, 2013, **43**, 1413-1419.
64. L. Dong, V. Gopalan, O. Holland and J. Neuzil, *Int. J. Mol. Sci.*, 2020, **21**.
65. R. M. Adlington, J. E. Baldwin, G. L. Challis, R. J. Cox and G. J. Pritchard, *Tetrahedron*, 2000, **56**, 623-628.
66. B. Toth, *Hydrazines and Cancer*, Taylor & Francis Ltd, London, 2000.
67. G. Le Goff and J. Ouazzani, *Bioorg. Med. Chem.*, 2014, **22**, 6529-6544.
68. H. Izumida, K. Adachi, A. Mihara, T. Yasuzawa and H. Sano, *J. Antibiot.*, 1997, **50**, 916-918.
69. L. Mani, S. Petek, A. Valentin, S. Chevalley, E. Folcher, W. Aalbersberg and C. Debitus, *Nat. Prod. Res.*, 2011, **25**, 1923-1930.
70. L. Chill, T. Yosief and Y. Kashman, *J. Nat. Prod.*, 2002, **65**, 1738-1741.
71. S. K. Chauthe, P. Sidduri, M. Reddy, R. Sistla, V. Byri, M. D. Uttaravalli, M. Botlagunta, H. Kumar, A. Gupta, A. K. Gupta, L. Bajpai, M. Bagadi and A. Mathur, *JPBA*, 2022, **212**, 114675.
72. M. Geffe, L. Andernach, O. Trapp and T. Opatz, *J. Org. Chem.*, 2014, **10**, 701-706.

7. Supplementary Information

Table of Figures

7.1. MB NUIG 361

Compound 1: white powder; 1H NMR (CD_3OD & DMSO-d_6, 600 MHz); *m/z* $[M+H]^+$ 212.1758 (calcd. for $C_{11}H_{22}N_3O^+$, 212.1757, Δ 0.47 ppm).

Compound 2: white powder; 1H NMR (CD_3OD & DMSO-d_6, 600 MHz); *m/z* $[M+H]^+$ 212.1754 (calcd. for $C_{11}H_{22}N_3O^+$, 212.1757 Δ −1.41 ppm).

Compound 3: white powder; $[\alpha]_D^{20}$ −148 (c 6.60 mg.mL^{-1}, CH_3OH); ^{1}H NMR (CD_3OD, 500 MHz) and ^{13}C NMR (CD_3OD, 125 MHz) spectral data, see table 1; *m/z* $[M+H]^+$ 369.3266 (calcd. for $C_{25}H_{41}N_2^+$, 369.3264, Δ 0.54 ppm).

Compound 4: white powder; $[\alpha]_D^{20}$ −17 (c 2.92 mg.mL^{-1}, CH_3OH); ^{1}H NMR (CD_3OD, 500 MHz) and ^{13}C NMR (CD_3OD, 125 MHz) spectral data, see table 1; *m/z* $[M+H]^+$ 369.3265 (calcd. for $C_{25}H_{41}N_2^+$, 369.3264, Δ 0.27 ppm).

Compound 5: white powder; $[\alpha]_D^{20}$ −27 (c 0.26 mg.mL^{-1}, CH_3OH); ^{13}C NMR had no signals HSQC carbon signals used instead (CD_3OD, 125 MHz), spectral data in Table 1; *m/z* $[M+H]^+$ 367.3112 (calcd. for $C_{25}H_{39}N_2^+$, 367.3108, Δ 1.09 ppm).

Bioassays done by: Rebeca Alvarino, Amparo Alfonso, Luis M. Botana

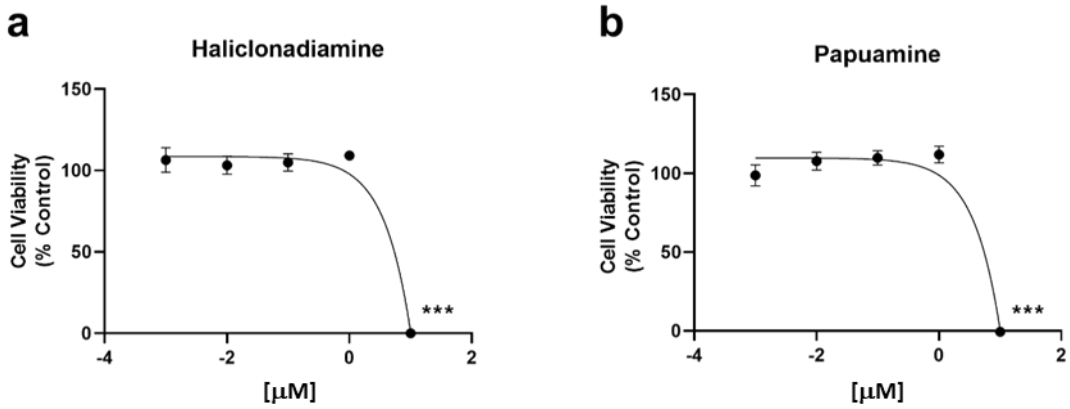

SI Figure 1 Effect of haliclonadiamine and papuamine on cell viability in SHSY5Y cells.

Dose-response curves. Cells were treated with haliclonadiamine (a) and papuamine (b) at different concentrations (0.01, 0.1, 1, and 10 μM) for 6 hours. Cell viability was measured by MTT assay. The values are shown as the difference between control cells *versus* cells treated by ANOVA statistical analysis followed by post hoc Dunnet's t-test.

***p < 0.001.

IC_{50} Haliclonadiamine: 3.69 μM [1.83-7.53]

IC_{50} Papuamine: 3.83 μM [1.82-8.21]

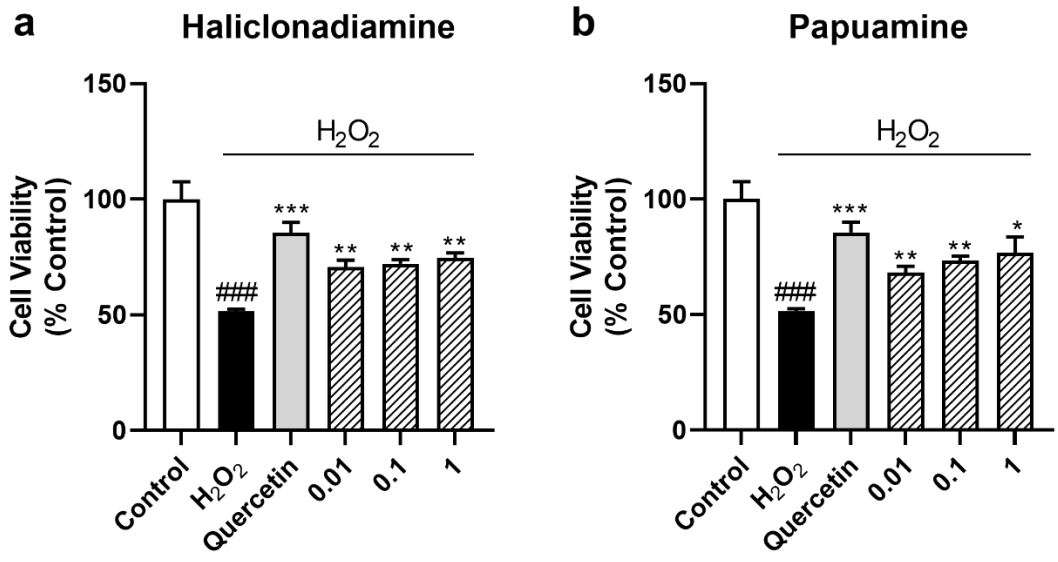

SI Figure 2 Effect of haliclonadiamine and papuamine on oxidative damage in SH-SY5Y cell line.

Cells were treated with haliclonadiamine (a) and papuamine (b) at different concentrations (0.01, 0.1, and 1 μM) in the presence of H_2O_2 (150 μM) for 6 h. Quercetin (10 μM) was used as a positive control. Cell viability was measured by MTT assay. Data are represented as a percentage, being the result of the average of absorbance ± SEM of a minimum of N = 3 independent experiments performed by triplicate. Statistical analysis: ANOVA followed by post hoc Dunnet's t-test. Significant differences between cells treated with H_2O_2 alone *versus* cells treated with compounds in the presence of H_2O_2 (*$p < 0.05$ and **$p < 0.01$) or cells treated with H_2O_2 versus control cells (###$p < 0.001$).

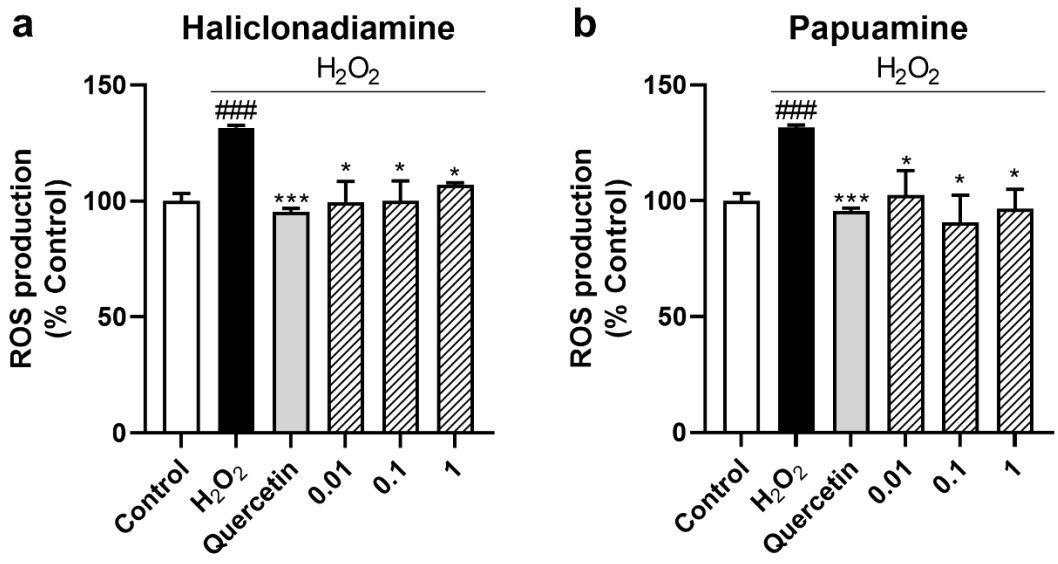

SI Figure 3 (1) Effect of haliclonadiamine and papuamine on intracellular ROS production in SH-SY5Y cell line. (2) Effect of haliclonadiamine and papuamine on intracellular ROS production in SH-SY5Y cell line.

Cells were treated with haliclonadiamine (a) and papuamine (b) at different concentrations (0.01, 0.1, and 1 μM) in the presence of H_2O_2 (150 μM) for 6 h. Quercetin (10 μM) was used as a positive control. ROS levels were measured with DCFH-DA dye. Data are represented as a percentage, being the result of the average of absorbance ± SEM of a minimum of N = 3 independent experiments performed by triplicate. Statistical analysis: ANOVA followed by post hoc Dunnet's t-test. Significant differences between cells treated with H_2O_2 alone *versus* cells treated with compounds in the presence of H_2O_2 (*$p < 0.05$) or cells treated with H_2O_2 versus control cells (###$p < 0.001$).

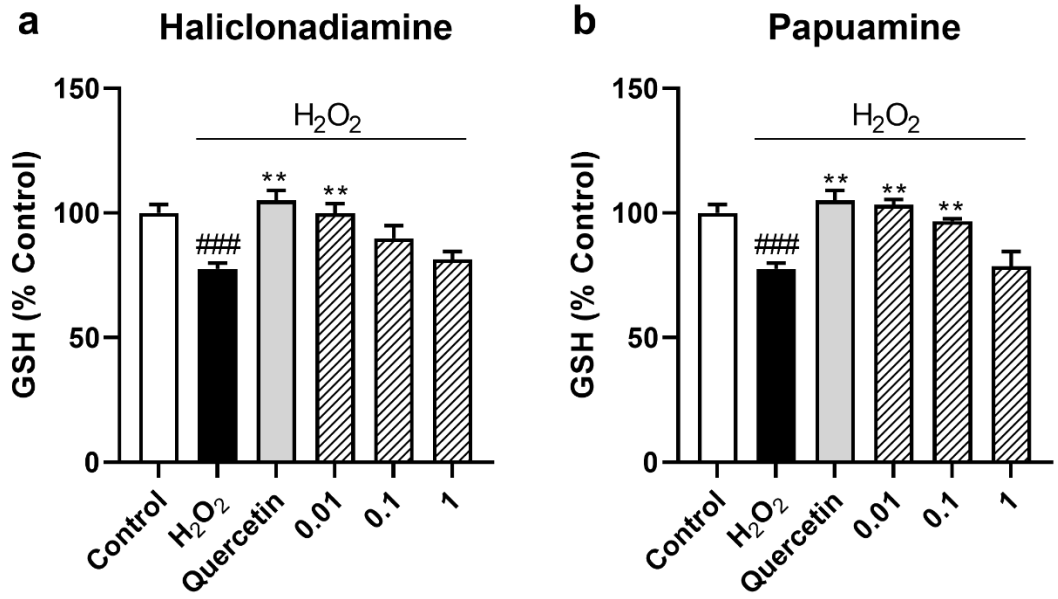

SI Figure 4 Effect of haliclonadiamine and papuamine on antioxidant systems in SH-SY5Y cell line.

Cells were treated with haliclonadiamine (a) and papuamine (b) at different concentrations (0.01, 0.1, and 1 μM) in the presence of H_2O_2 (150 μM) for 6 h. Quercetin (10 μM) was used as a positive control. GSH levels were determined with Thiol Tracker Violet dye. Data are represented as a percentage, being the result of the average of absorbance ± SEM of a minimum of N = 3 independent experiments performed by triplicate. Statistical analysis: ANOVA followed by post hoc Dunnet's t-test. Significant differences between cells treated with H_2O_2 alone *versus* cells treated with compounds in the presence of H_2O_2 (**$p < 0.01$) or cells treated with H_2O_2 versus control cells (###$p < 0.001$).

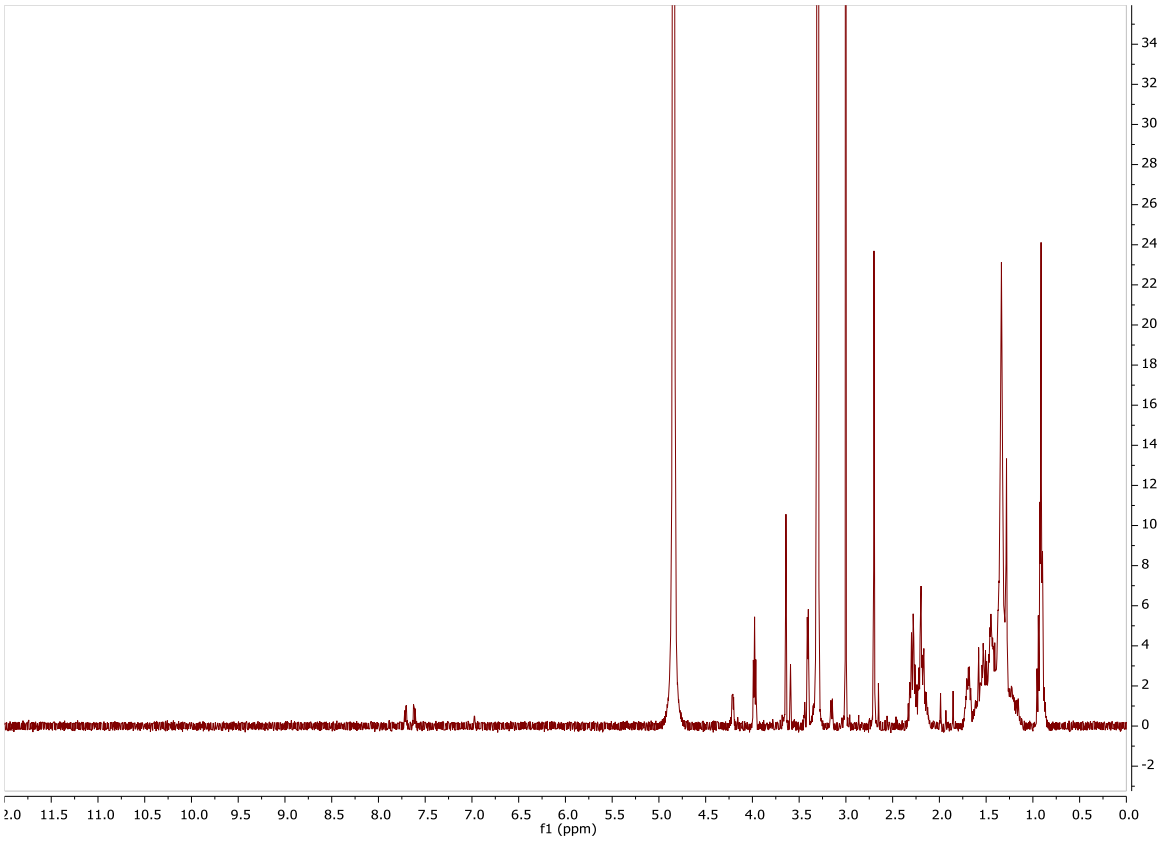

SI Figure 5 ^{1}H NMR spectrum (600 MHz, CD_3OD) of compound **1**

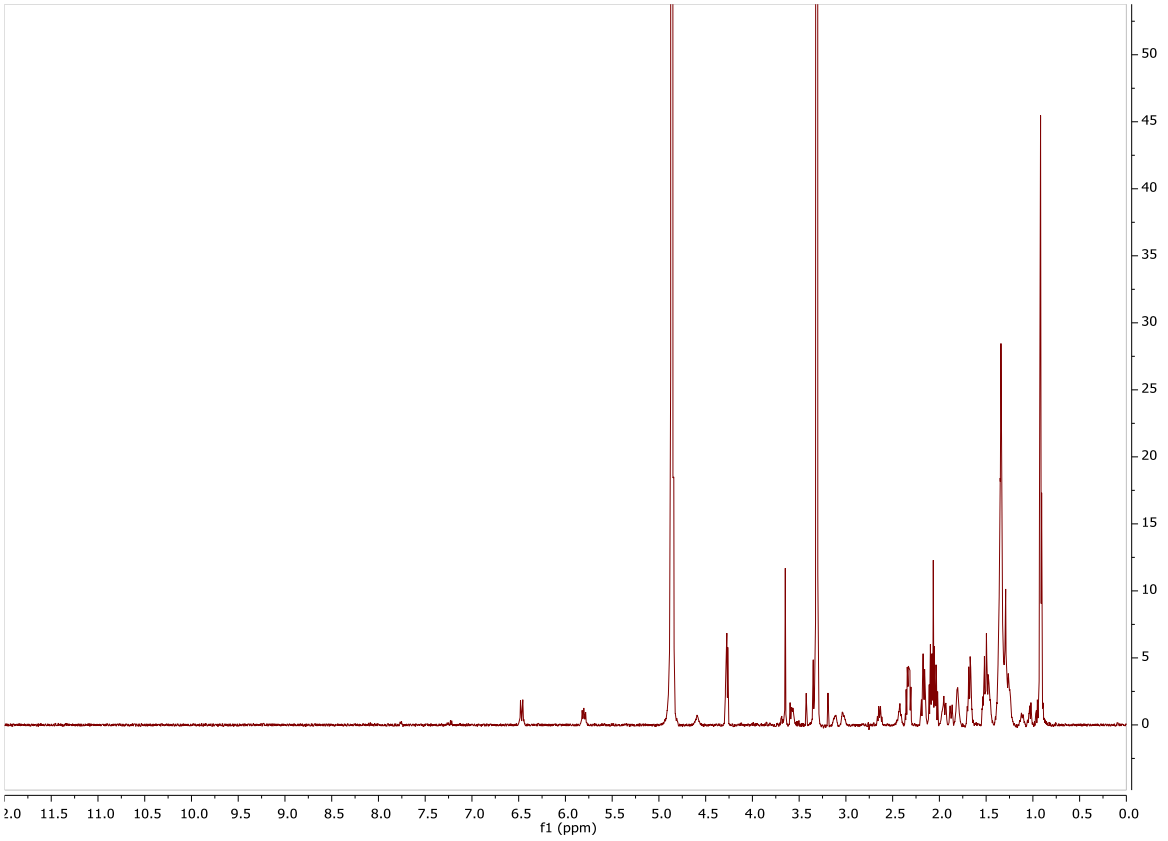

SI Figure 6 ^{1}H NMR spectrum (600 MHz, CD_3OD) of compound **2**

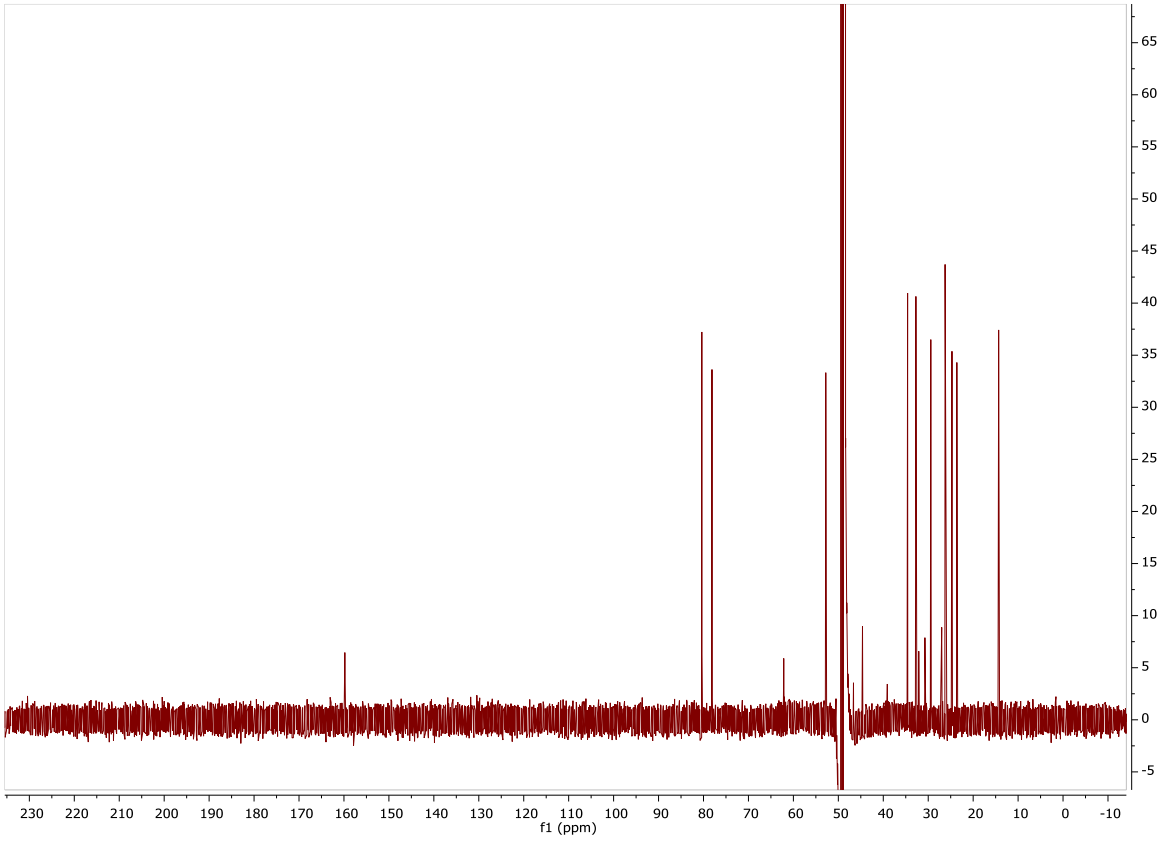

SI Figure 7 ^{13}C NMR spectrum (600 MHz, CD_3OD) of compound **2**

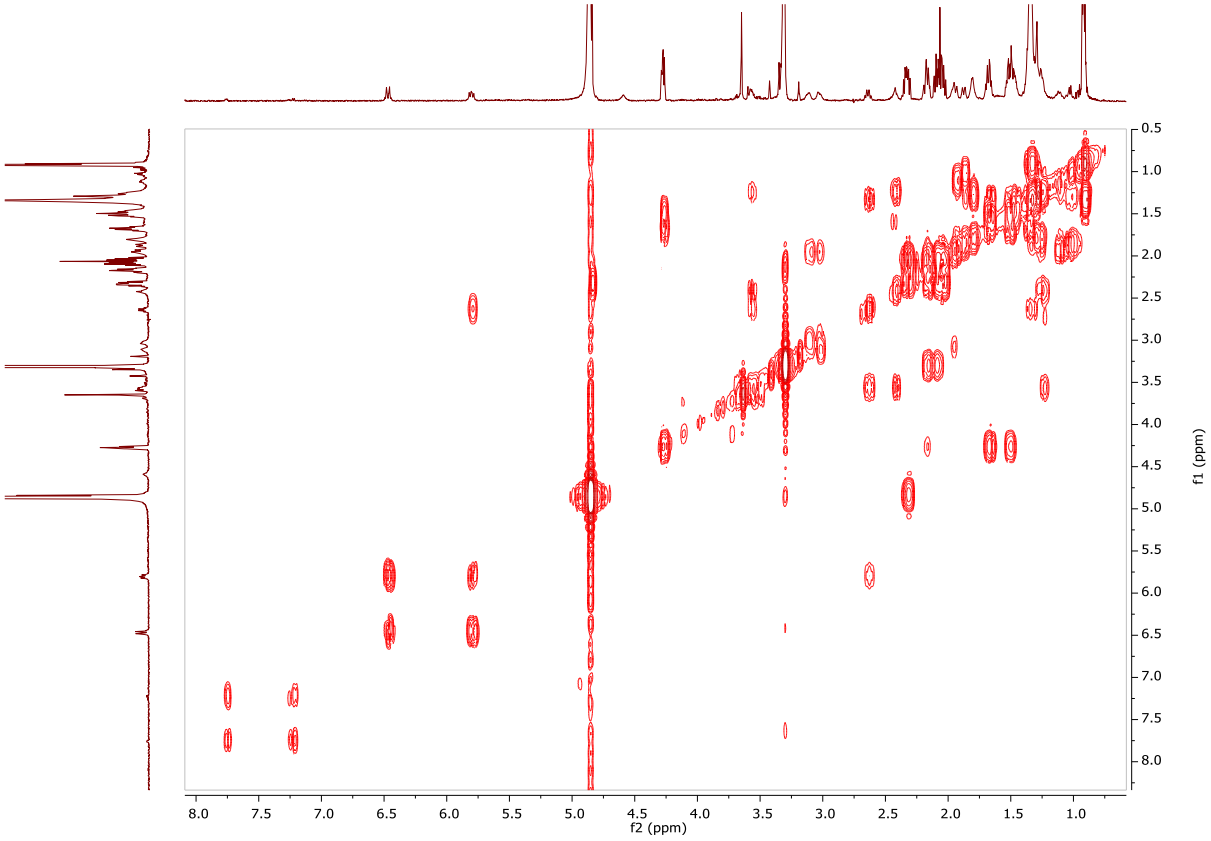

SI Figure 8 COSY spectrum (600 MHz, CD_3OD) of compound **2**

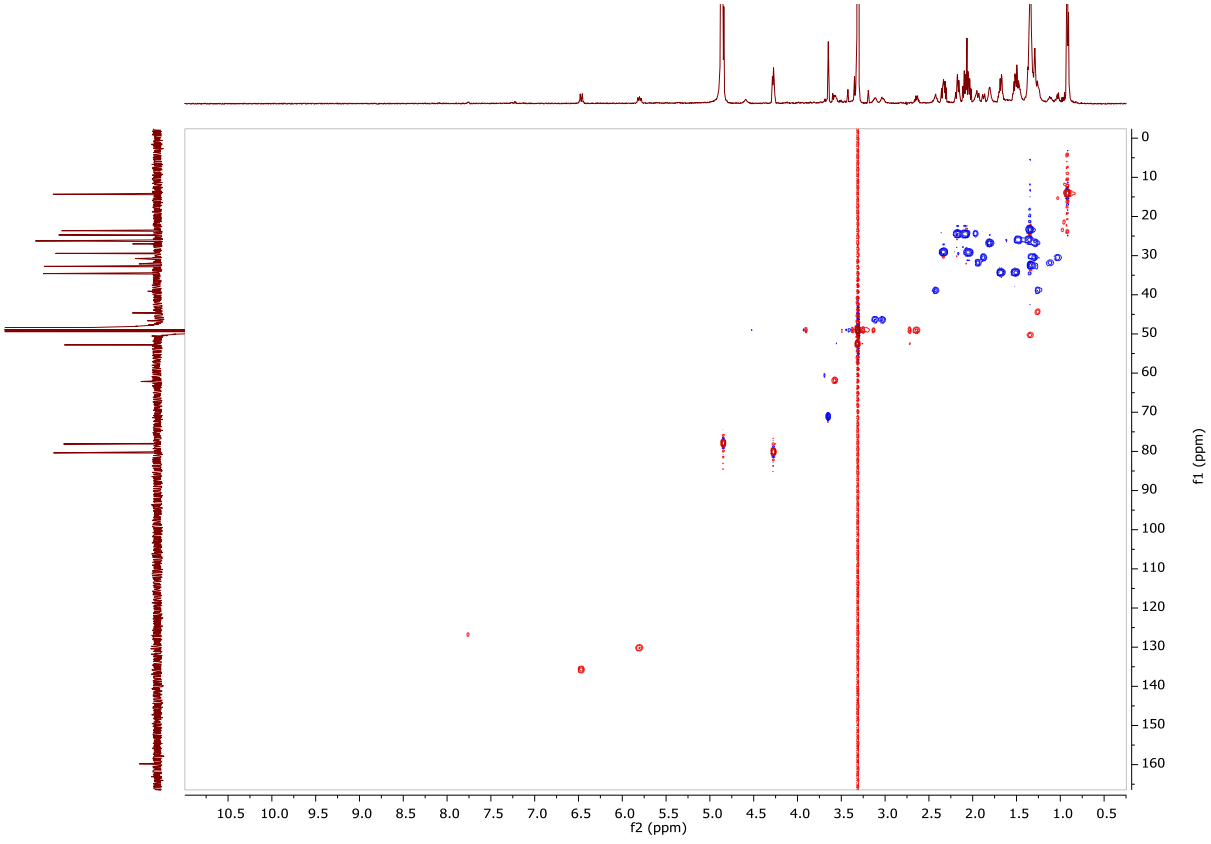

SI Figure 9 HSQC spectrum (600 MHz, CD_3OD) of compound **2**

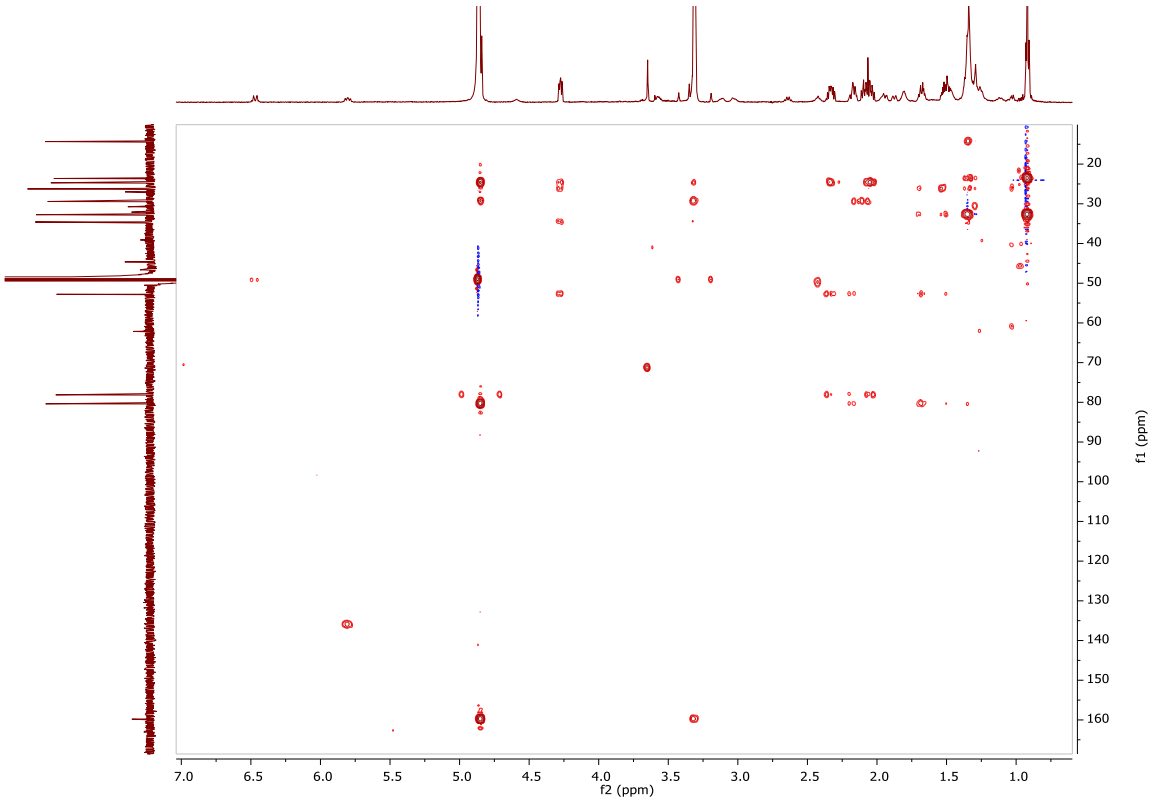

SI Figure 10 HMBC spectrum (600 MHz, CD_3OD) of compound **2**

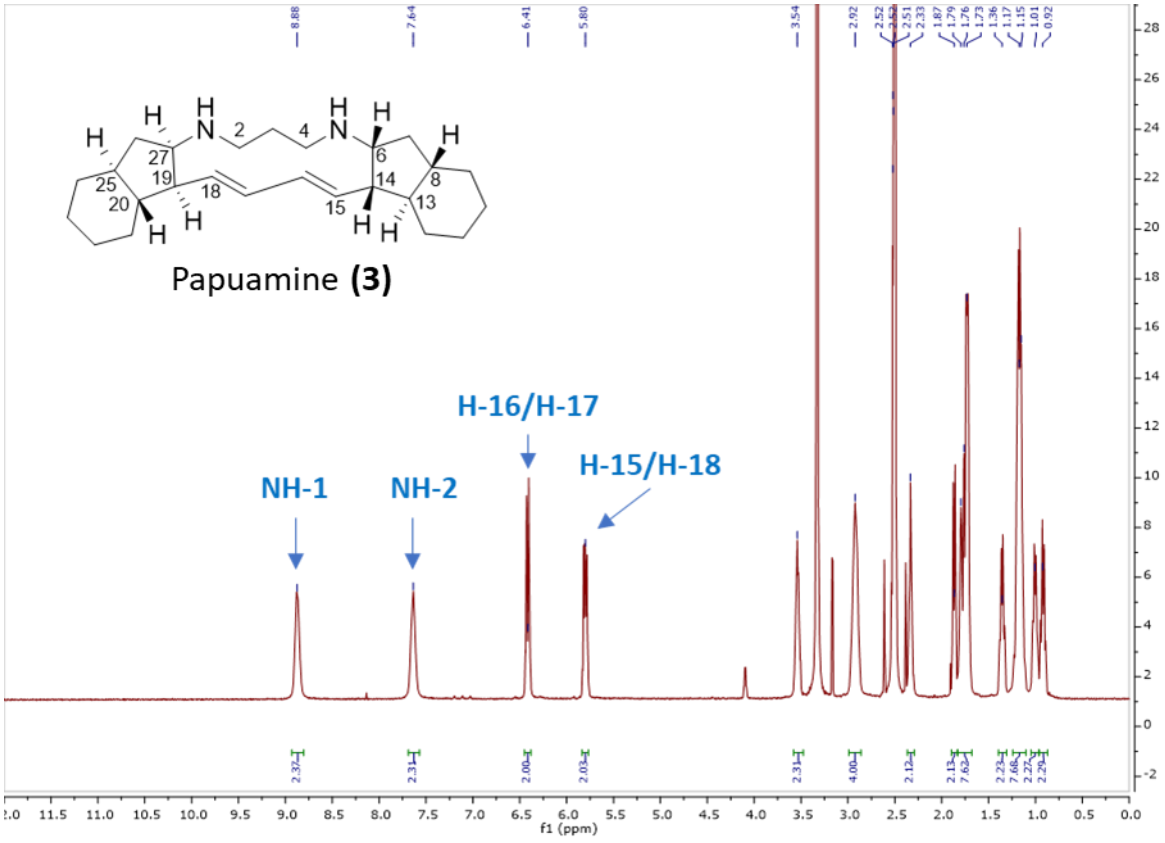

SI Figure 11 ^{1}H NMR spectrum (600 MHz, DMSO-d_6) of compound **3**

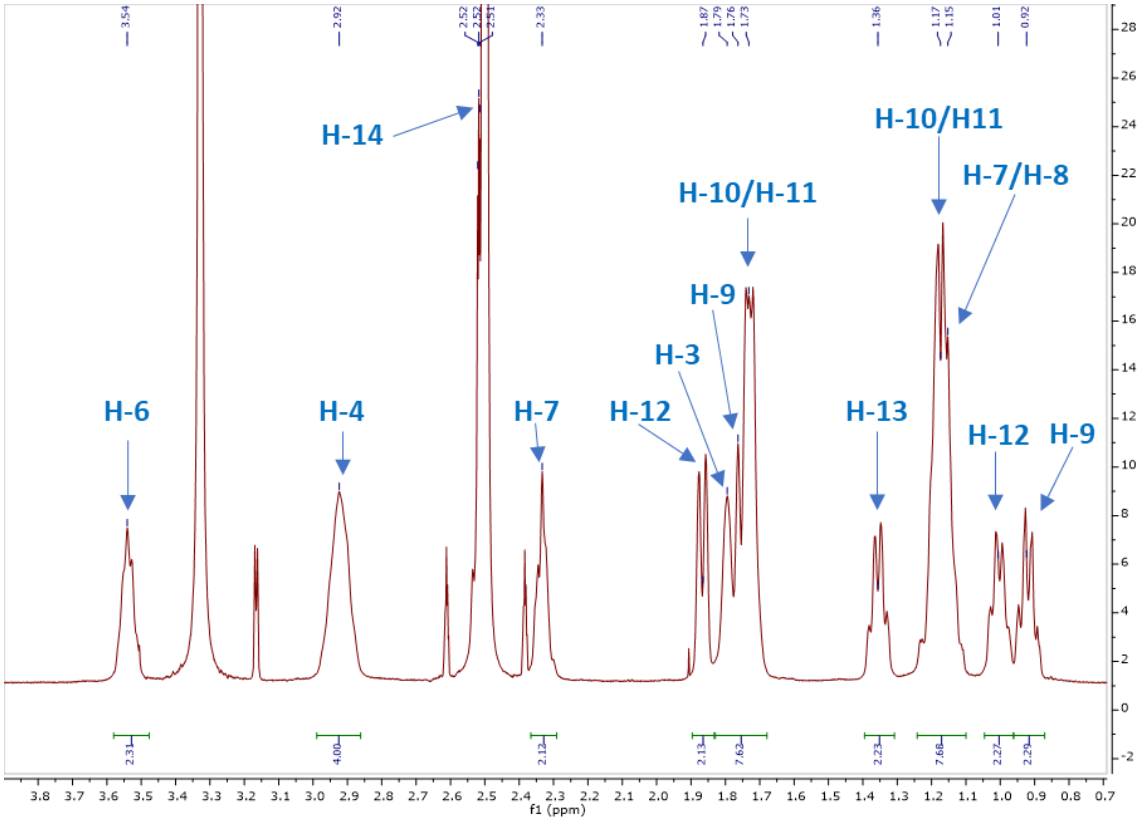

SI Figure 12 Expanded ^{1}H NMR spectrum (600 MHz, DMSO-d_6) of compound **3**

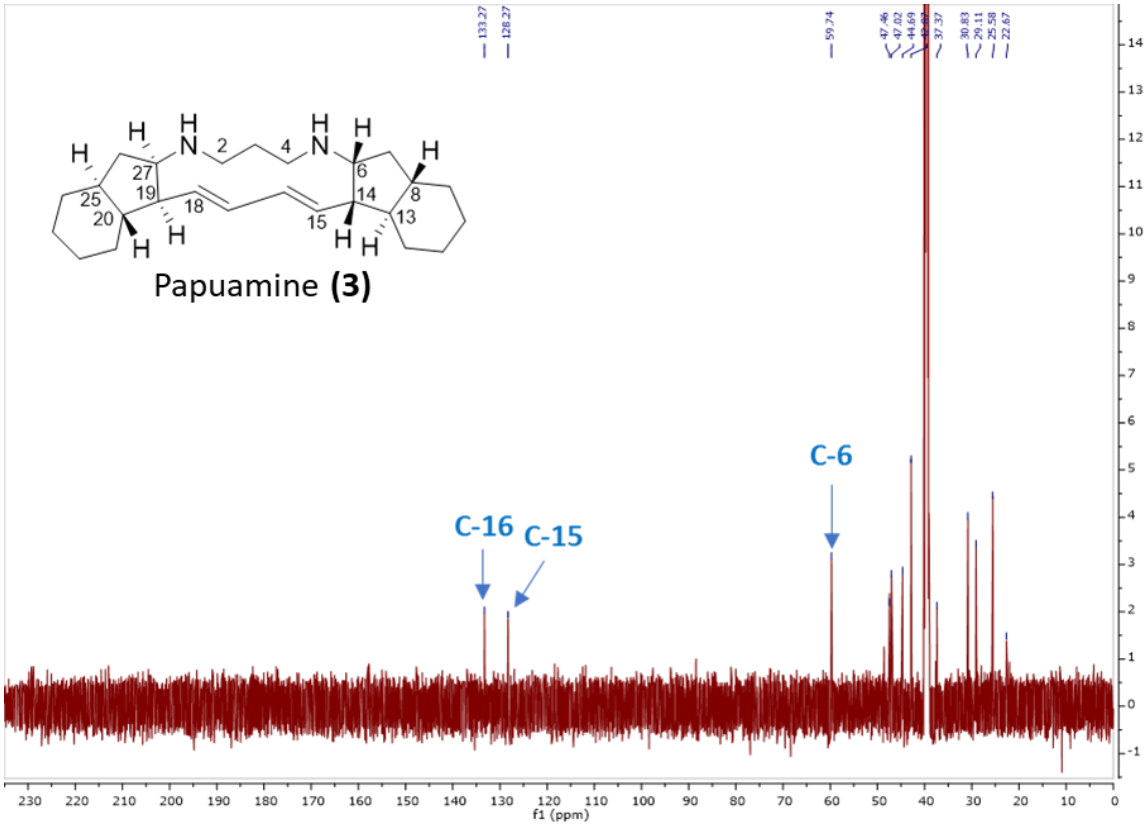

SI Figure 13 ^{13}C NMR spectrum (150 MHz, DMSO-d_6) of compound **3**

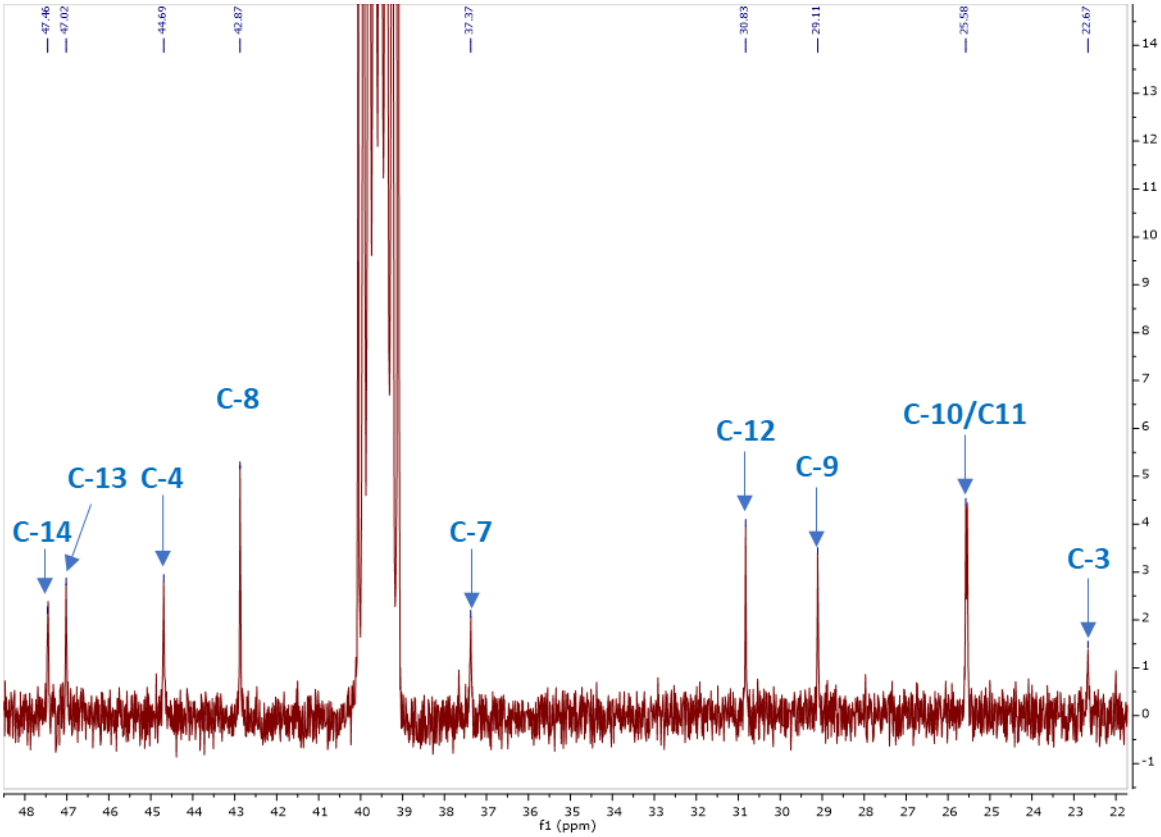

SI Figure 14 Expanded ^{13}C NMR spectrum (150 MHz, DMSO-d_6) of compound **3**

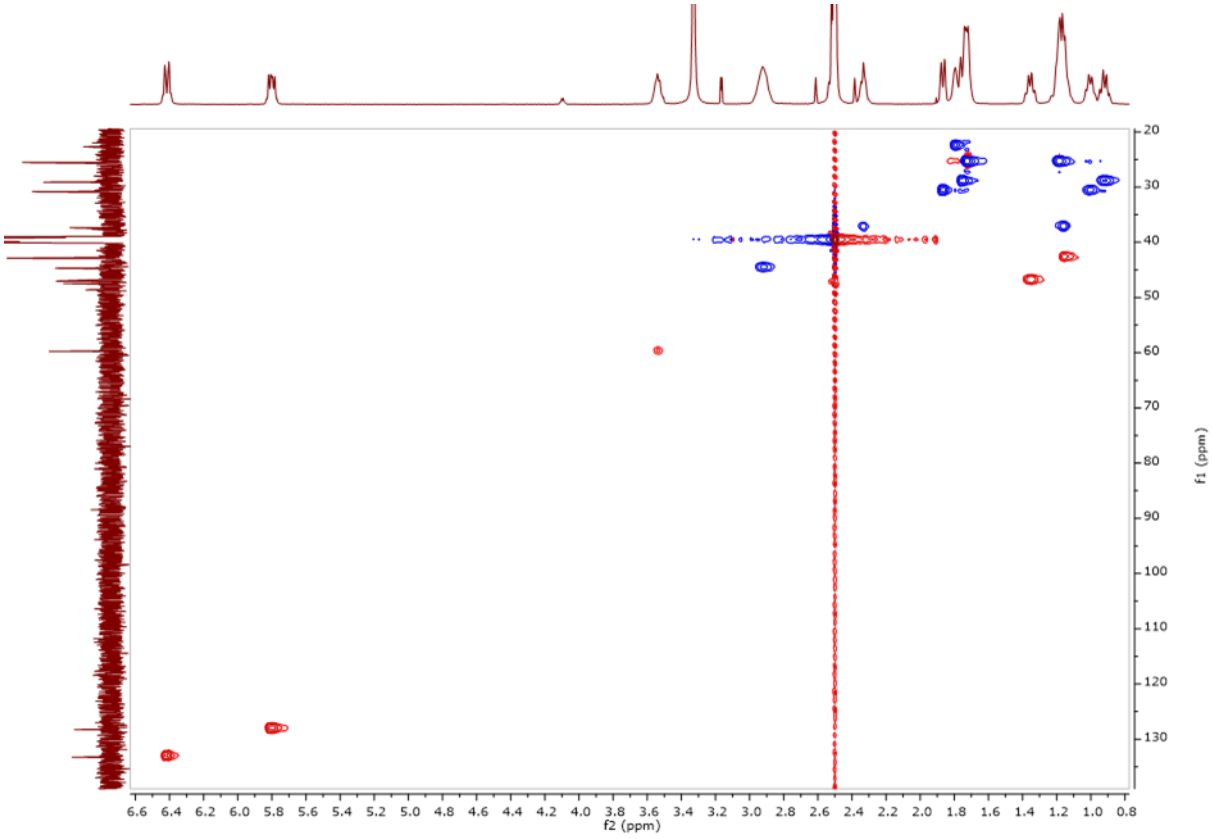

SI Figure 15 HSQC spectrum (600 MHz, DMSO-d_6) of compound **3**

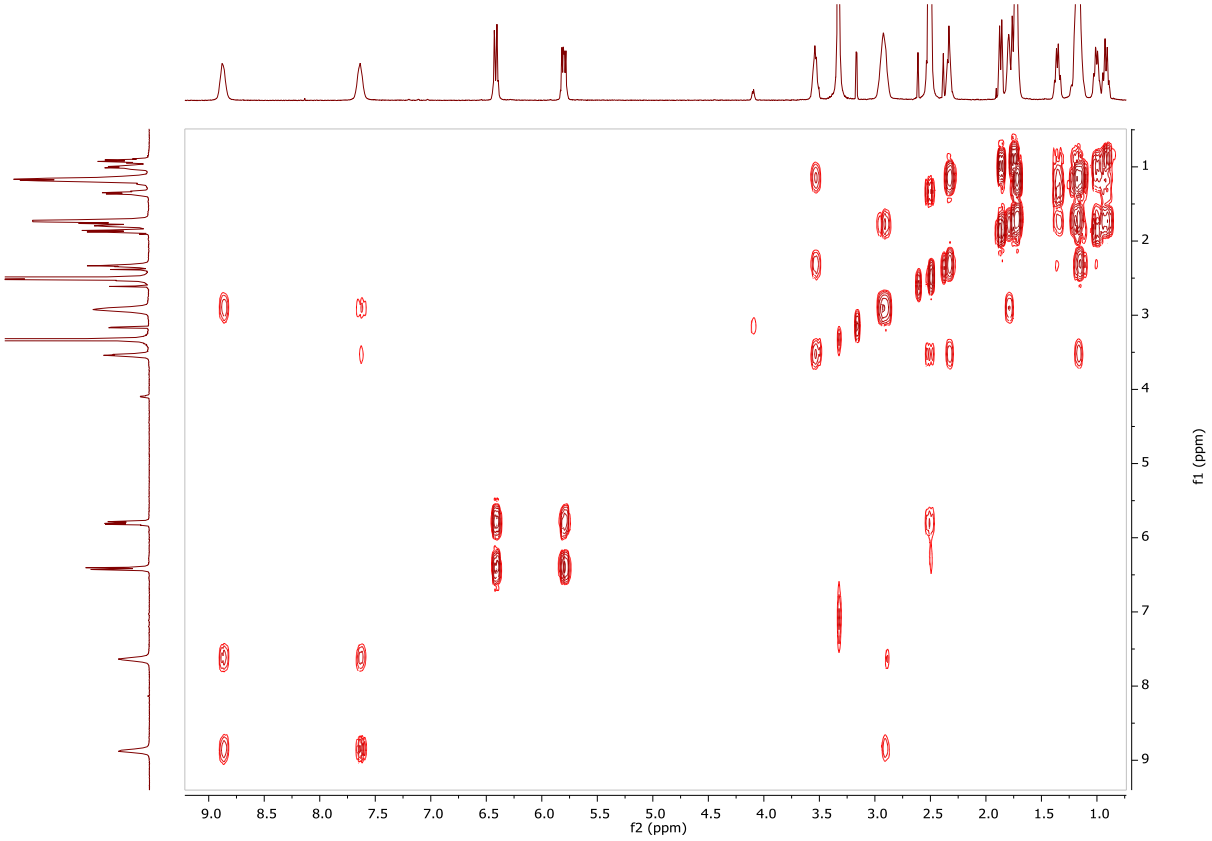

SI Figure 16 ^{1}H-^{1}H COSY spectrum (600 MHz, DMSO-d_6) for compound **3**

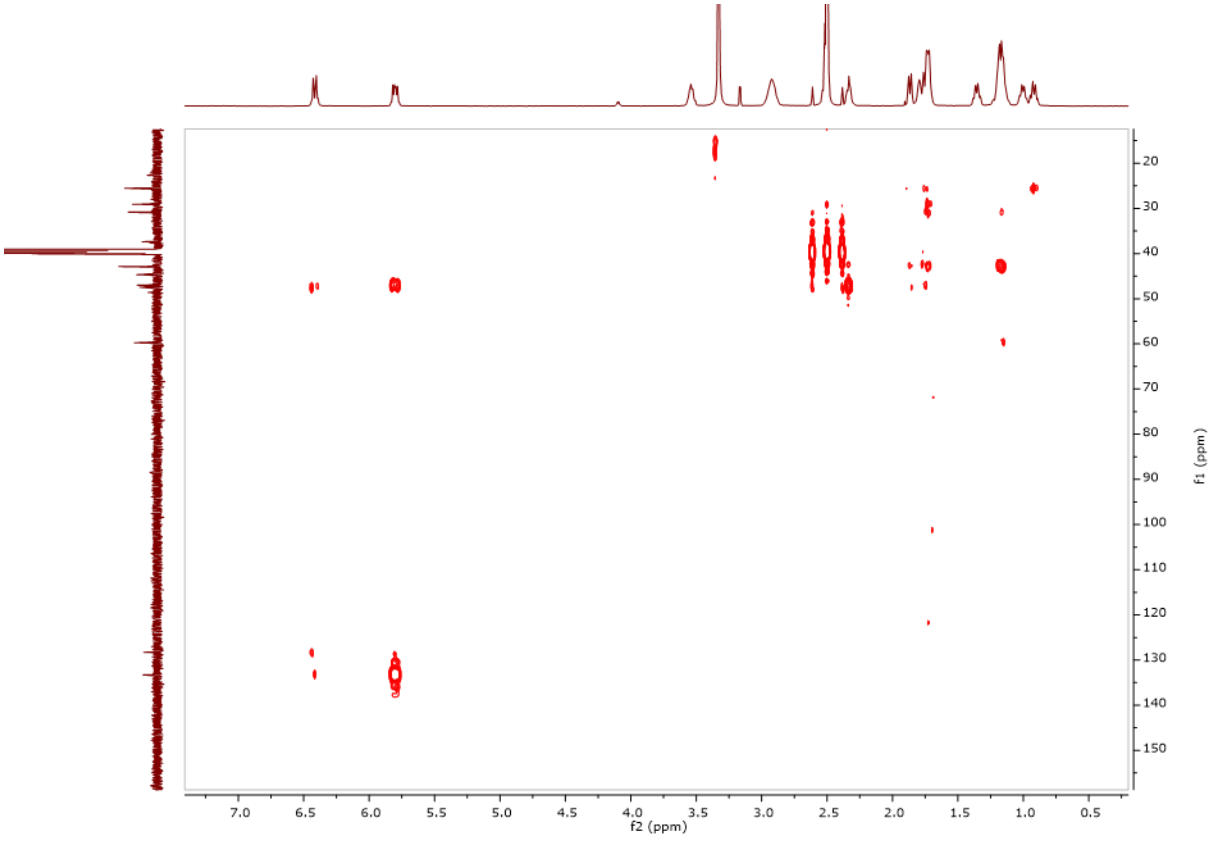

SI Figure 17 HMBC spectrum (600 MHz, DMSO-d_6) for compound **3**

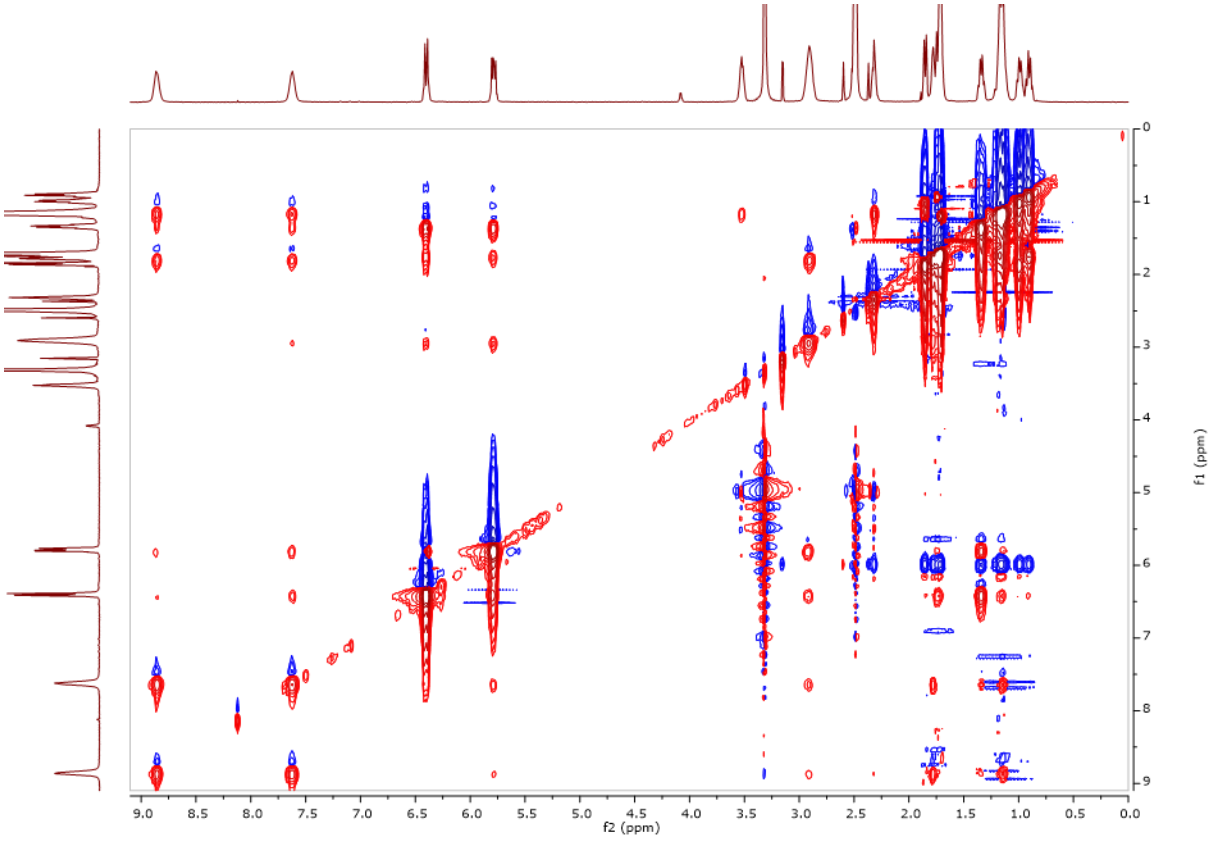

SI Figure 18 NOESY spectrum (600 MHz, DMSO-d_6) for compound **3**

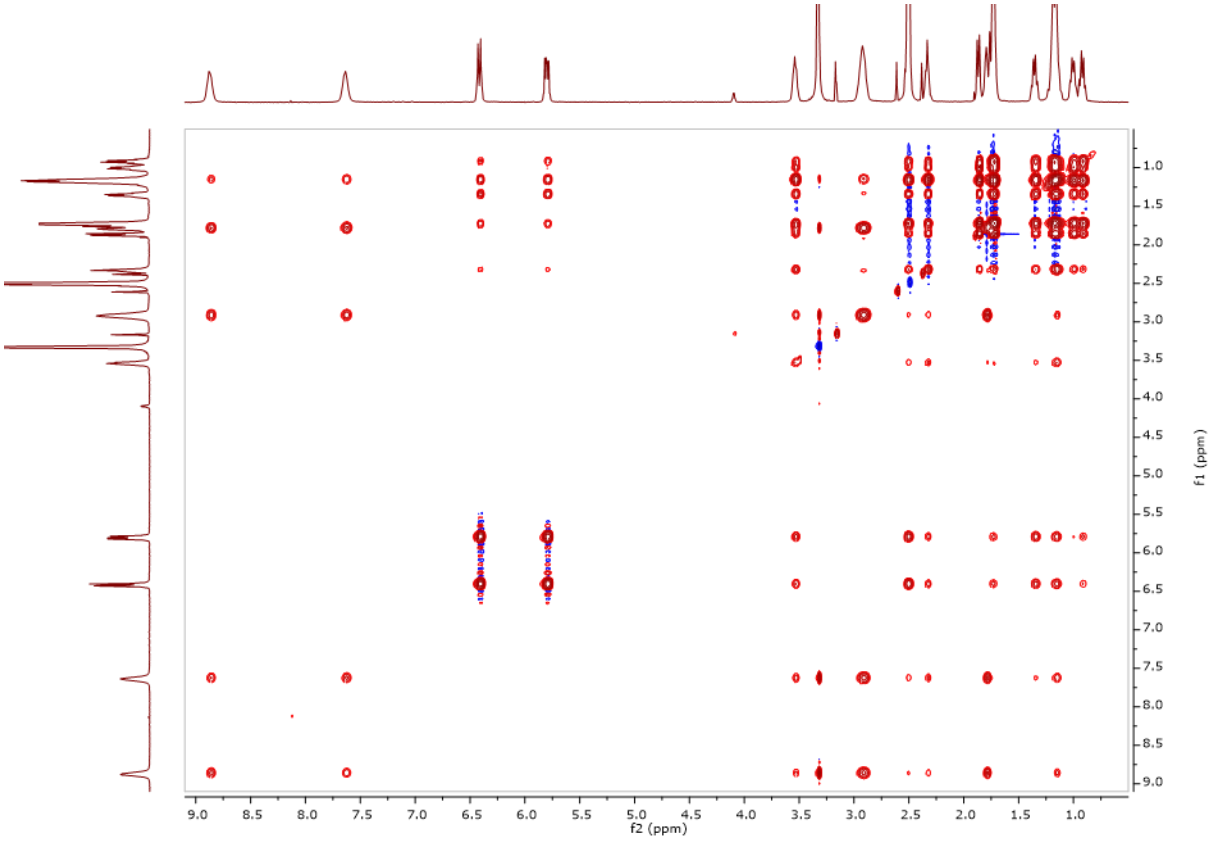

SI Figure 19 TOCSY spectrum (600 MHz, DMSO-d_6) for compound 3

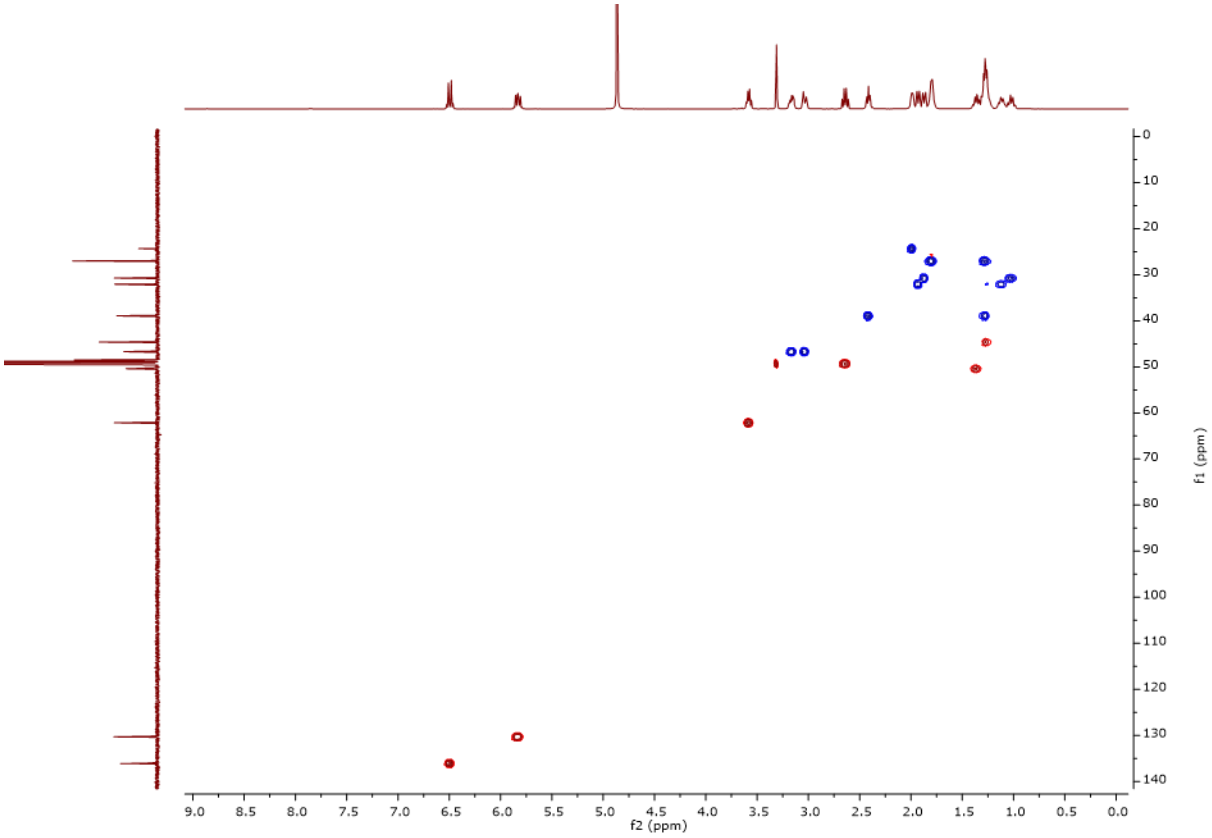

SI Figure 20 HSQC spectrum (500 MHz, CD_3OD) of compound **3**

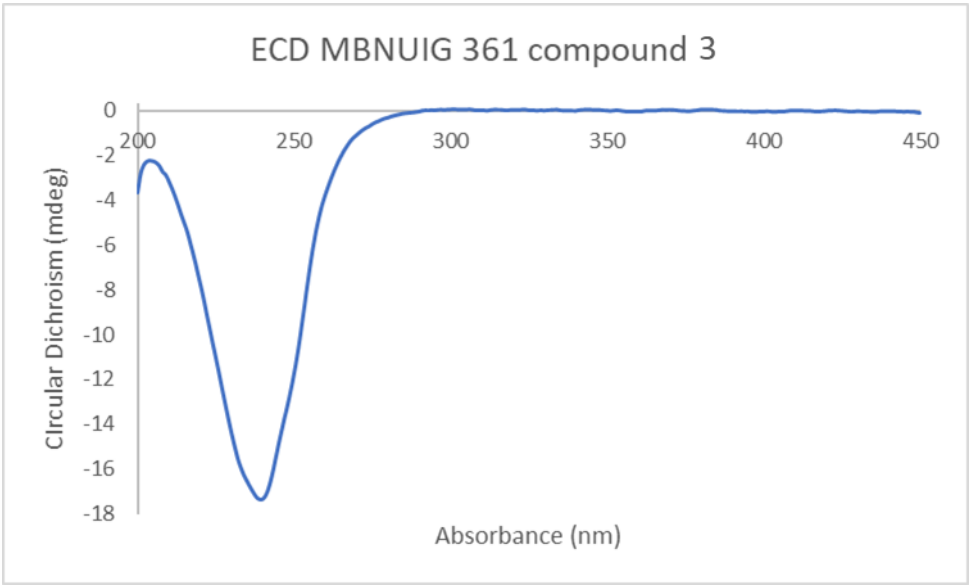

SI Figure 21 ECD spectrum (c 0.016 $mg.mL^{-1}$, MeOH) of compound **3**

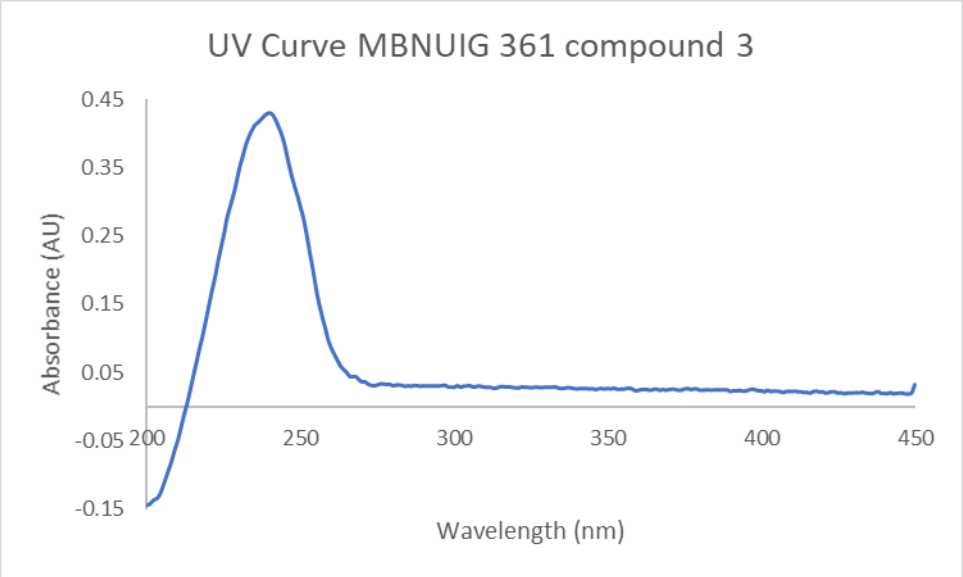

SI Figure 22 UV curve (c 0.016 mg.mL^{-1}, MeOH) of compound **3**

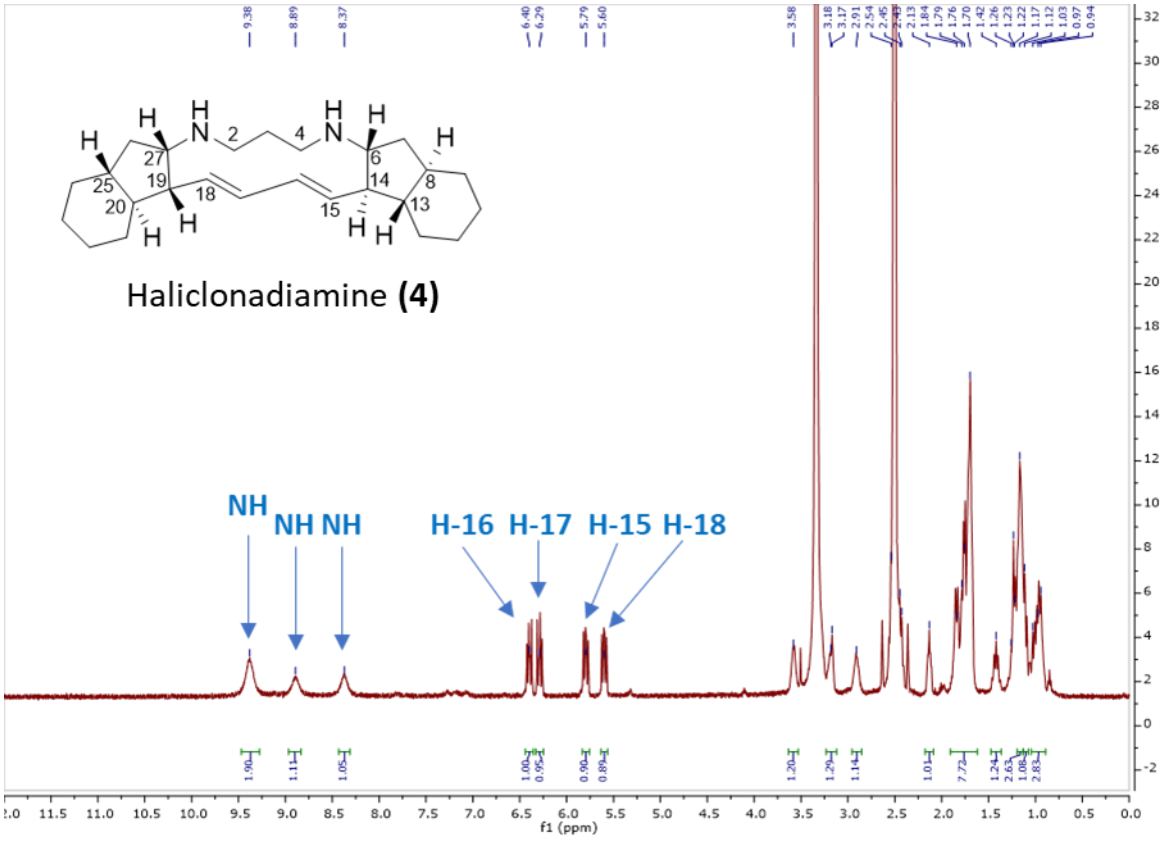

SI Figure 23 ^{1}H NMR spectrum (500 MHz, DMSO-d$_6$) of compound **4**

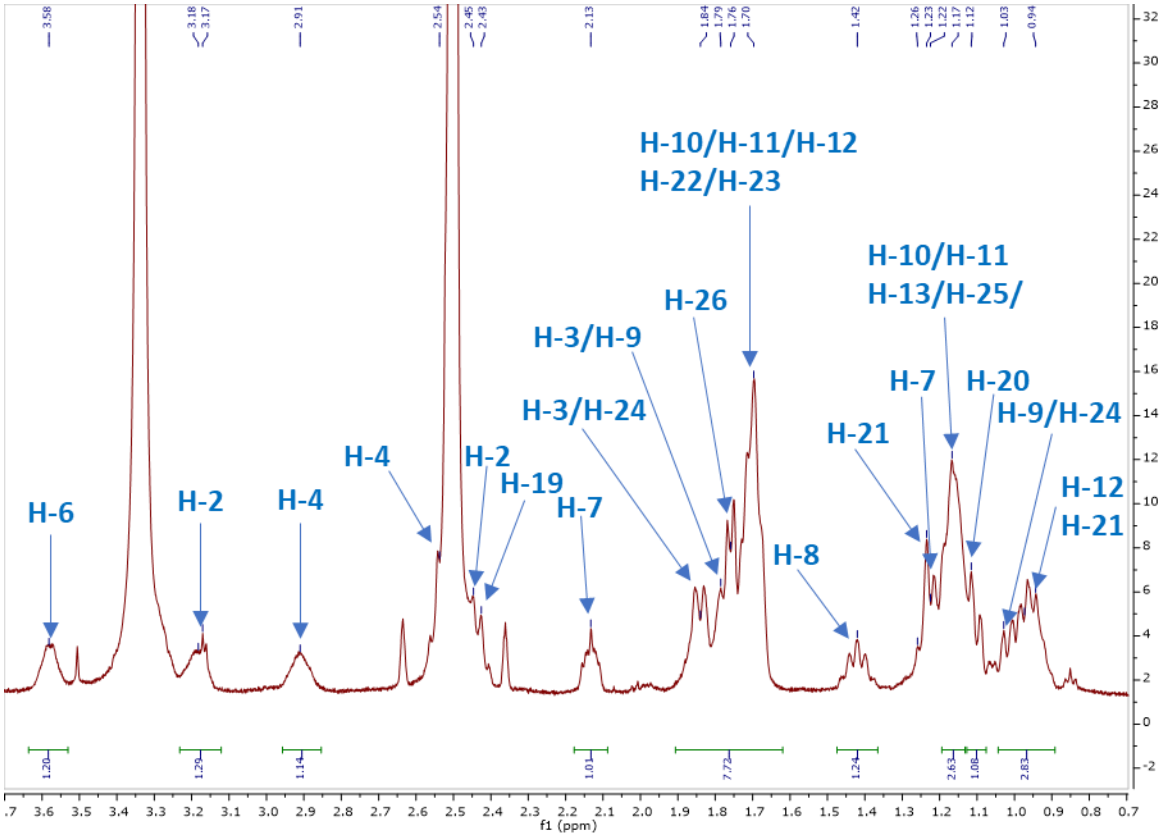

SI Figure 24 Expanded ^{1}H NMR spectrum (500 MHz, DMSO-d_6) of compound **4**

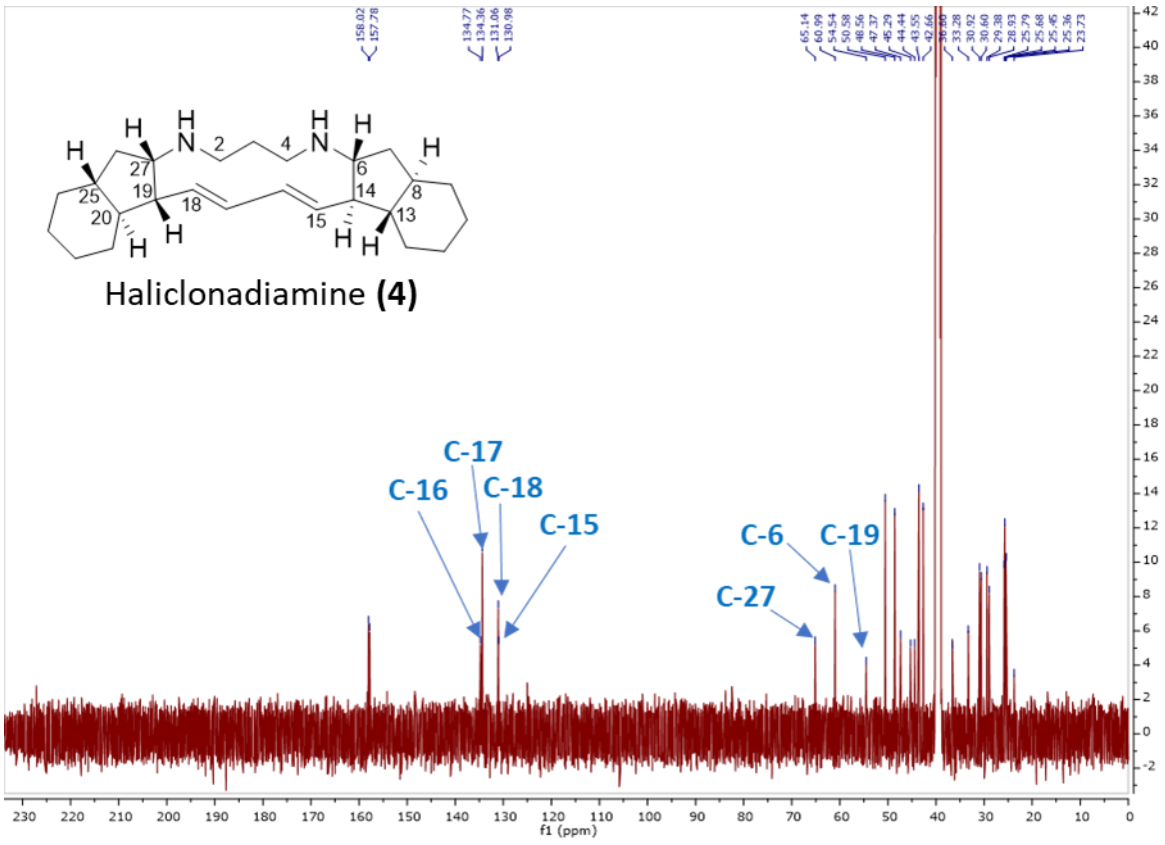

SI Figure 25 13C NMR spectrum (150 MHz, DMSO-d6) of compound 4

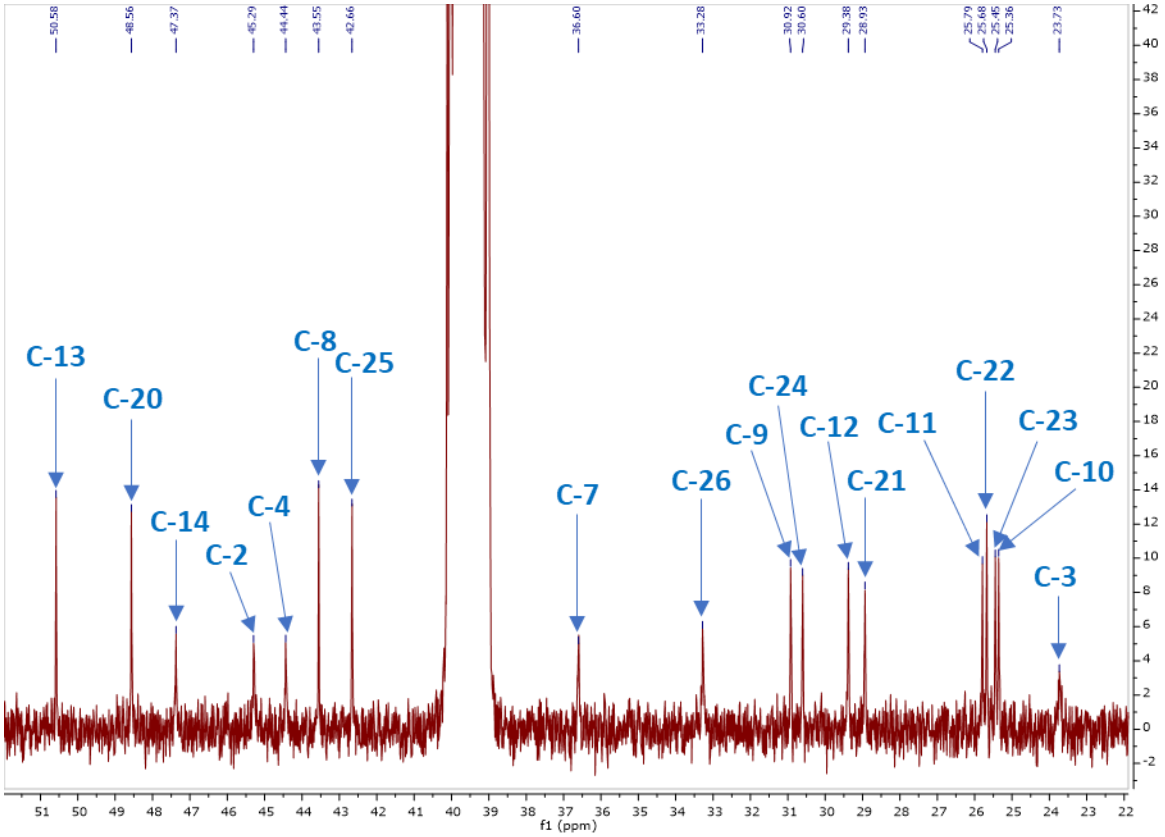

SI Figure 26 ^{13}C NMR spectrum (150 MHz, DMSO-d_6) of compound **4**

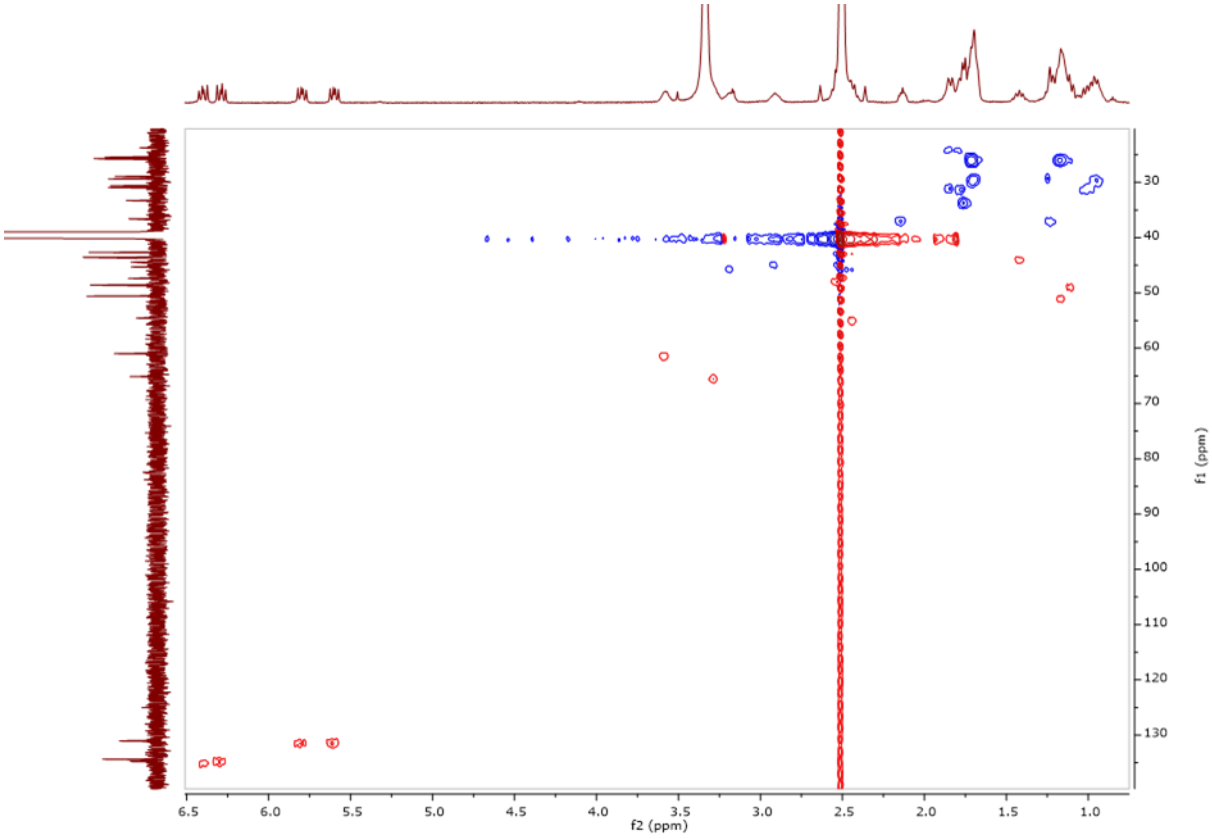

SI Figure 27 HSQC spectrum (500 MHz, DMSO-d_6) of compound **4**

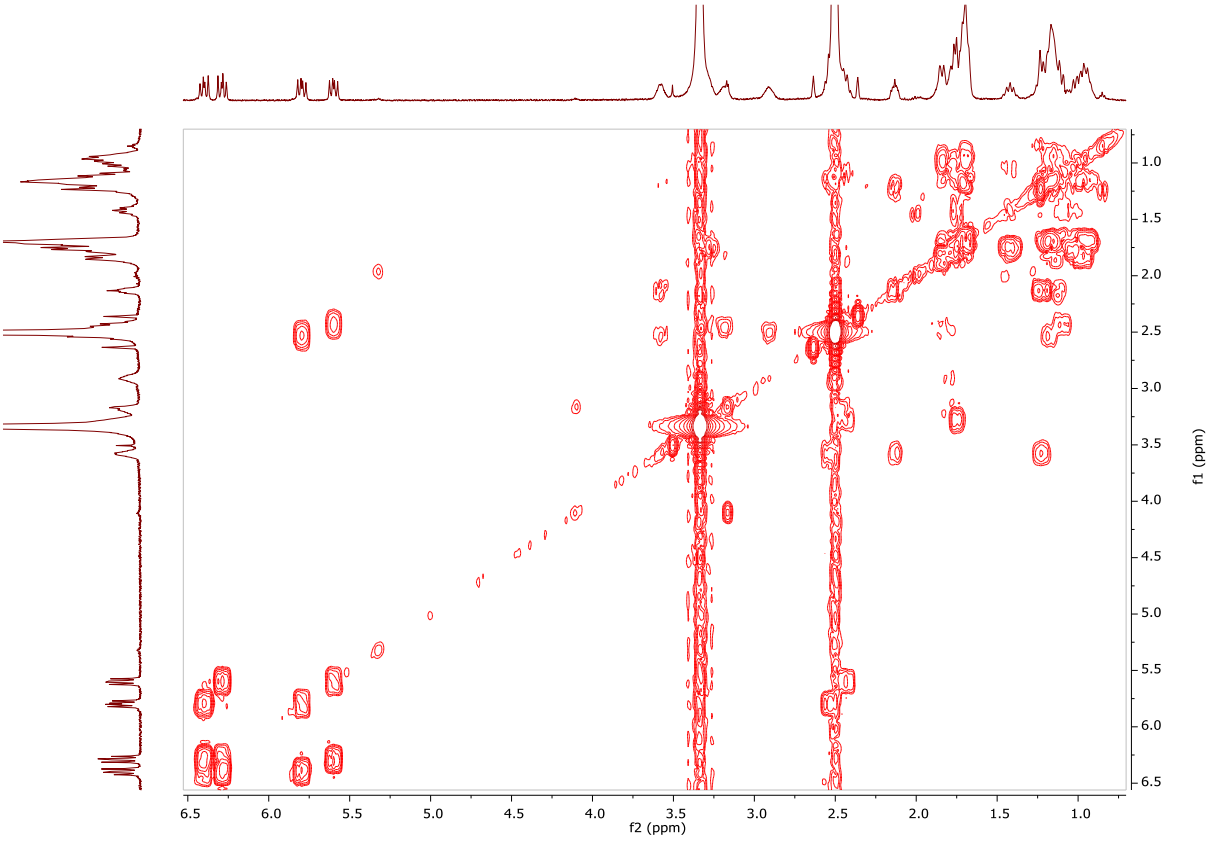

SI Figure 28 ^{1}H-^{1}H COSY spectrum (500 MHz, DMSO-d_6) of compound **4**

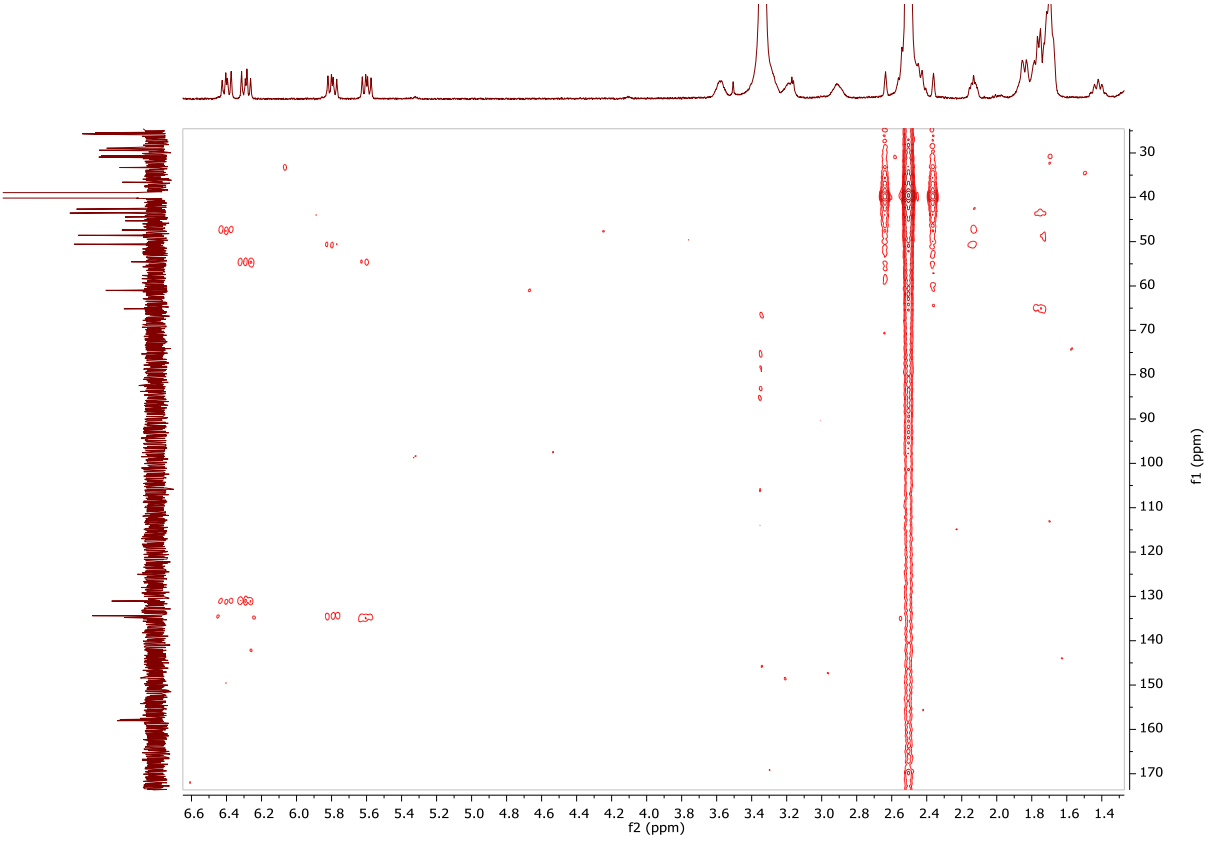

SI Figure 29 HMBC spectrum (500 MHz, DMSO-d_6) of compound **4**

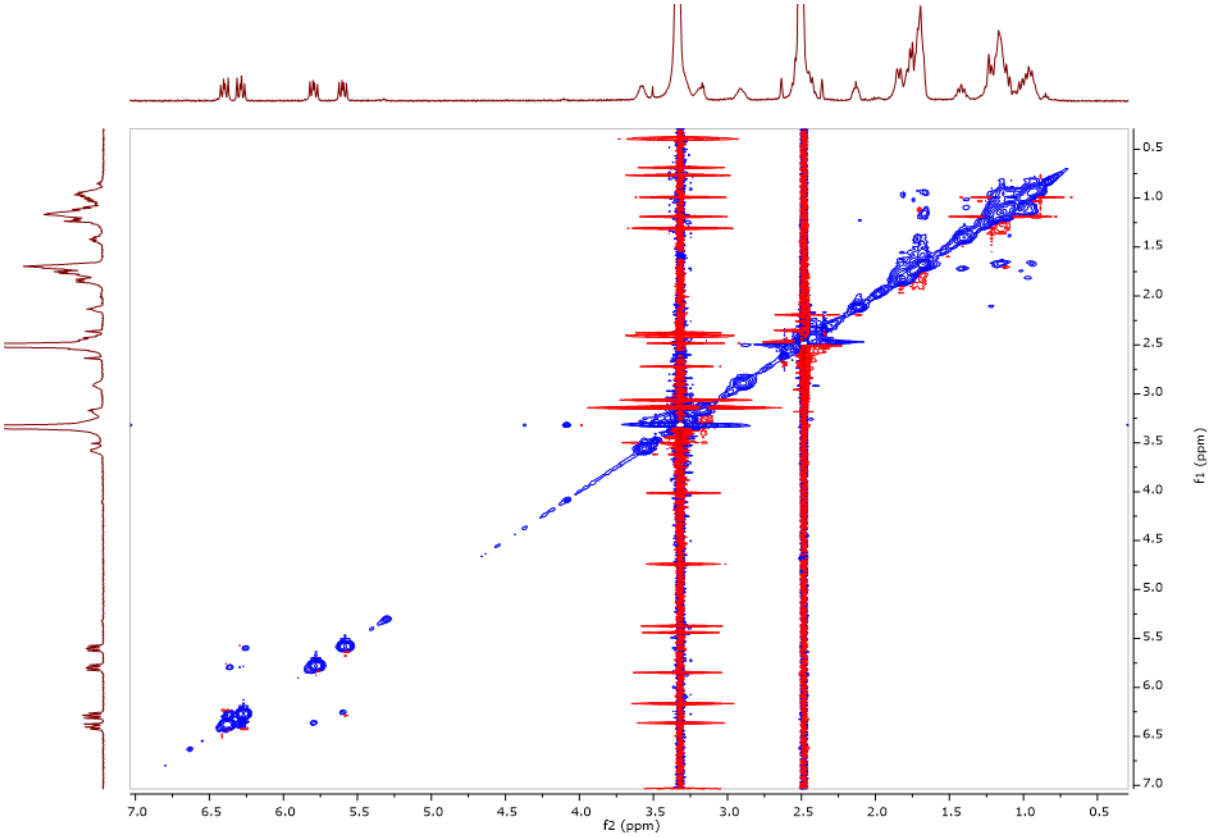

SI Figure 30 NOESY spectrum (500 MHz, DMSO-d_6) of compound **4**

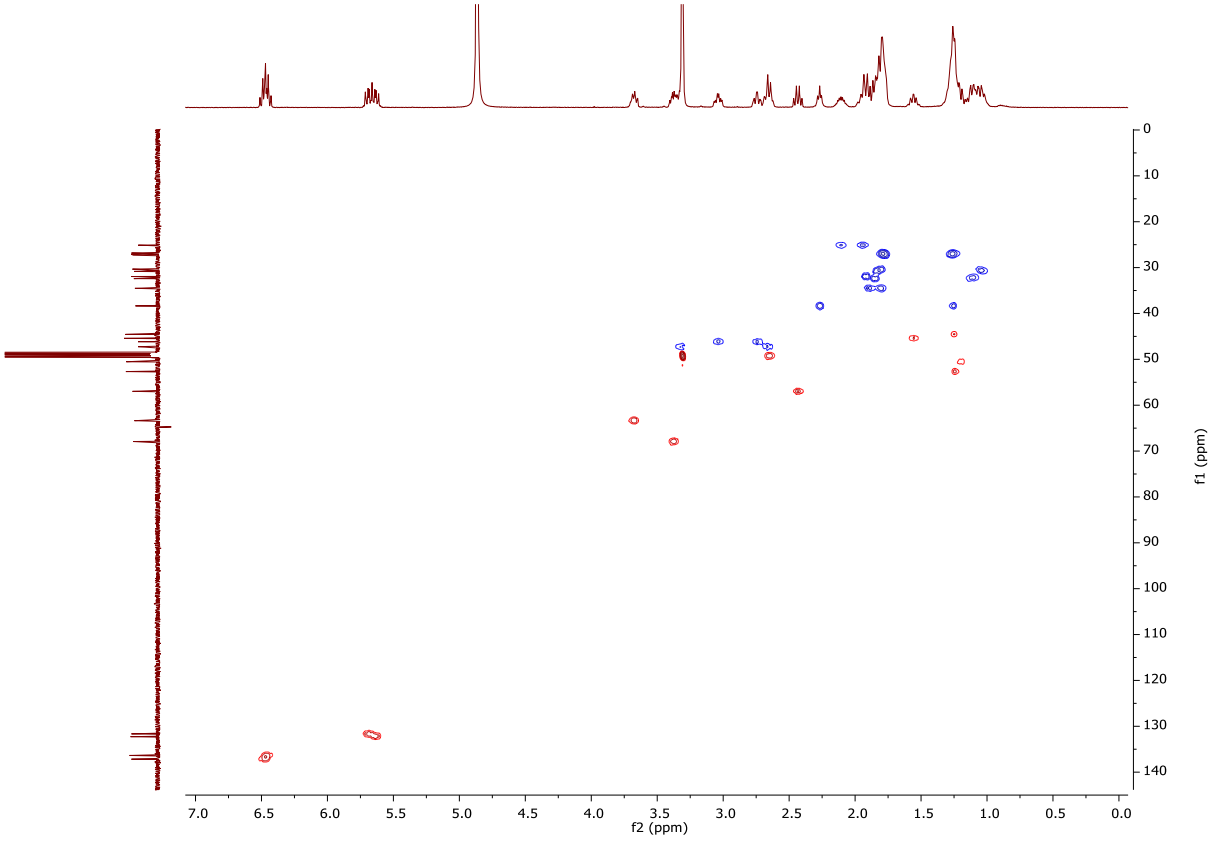

SI Figure 31 HSQC spectrum (500 MHz, CD_3OD) of compound **4**

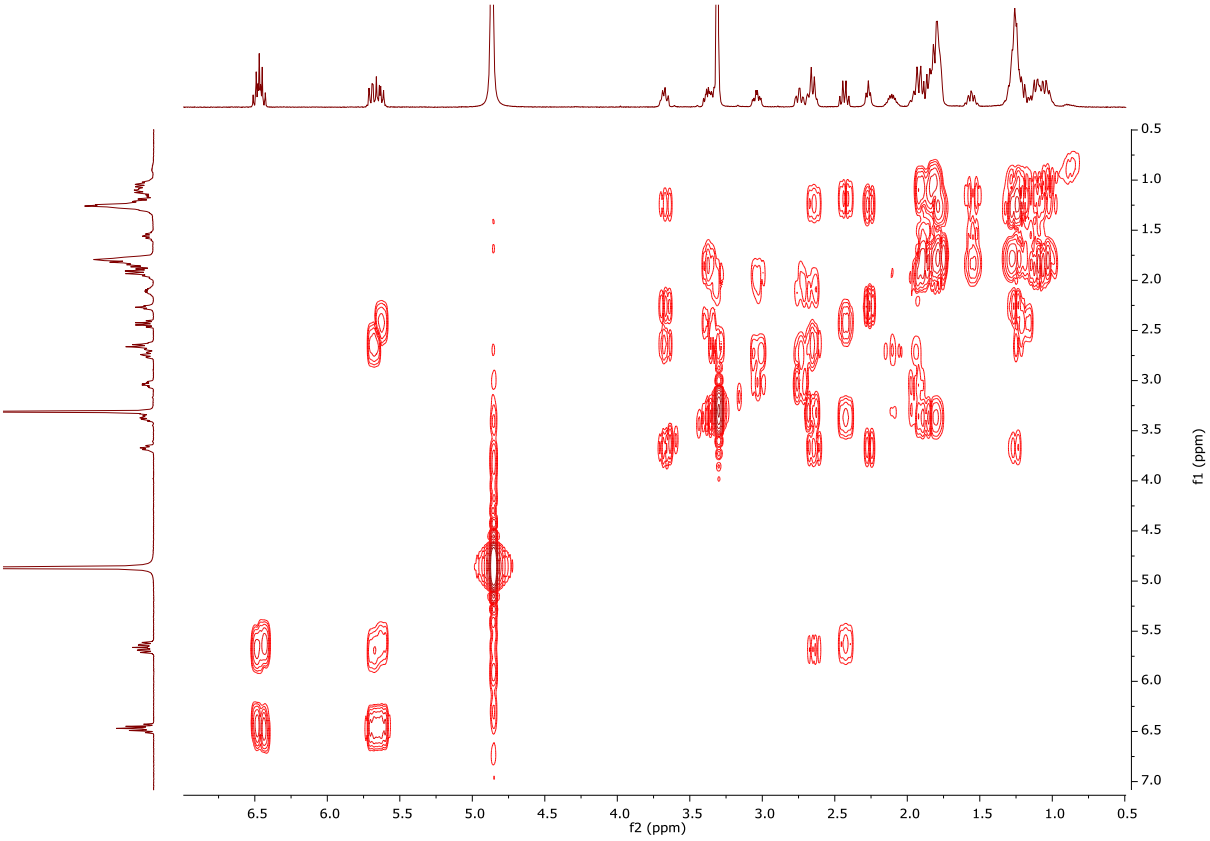

SI Figure 32 ^{1}H-^{1}H COSY spectrum (500 MHz, CD_3OD) of compound **4**

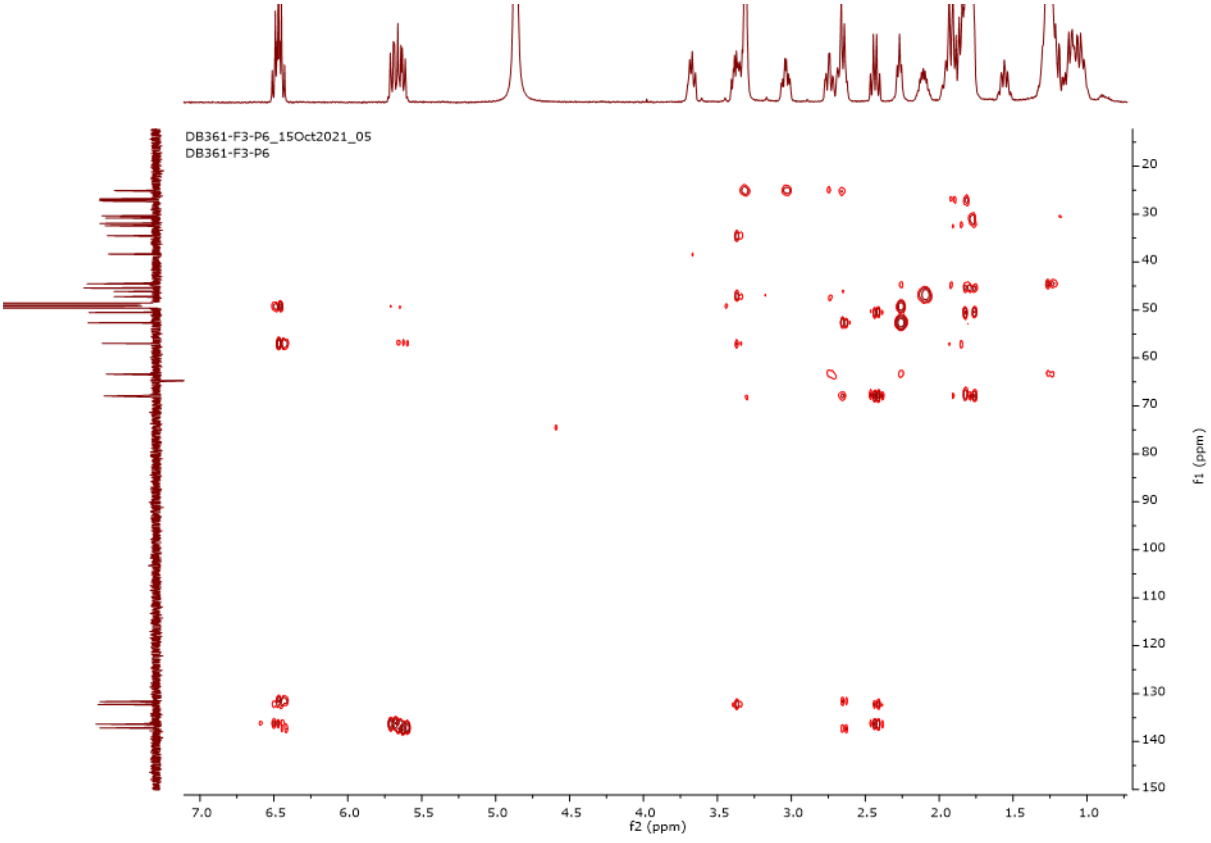

SI Figure 33 HMBC spectrum (500 MHz, CD_3OD) of compound **4**

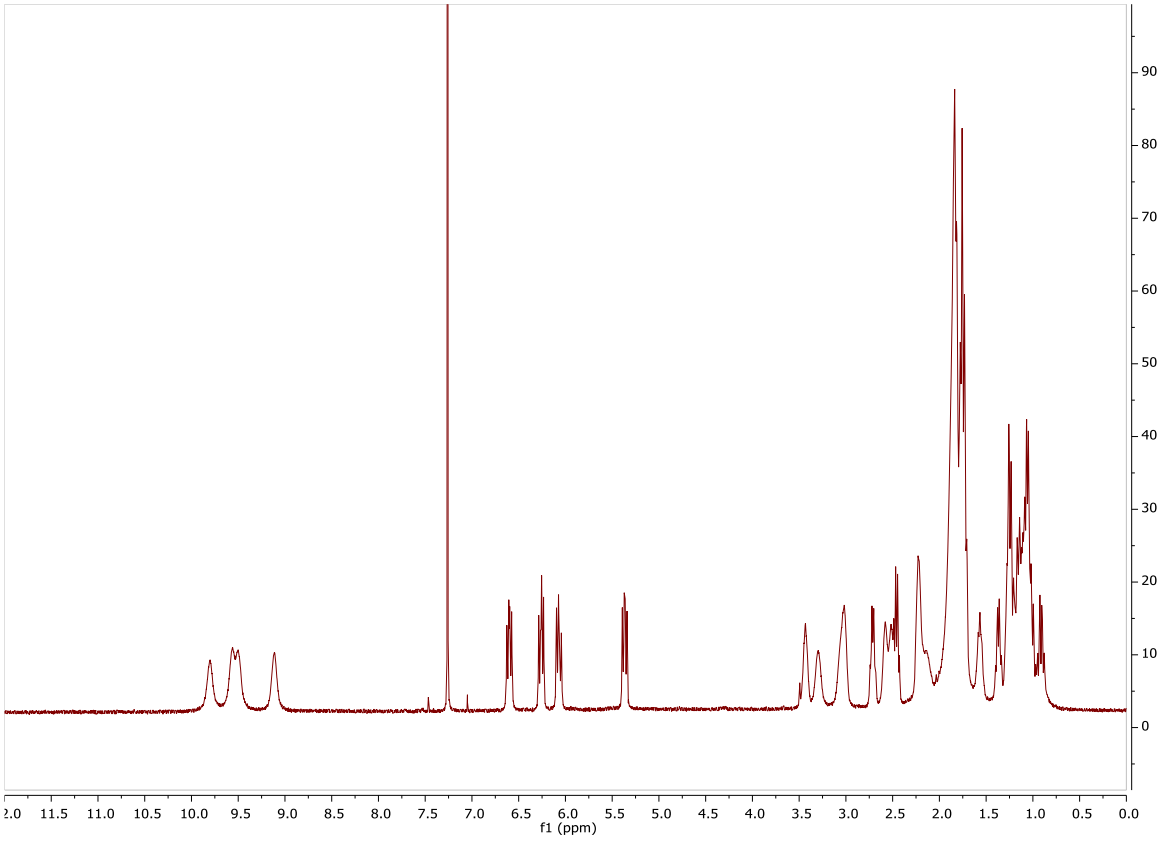

SI Figure 34 ^{1}H NMR (600 MHz, $CDCl_3$) of compound **4**

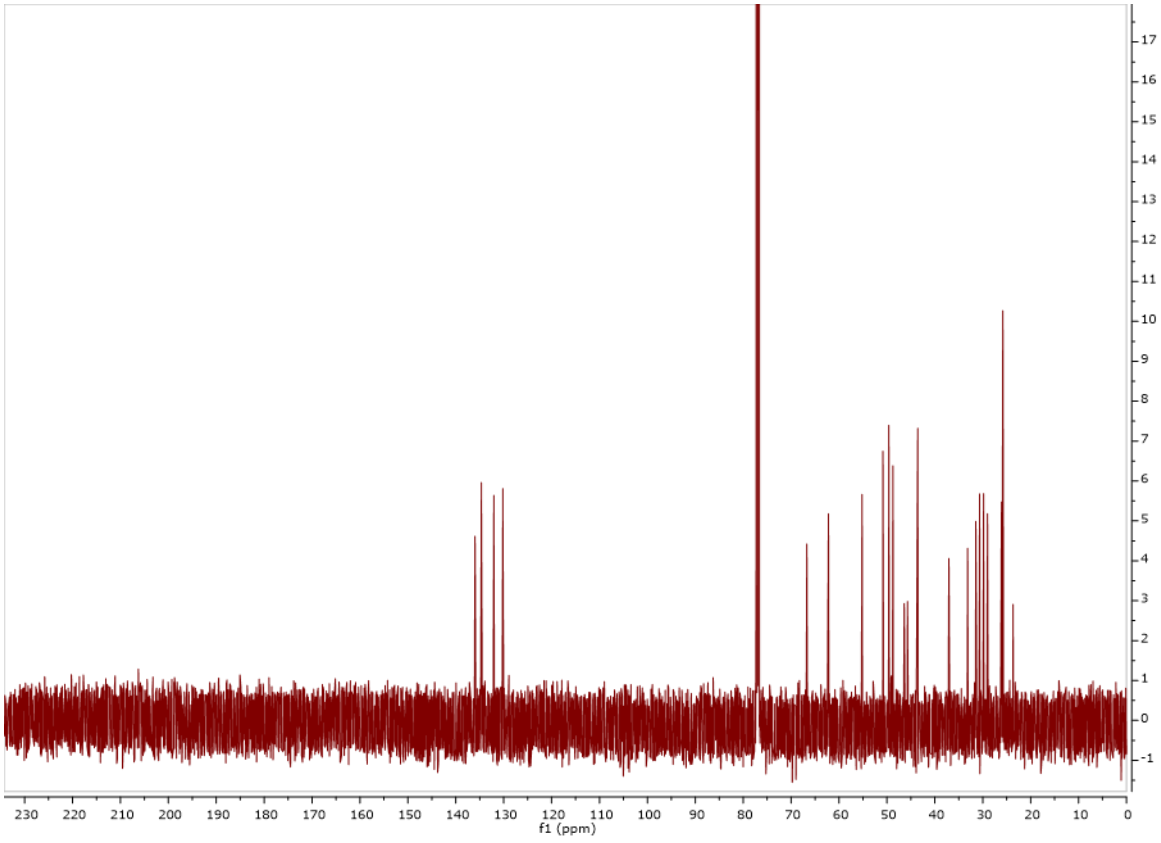

SI Figure 35 ^{13}C NMR (600 MHz, $CDCl_3$) of compound **4**

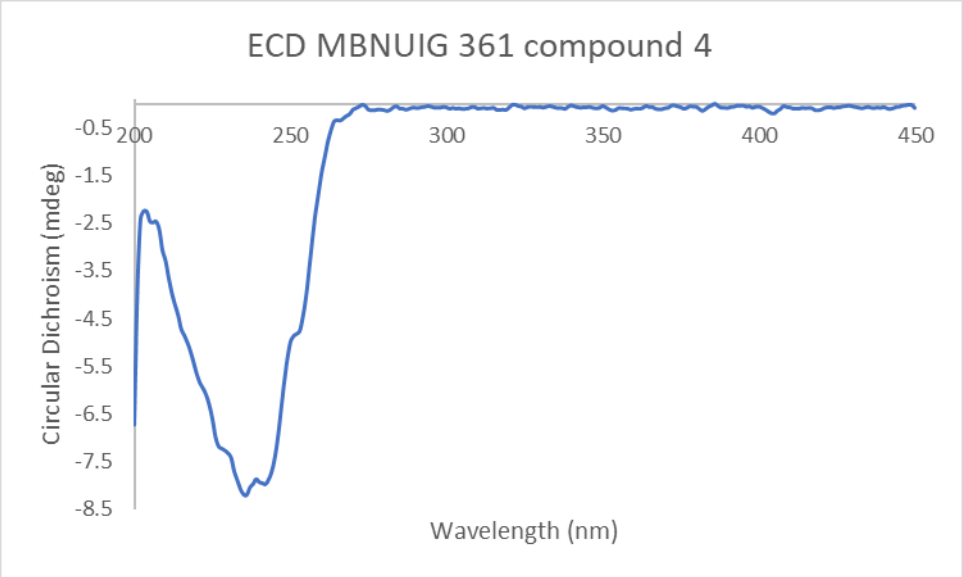

SI Figure 36 ECD spectrum (c 0.05 mg.mL^{-1}, MeOH) of compound **4**

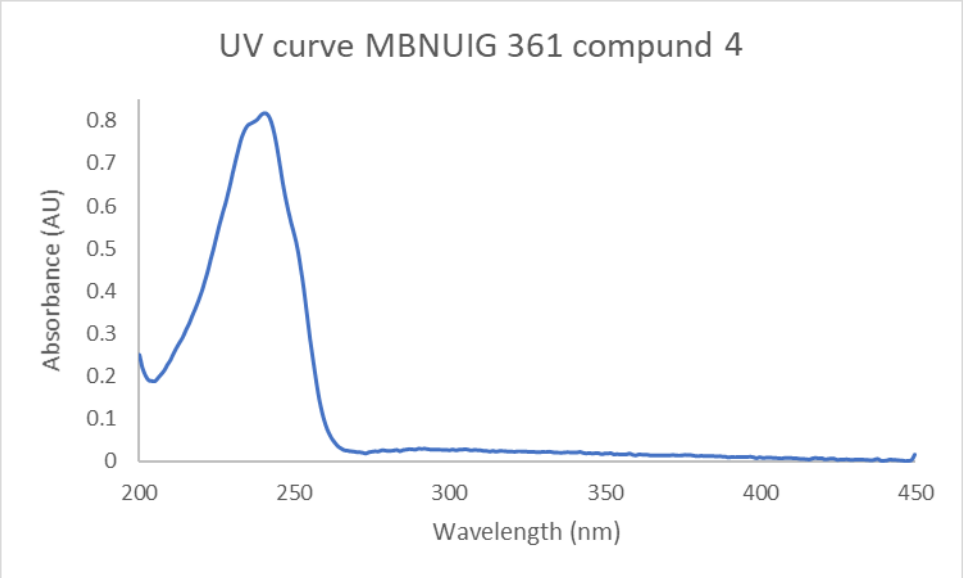

SI Figure 37 UV curve (c 0.05 mg.mL^{-1}, MeOH) of compound **4**

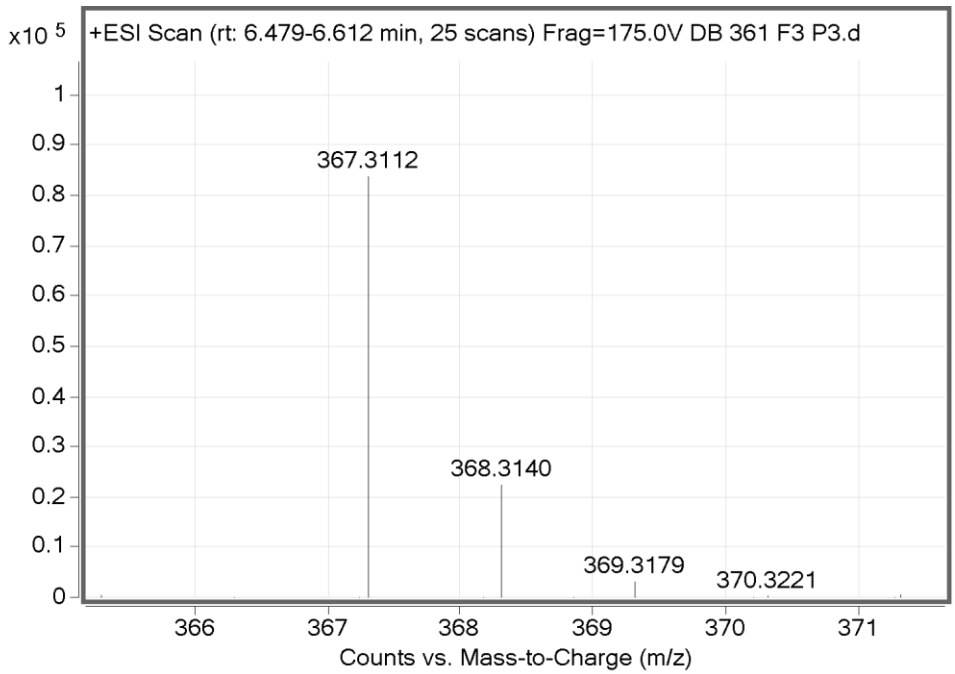

SI Figure 38 MS data for compound **5**

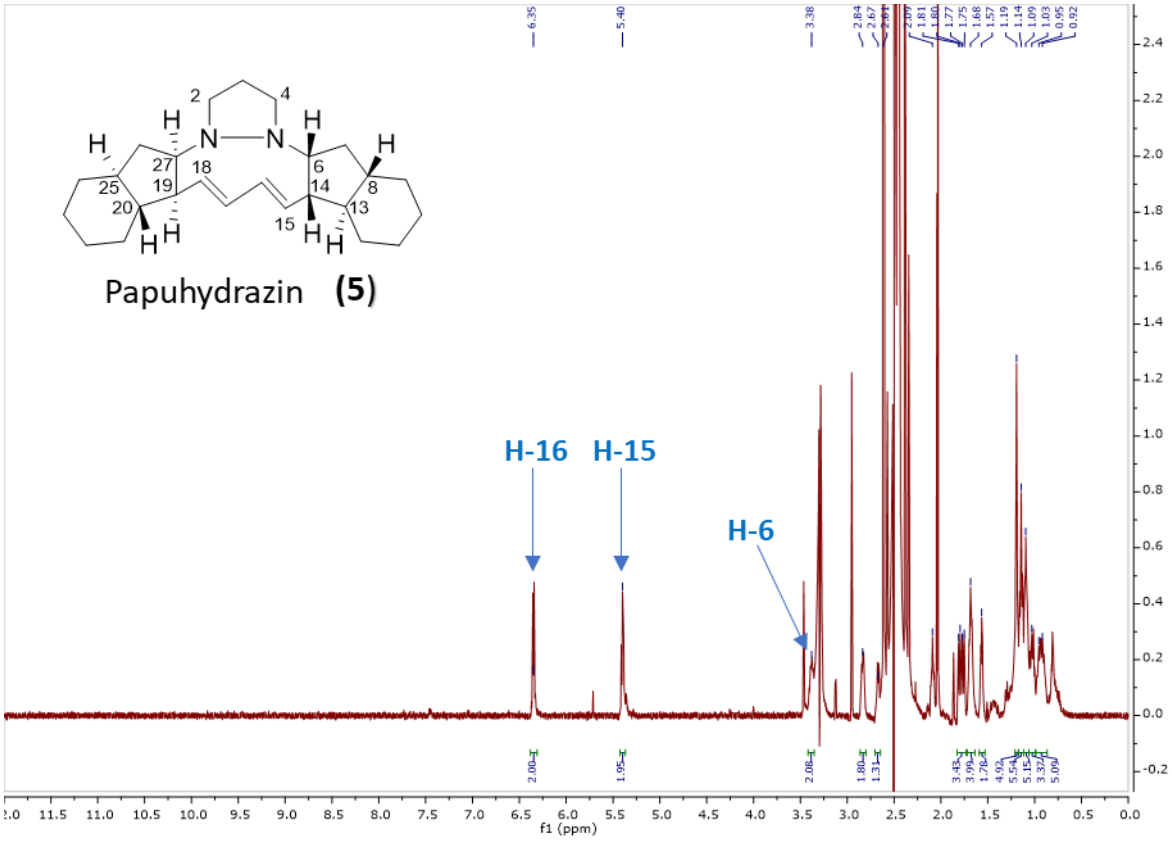

SI Figure 39 ^{1}H NMR spectrum (600 MHz, DMSO-d_6) of compound **5**

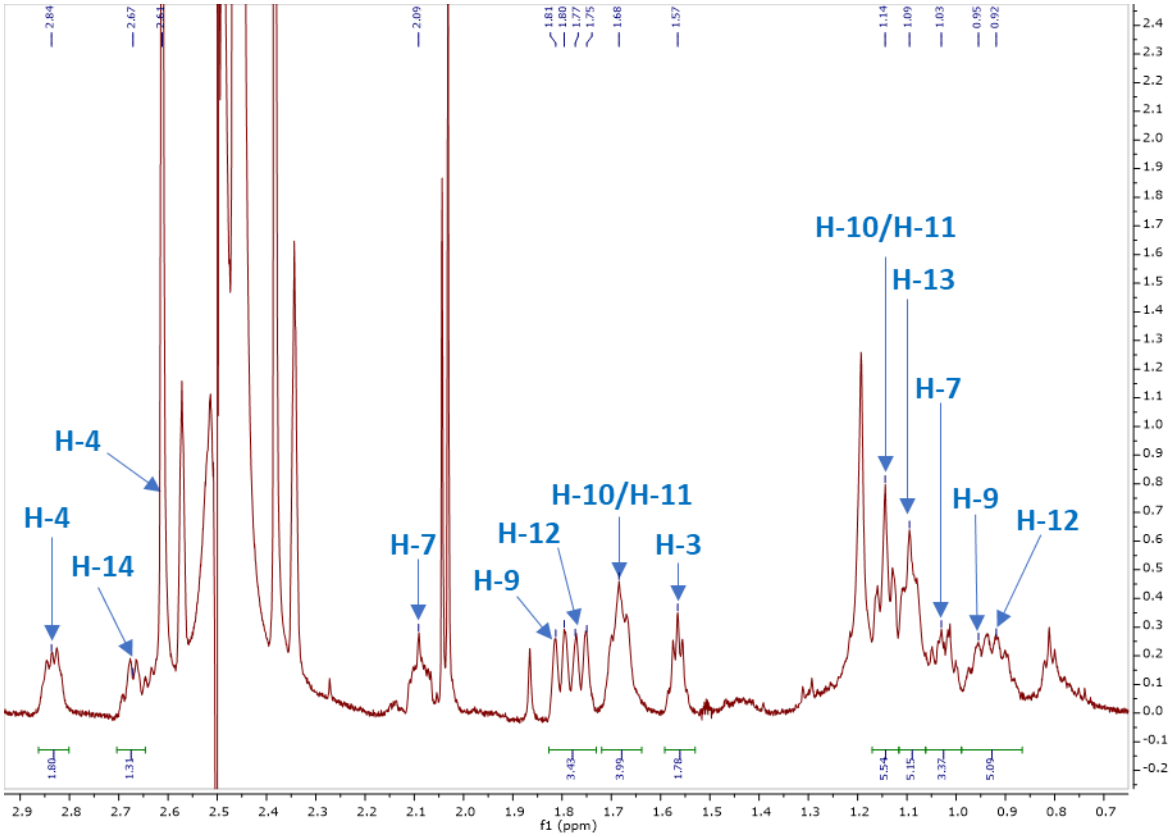

SI Figure 40 Expanded ^{1}H NMR spectrum (600 MHz, DMSO-d_6) of compound **5**

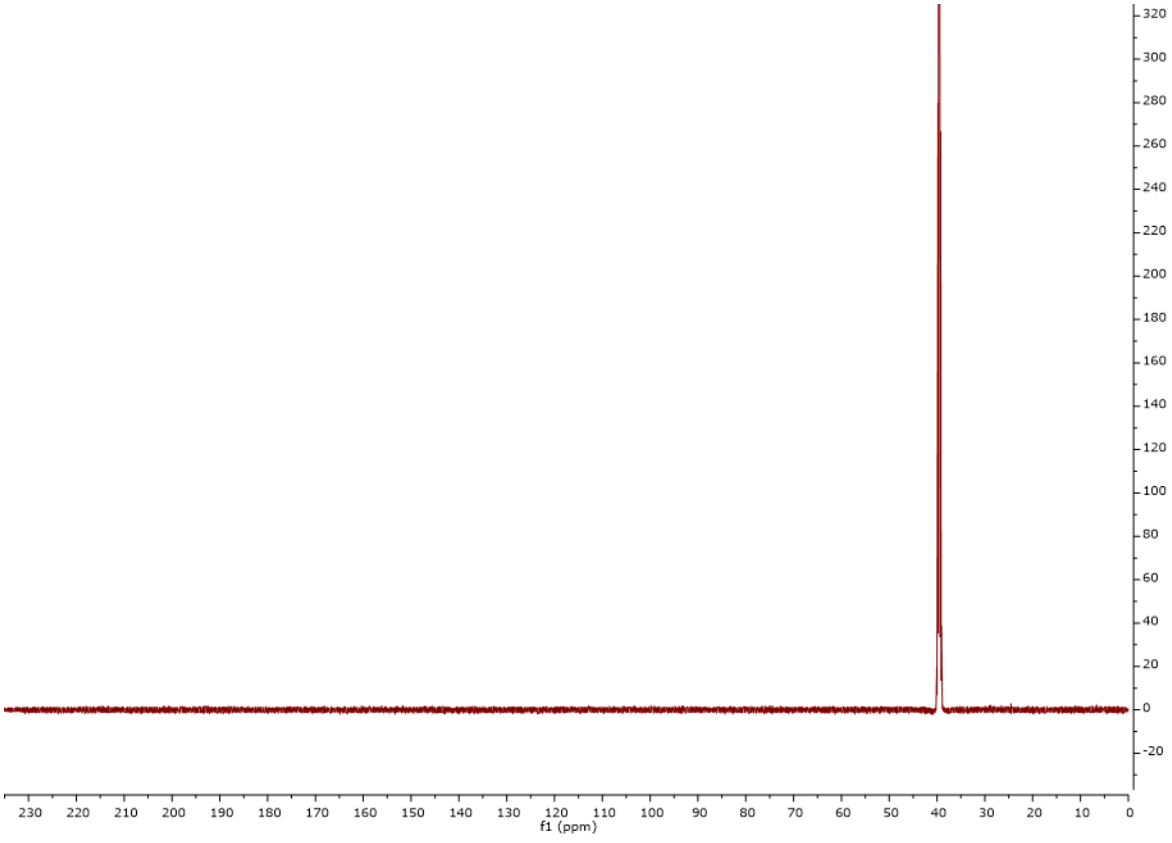

SI Figure 41 ^{13}C NMR spectrum (600 MHz, DMSO-d_6) of compound **5**

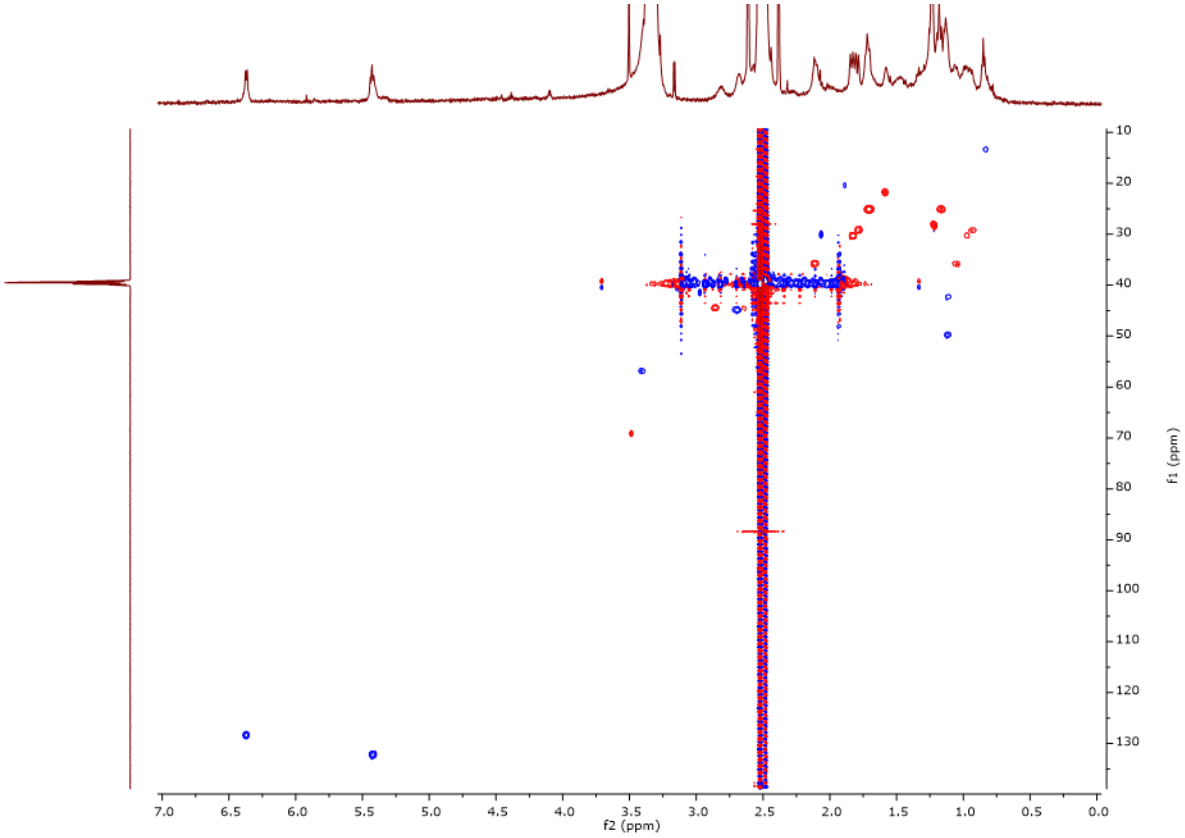

SI Figure 42 HSQC spectrum (600 MHz, DMSO-d_6) of compound **5**

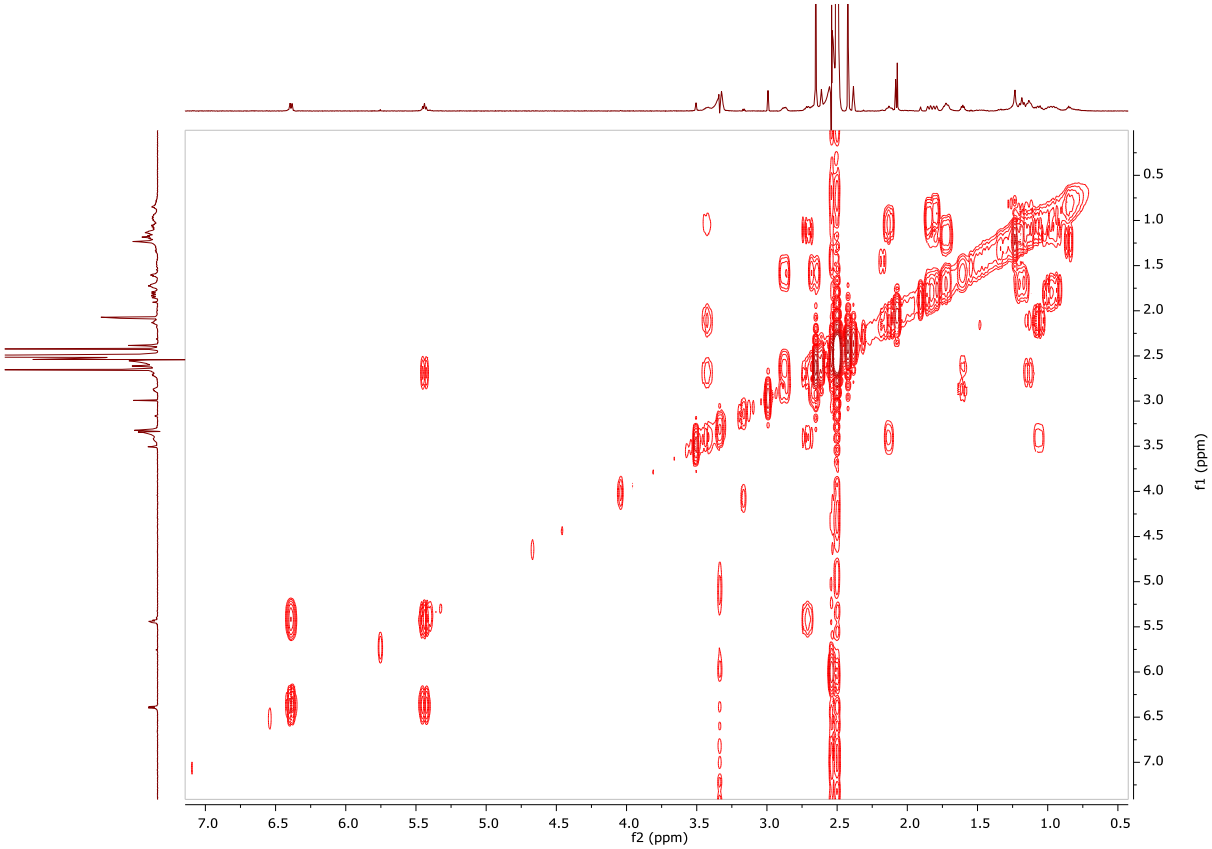

SI Figure 43 ^{1}H-^{1}H COSY spectrum (600 MHz, DMSO-d_6) of compound **5**

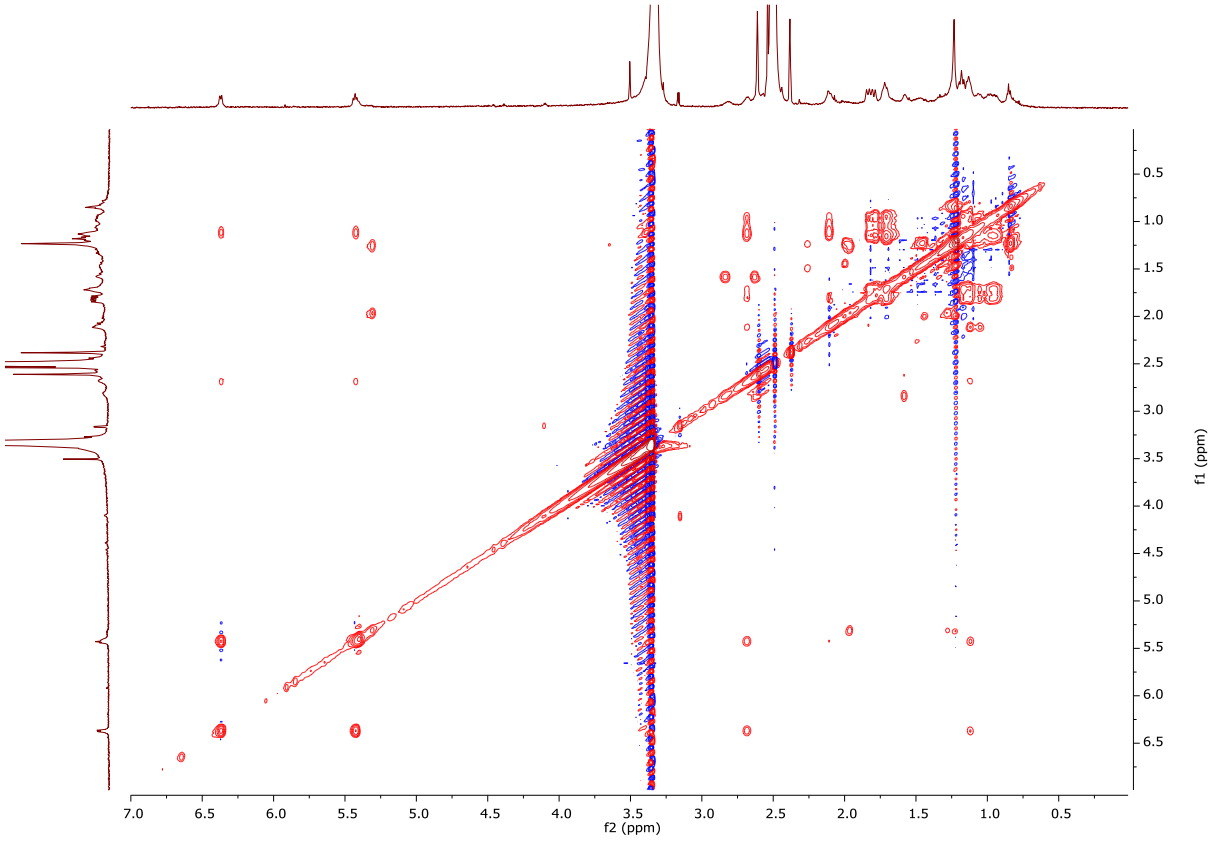

SI Figure 44 TOCSY spectrum (600 MHz, DMSO-d_6) of compound **5**

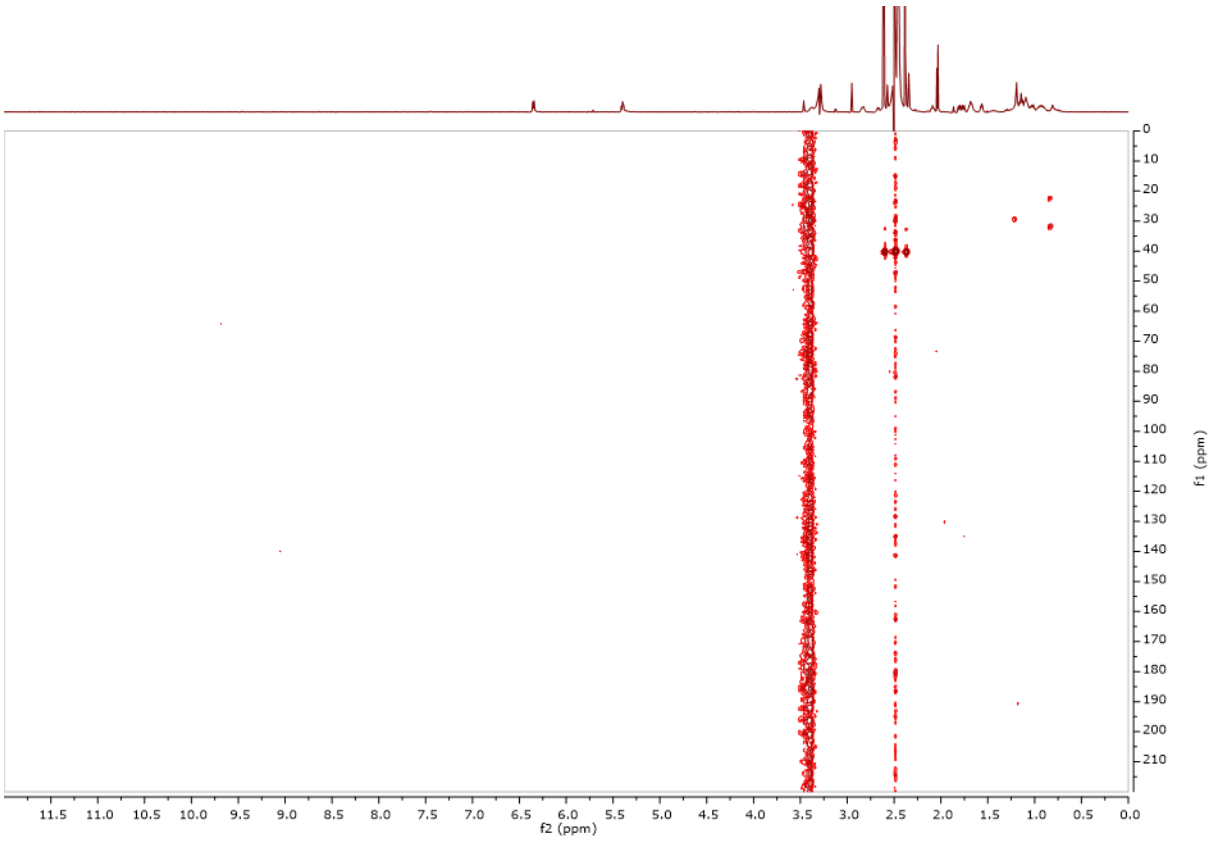

SI Figure 45 HMBC spectrum (600 MHz, DMSO-d_6) of compound **5**

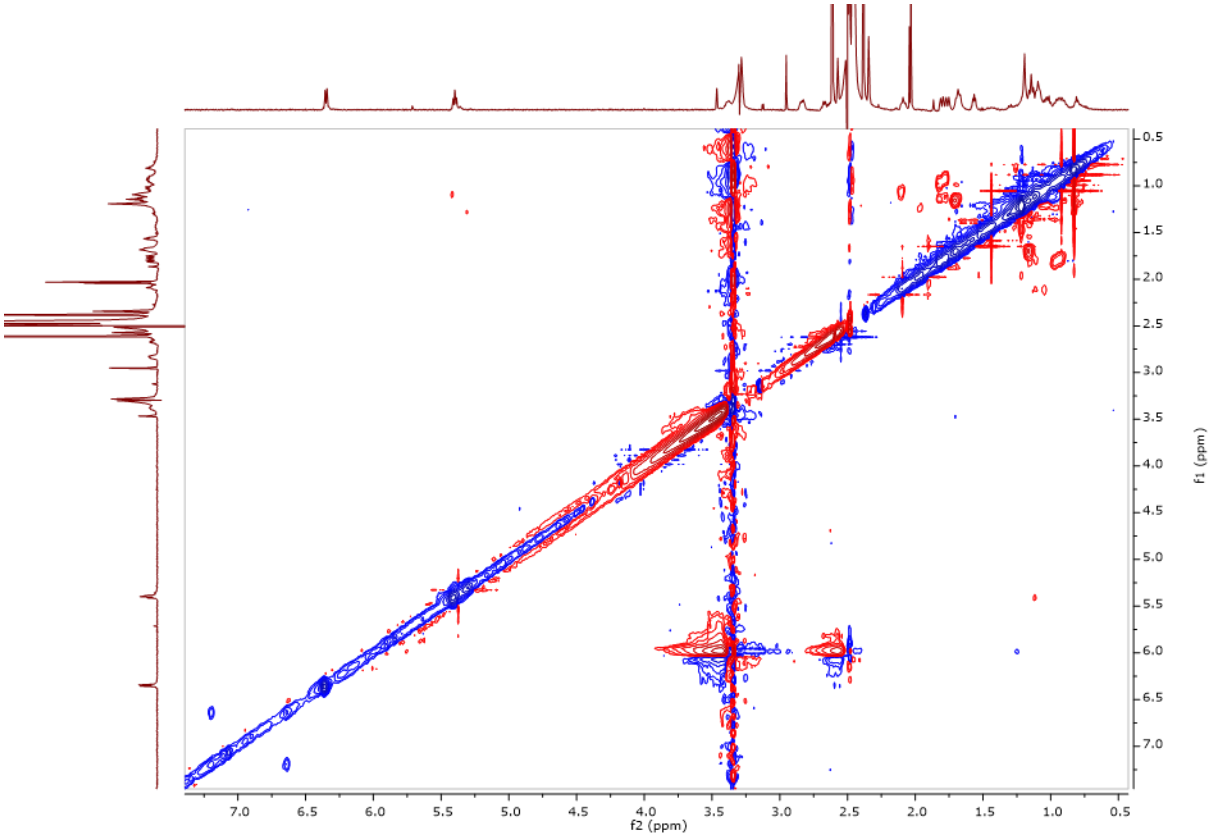

SI Figure 46 NOESY spectrum (600 MHz, DMSO-d_6) of compound **5**

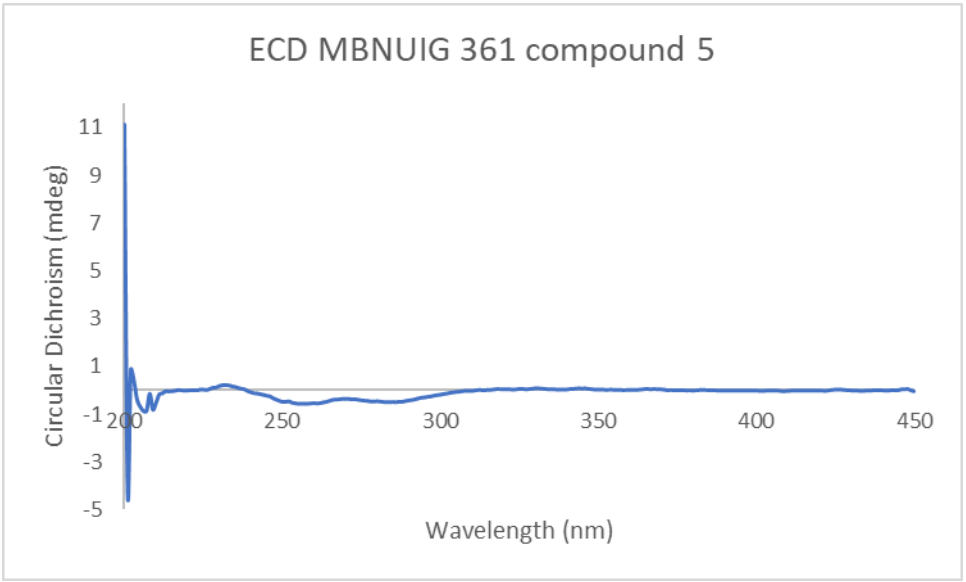

SI Figure 47 ECD spectrum (c 0.26 mg.mL^{-1}, MeOH) of compound **5**

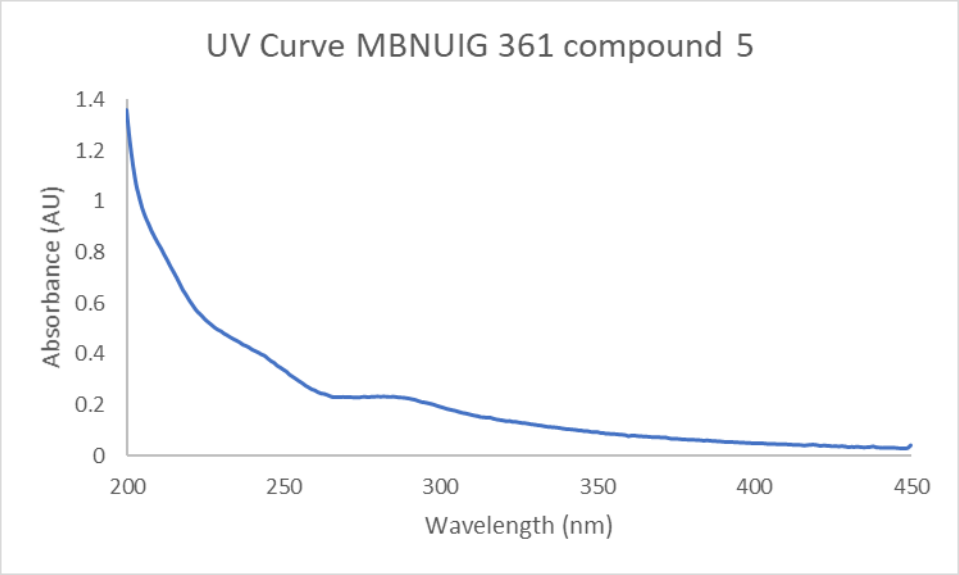

SI Figure 48 UV curve (c 0.26 mg.mL^{-1}, MeOH) of compound **5**

7.2. MB NUIG 368

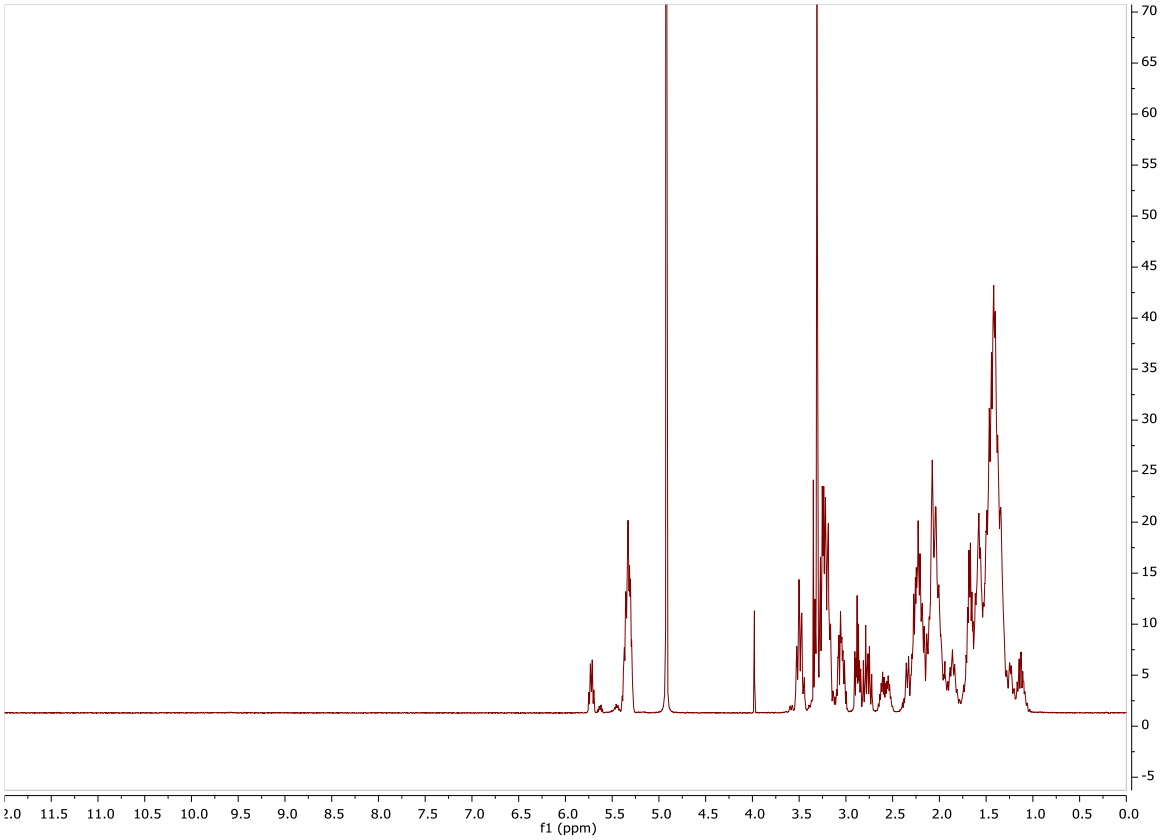

SI Figure 49 ^{1}H NMR spectrum (600 MHz, CD_3OD) of compound **3**

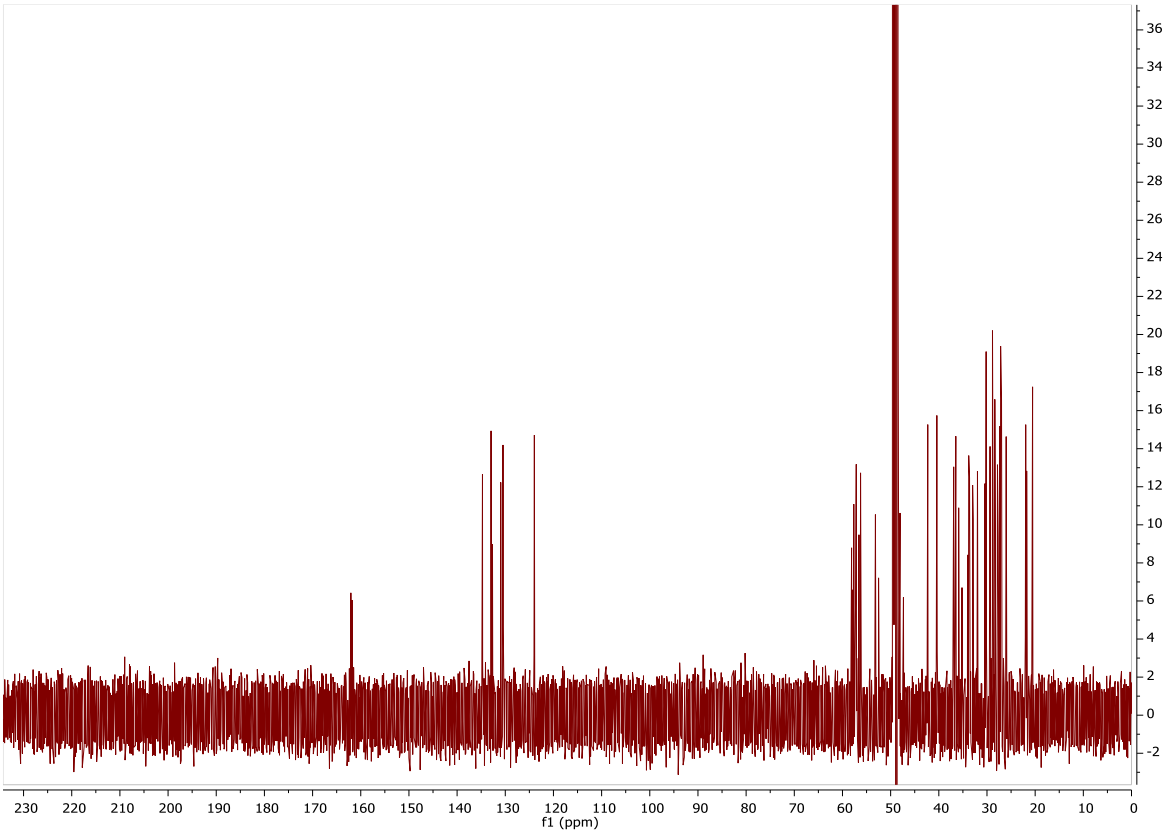

SI Figure 50 ^{13}C NMR spectrum (600 MHz, CD_3OD) of compound **3**

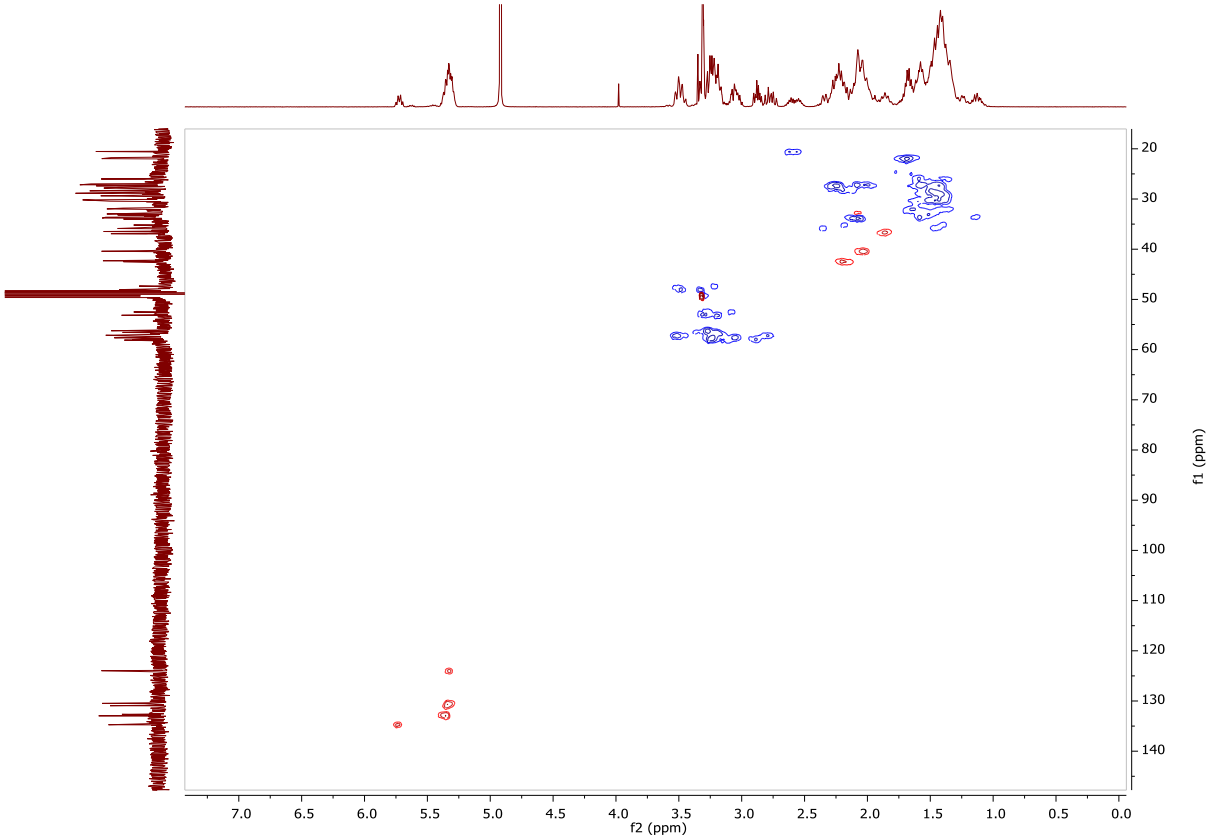

SI Figure 51 HSQC spectrum (600 MHz, CD_3OD) of compound **3**

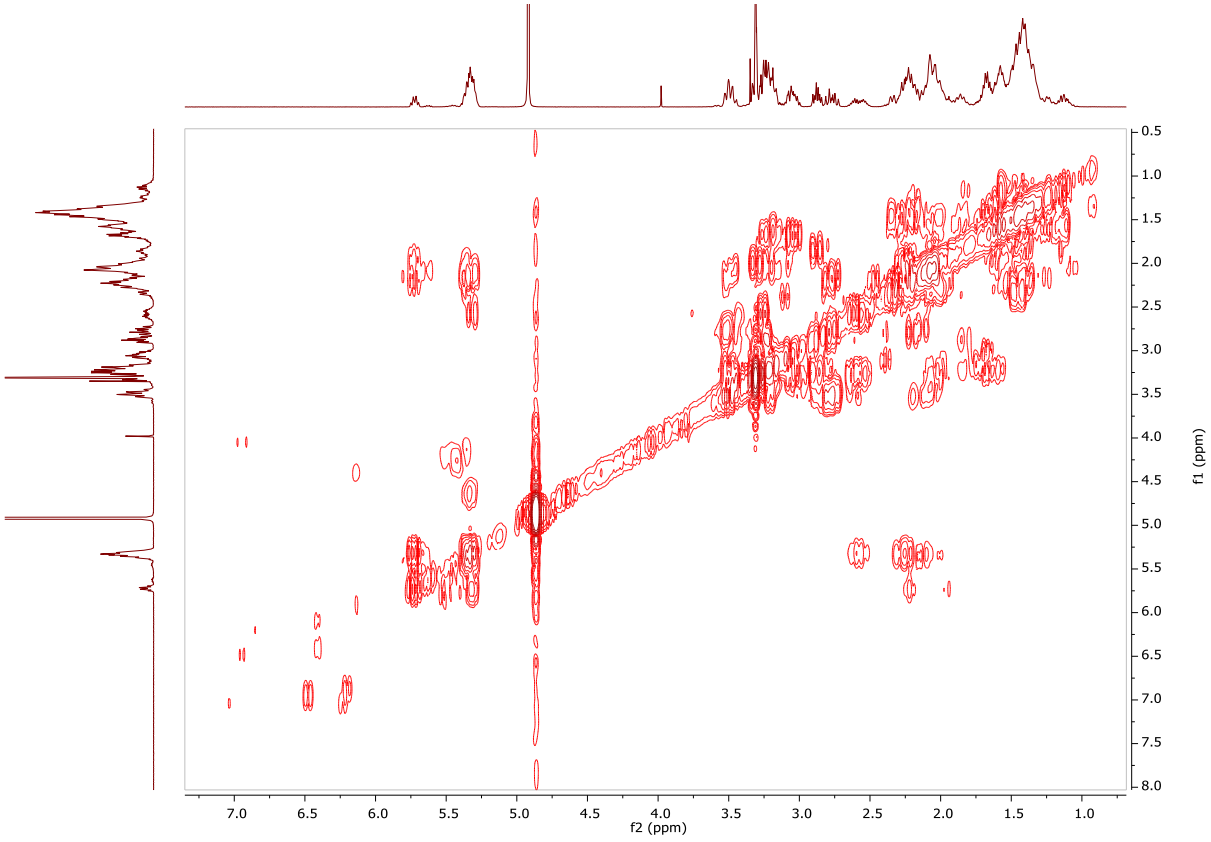

SI Figure 52 COSY spectrum (600 MHz, CD_3OD) of compound **3**

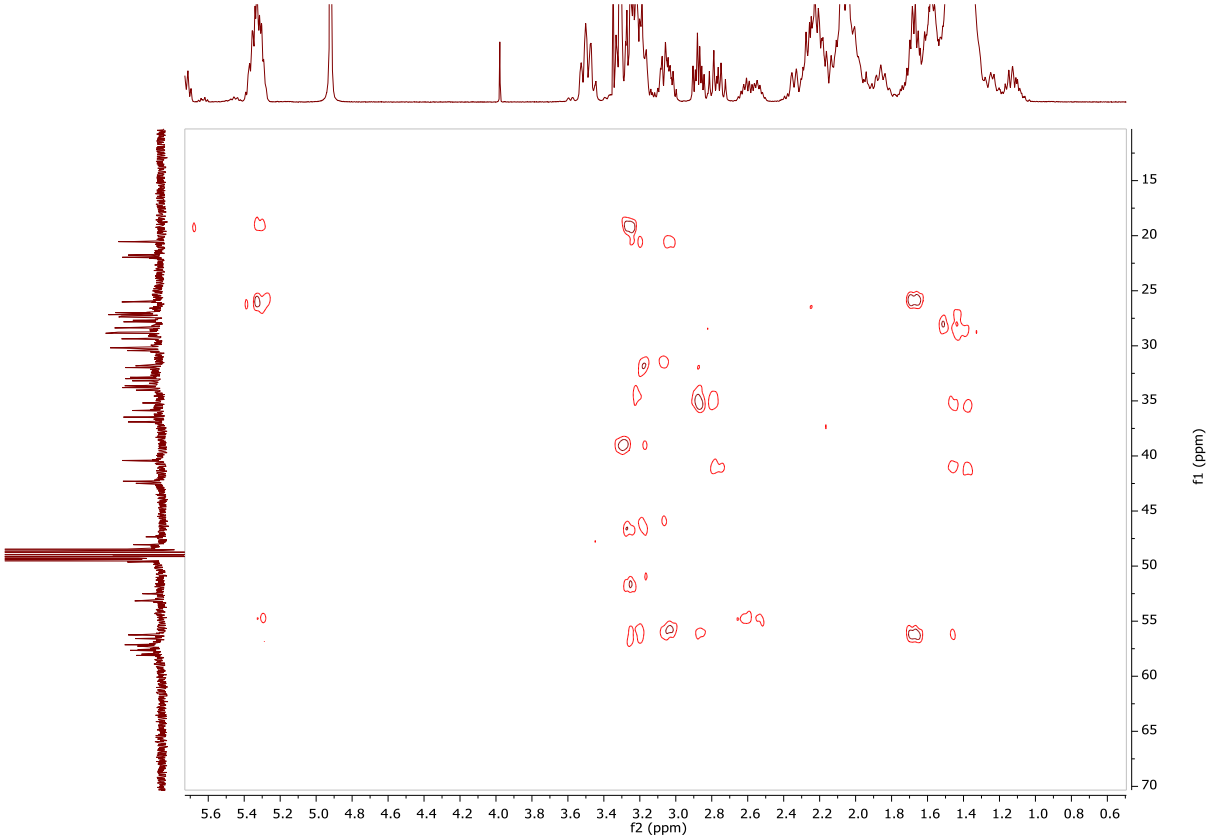

SI Figure 53 HMBC spectrum (600 MHz, CD_3OD) of compound **3**

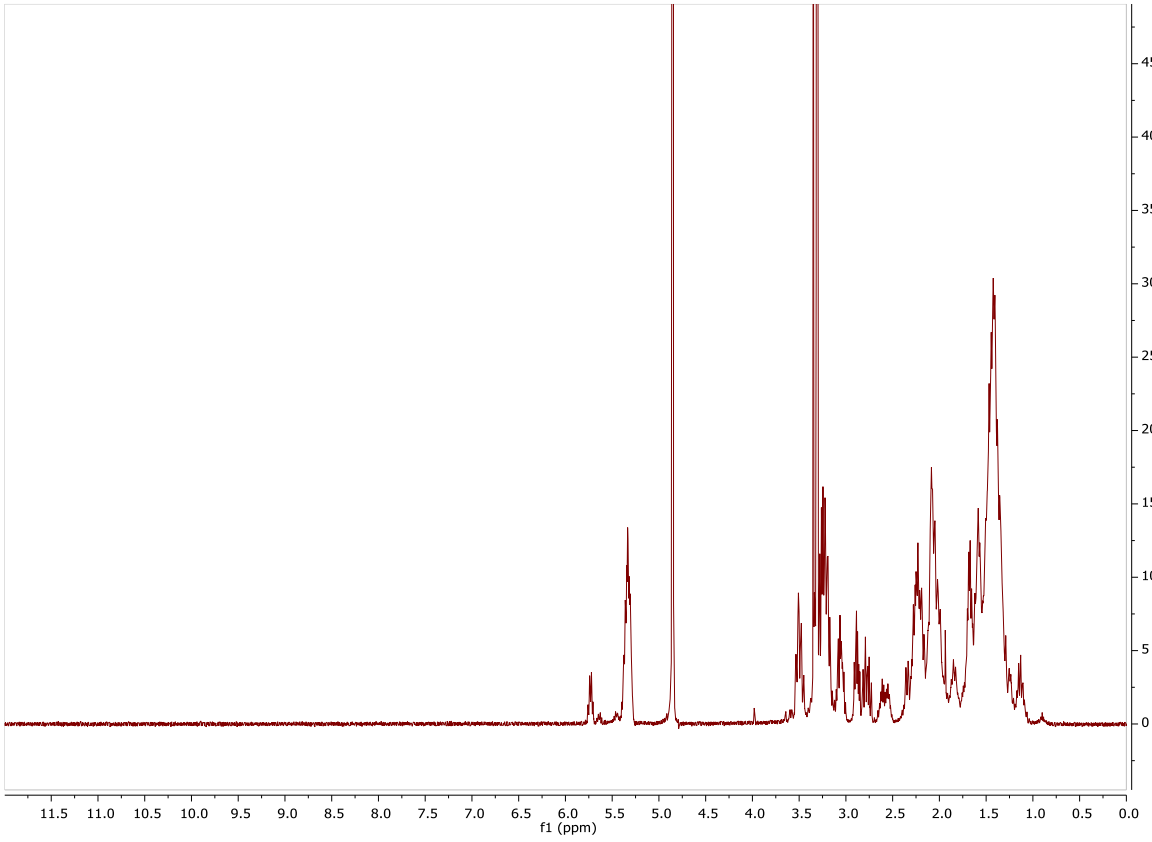

SI Figure 54 ^1H NMR spectrum (600 MHz, CD_3OD) of compound **4**

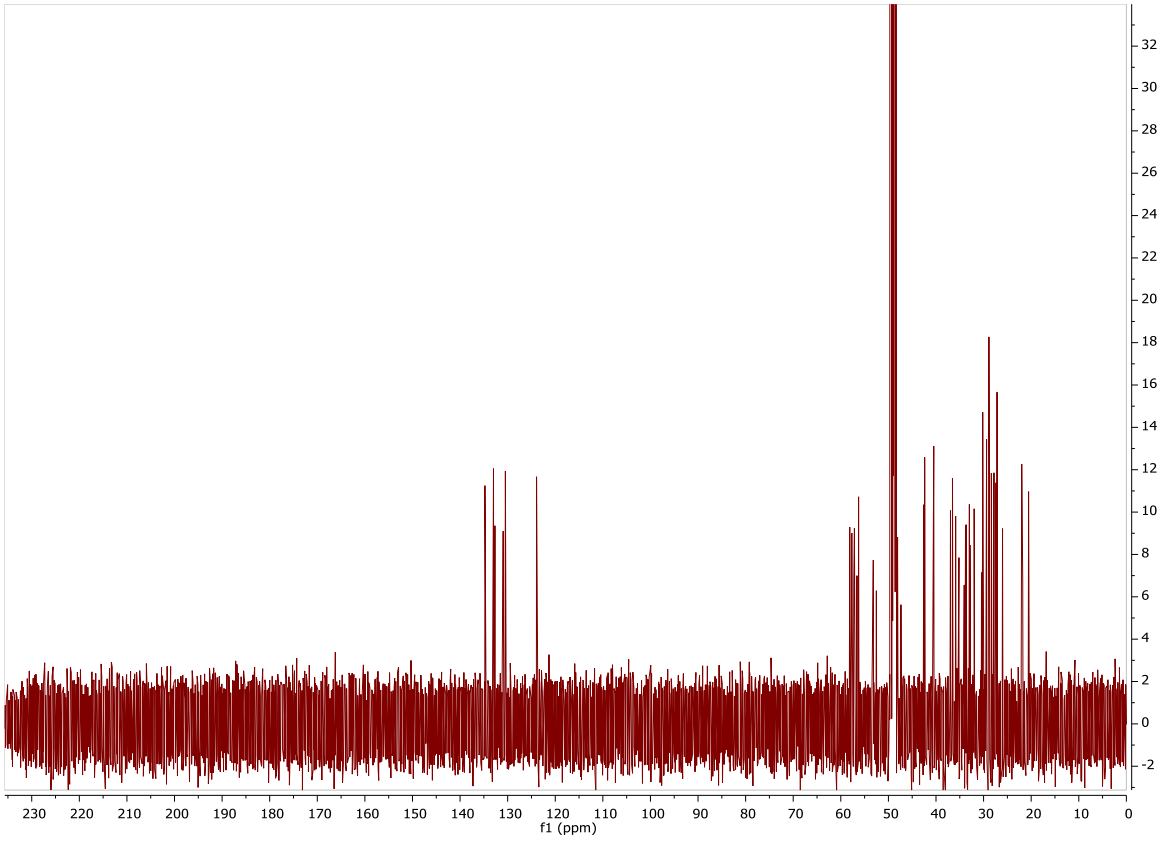

SI Figure 55 ^{13}C NMR spectrum (600 MHz, CD_3OD) of compound **4**

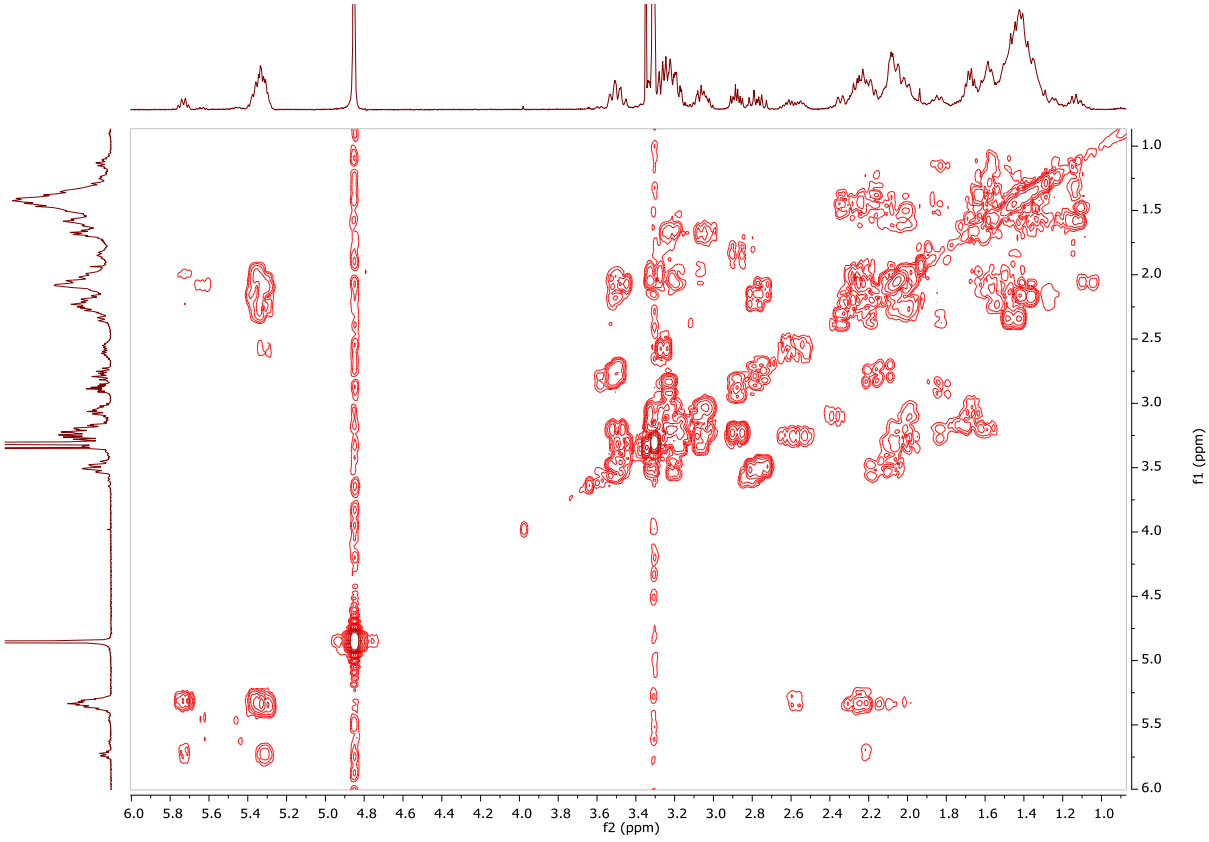

SI Figure 56 COSY spectrum (600 MHz, CD_3OD) of compound **4**

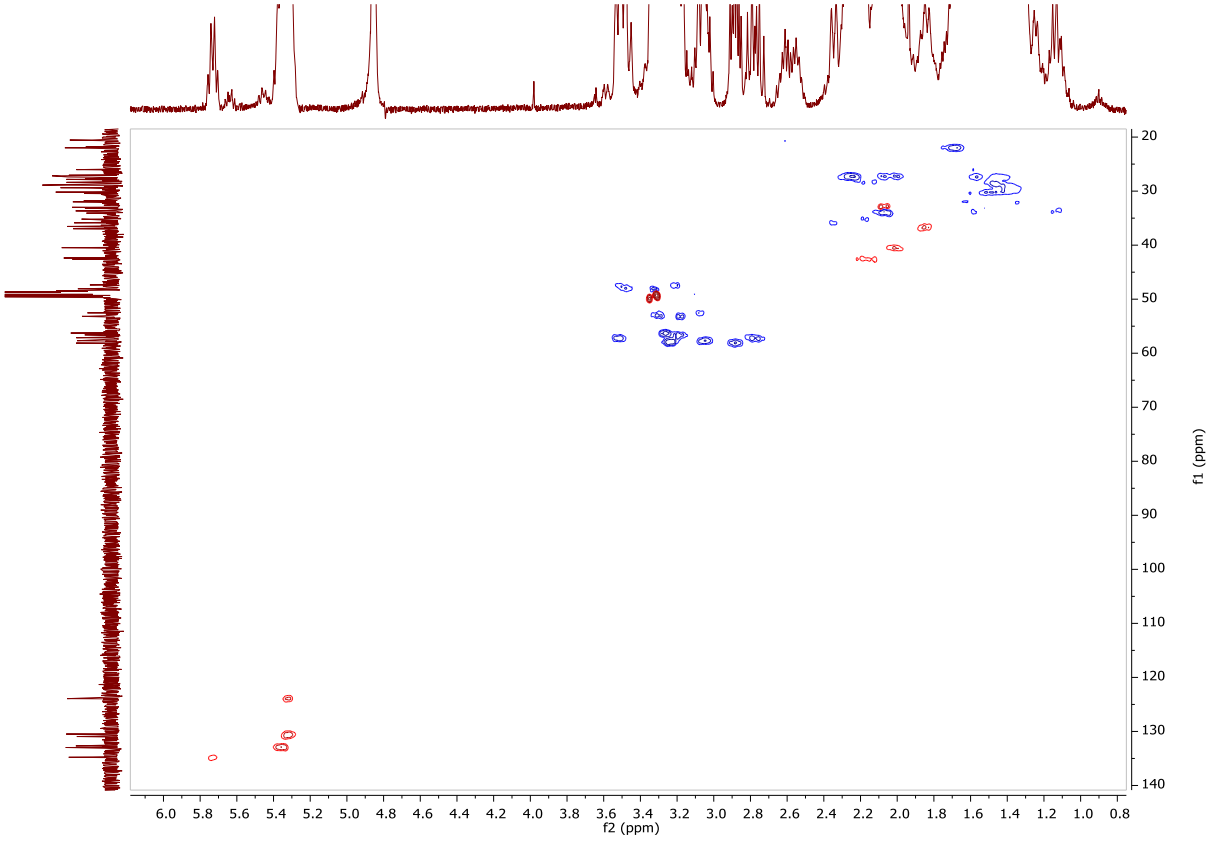

SI Figure 57 HSQC spectrum (600 MHz, CD_3OD) of compound **4**

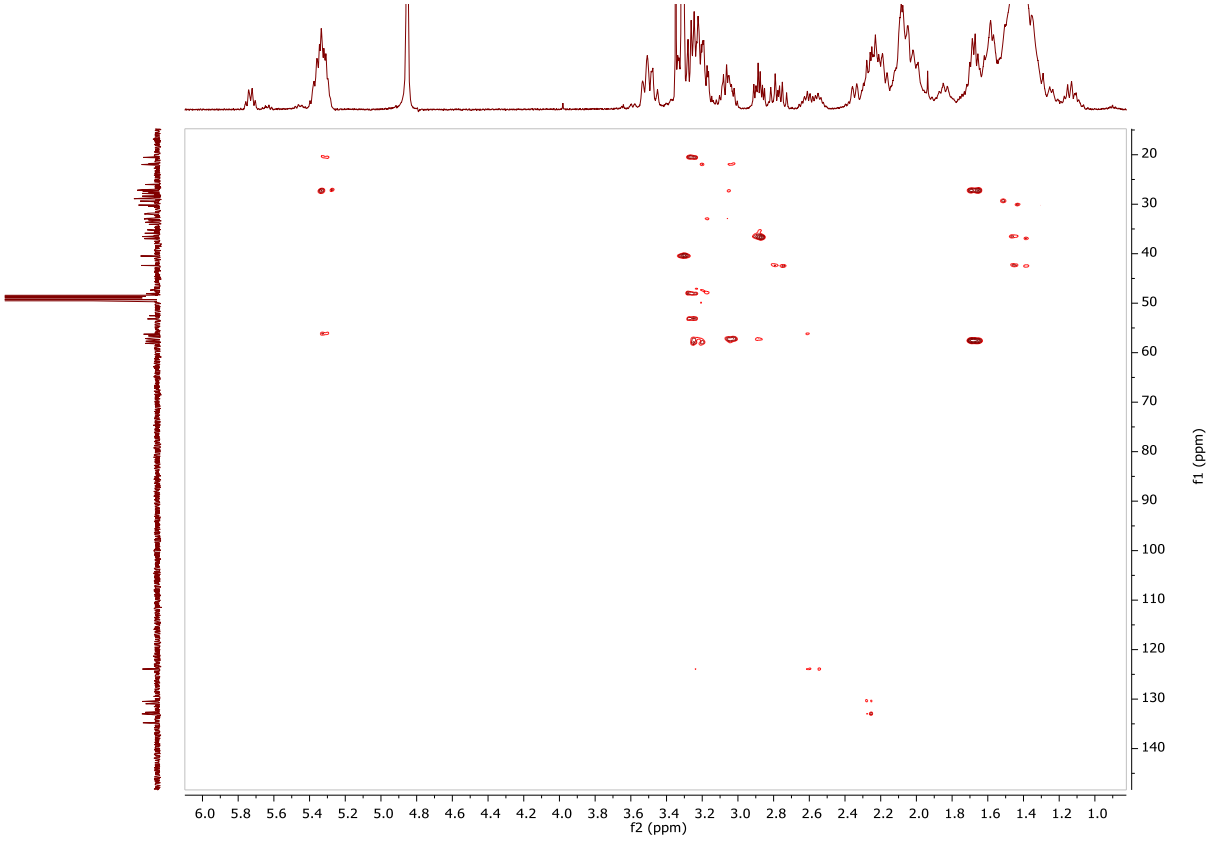

SI Figure 58 HMBC spectrum (600 MHz, CD_3OD) of compound **4**